

2018

Designed Polymer Brush Interfaces For Plutonium Separations And Polyethylene Nanocomposites

Julia G. Pribyl

University of South Carolina - Columbia

Follow this and additional works at: <https://scholarcommons.sc.edu/etd>

 Part of the [Chemistry Commons](#)

Recommended Citation

G. Pribyl, J. (2018). *Designed Polymer Brush Interfaces For Plutonium Separations And Polyethylene Nanocomposites*. (Doctoral dissertation). Retrieved from <https://scholarcommons.sc.edu/etd/4933>

This Open Access Dissertation is brought to you by Scholar Commons. It has been accepted for inclusion in Theses and Dissertations by an authorized administrator of Scholar Commons. For more information, please contact dillarda@mailbox.sc.edu.

DESIGNED POLYMER BRUSH INTERFACES FOR PLUTONIUM SEPARATIONS
AND POLYETHYLENE NANOCOMPOSITES

by

Julia G. Pribyl

Bachelor of Science
University of South Carolina, 2014

Submitted in Partial Fulfillment of the Requirements

For the Degree of Doctor of Philosophy in

Chemistry

College of Arts and Sciences

University of South Carolina

2018

Accepted by:

Brian Benicewicz, Major Professor

Morgan Stefik, Committee Member

Stephen Morgan, Committee Member

Ehsan Jabbarzadeh, Committee Member

Cheryl L. Addy, Vice Provost and Dean of the Graduate School

© Copyright by Julia G. Pribyl, 2018
All Rights Reserved.

DEDICATION

To my parents. Thank you for your unending and enthusiastic support.

And in loving memory of my grandfather, Lawrence E. Pribyl.

ACKNOWLEDGEMENTS

A deep debt of gratitude is owed to my advisor, Prof. Brian Benicewicz. As an advisor he is kind, a teacher, a motivator, and has taught me that as scientists we should probe deeply but also endeavor to see the forest through the trees. I owe a great deal of my success to him and offer him my sincerest thanks. I have been very privileged to work here, where he has cultivated an environment which has and will continue to produce excellent scientists. More importantly, this is a place where we all begin our time as colleagues and end as friends, and I have cherished these years as time well spent. Thank you to my committee members Prof. Morgan Stefik, Prof. Stephen Morgan, and Prof. Ehsan Jabbarzadeh for their encouragement, helpful advice, and honest criticism throughout my doctoral work. Special thank you to each of my collaborators at Rensselaer Polytechnic Institute, Prof. Linda Schadler (now at the University of Vermont), Marissa Giovino, and Xin Ning; also Prof. Sanat Kumar and Andrew Jimenez at Columbia University. This triumvirate of collaboration between Professors Benicewicz, Schadler, and Kumar has taught me much about the power of interdisciplinary teamwork which I hope to someday emulate. Thank you also to Dr. Kathryn Taylor-Pashow and Dr. Thomas Shehee at Savannah

River National Laboratory. I am especially grateful to them for their many invitations to observe experiments at SRNL and their eagerness to share their love of actinide science with me.

I would also like to express my gratitude towards the organizations which have funded my research including the SRNL LDRD Program and the US Department of Energy. It has been a pleasure to be able to spend many semesters focused solely on research. Some of my fondest memories of these past few years have been the days when I lost track of time in lab in pursuit of exciting results.

Here I have known the great joy that is working with excellent lab mates, many of whom have become my very good friends. First, thank you to Dr. Tony Neely for his patience during my training and for his wicked sense of humor. Working with him really set the tone for the rest of my time in this group. I am grateful to Dr. Michael Bell for his example as an excellent synthetic chemist, and his willingness to work together after his departure. Thank you also to Dr. Mohammad Mohammadkhani, Dr. Kayley Hayat, Dr. Yang Zheng, Dr. Yucheng Huang, Warren Steckle, Dr. Quoqing Qian, Dr. Anand Viswanath, Zaid "The Sheikh" Abbas, Andrew Pingitore, Maan Al Ali, Laura Murdock, Dr. Amin Daryaei, Dr. Fei Huang, Dr. Lihui Wang, Dr. Ran Liu, Massimo Tawfilas, Dennis Huebner, Brock Fletcher, Christopher Ott, James Sitter, Karl Golian, Kayla Lantz, Dr. Amrita Sarkar, Zack Marsh, Ben Lamm, Dr. Hasala (Nadee) Lokupitiya, Prof.

Chuanbing Tang, Md. Anisur Rahman, Meghan Lamm, and Dr. Mitra

Ganewatta. I count all these people among my friends and I will miss them greatly.

Of course, the Benicewicz group would not be what it is without the magnificent Susan Hipp. Special thank you to her for many great conversations, encouragement, advice, help, and friendship during my time here. Thanks also to Dr. Pamela Benicewicz for her hospitality during the many times she graciously hosted ACS Poly/PMSE functions at her home. Many fun (and delicious) nights were enjoyed because of her efforts. Thank you to Prof. Sheryl Wiskur and Dr. Ravish Akhani for their guidance and encouragement in my early days in the lab. I would also be remiss not to mention my gratitude towards Dr. Kenneth Wagener. Many thanks to him for the opportunity to spend a month in the Butler Labs at the University of Florida working in his group, and for sharing his unique perspectives with me. The way he loves and thinks about science is contagious.

Finally, my deepest love and gratitude to my family, friends, and beloved dog Oliver.

ABSTRACT

Modification of surfaces with polymer brushes has become an important area of research for developing materials with a variety of advanced properties. Flat or continuous surfaces modified with polymer brushes can serve as surfaces where chemical reactions or separations take place, and discrete nanoparticles covered in a polymer brush can disperse within a miscible surrounding polymer, generating a composite which retains the processability of the polymer but becomes endowed with the properties of the filler as well. Presented herein are new synthetic approaches to modify both continuous surfaces as well as discrete particles with polymer brushes for complex applications.

In the first chapter which details new work, the ability of foam monoliths grafted with a polymer brush to serve as a scaffold for plutonium separations is discussed. In this first part of a two-part story, a photoinitiated polymerization generates surface grafted chains of a functional polymer brush on a foam surface, and the resulting monoliths were tested for their plutonium capacity as well as separation efficiency compared to a commercial resin used for the same purpose. The light used to initiate the surface polymerization was found to have poor penetration into the center of the opaque monoliths which negatively affected the

monolith's capacity, but narrow elution profiles of the loaded plutonium hinted at the potential for macroporous foams to serve as very efficient scaffolds for separations.

An extension of this work saw the development of an improved synthetic strategy with the aim of improving the plutonium capacity of the foam as well as devising a strategy to control the graft density and molecular weight of grafted polymer chains. The separation characteristics and recyclability of these materials was investigated and is discussed in detail.

Focus then shifted to the development of well-defined polyethylene grafted silica nanoparticles. Polyethylene represents the largest class of commodity plastics used globally but is underexplored in the nanocomposites community due to the synthetic challenge of making well-defined polyethylene and attaching it to surfaces. A unique synthetic approach to prepare polyethylene grafted particles was devised, and the materials made using this procedure were thoroughly characterized.

Finally, some conclusions about what was learned as well as some suggestions about how this work might proceed are offered in light of the work presented herein.

TABLE OF CONTENTS

DEDICATION.....	iii
ACKNOWLEDGEMENTS.....	iv
ABSTRACT	vii
LIST OF TABLES	xii
LIST OF FIGURES	xiii
LIST OF SCHEMES	xvii
LIST OF ABBREVIATIONS.....	xix
CHAPTER 1: INTRODUCTION	1
1.1 Polymer Brushes	2
1.2 Polymeric High Internal-Phase Emulsion (polyHIPE) Foams	6
1.3 Polymer Nanocomposites	21
1.4 Dissertation Outline	34
1.5 References	36
CHAPTER 2: PHOTOINITIATED POLYMERIZATION OF 4-VINYLPYRIDINE ON POLYHIPE FOAM SURFACE TOWARDS IMPROVED PLUTONIUM SEPARATIONS.....	48
2.1 Abstract	49
2.2 Introduction	49

2.3 Experimental.....	52
2.4 Results and Discussion	56
2.5 Conclusions.....	61
2.6 References	62

CHAPTER 3: HIGH-CAPACITY POLY(4-VINYLPYRIDINE) GRAFTED POLYHIPE FOAMS FOR EFFICIENT PLUTONIUM SEPARATION AND PURIFICATION	66
---	----

3.1 Abstract	67
3.2 Introduction	67
3.3 Experimental.....	71
3.4 Results and Discussion	82
3.5 Conclusions.....	99
3.6 References	101

CHAPTER 4: SYNTHESIS AND CHARACTERIZATION OF POLYETHYLENE GRAFTED NANOPARTICLES TOWARD POLYETHYLENE NANOCOMPOSITES.....	106
---	-----

4.1 Abstract	107
4.2 Introduction	107
4.3 Experimental.....	114
4.4 Results and Discussion	118
4.5 Conclusions.....	126
4.6 References	127

CHAPTER 5: SUMMARY AND OUTLOOK.....	131
APPENDIX A: NMR SPECTRA.....	137
APPENDIX B: PERMISSION TO REPRINT.....	140

LIST OF TABLES

Table 2.1: Dimensions of materials tested and elemental analysis data for synthesized polyHIPE foams	55
Table 2.2: Chemical and physical characteristics of synthesized polyHIPE foam columns and Reillex® HPQ	57
Table 3.1: Dimensions and formulation information of materials tested	77
Table 3.2: Physical and chemical characteristics of synthesized polyHIPE foams and Reillex HPQ resin.....	85
Table 4.1: Physical and chemical characteristics of selected samples	120

LIST OF FIGURES

Figure 1.1: Illustration of polymer brush conformations (A) "pancake" (B) "mushroom" and (C) "brush"	2
Figure 1.2: Polymer brush grafting techniques (A) physisorption (B) grafting-to (C) grafting-from (D) grafting-through	4
Figure 1.3: Polymer brush architectures (A) bimodal (molecular weight) (B) mixed-bimodal (different chemistries) (C) block copolymer (D) Janus (two faces, or "patchy")	5
Figure 1.4: Diffusive mass transfer versus convective mass transfer.....	8
Figure 1.5: PolyHIPE absorption of n-hexane (dyed with Sudan 1) over time	17
Figure 1.6: Illustration of thermomechanical deformation and recovery in shape memory polyHIPEs.....	20
Figure 1.7: Dispersion states of bare nanoparticles versus polymer-grafted nanoparticles in a polymer matrix (in gray)	22
Figure 1.8: Illustration of relative interfacial volume (in blue) between larger and smaller fillers in a polymer matrix.....	23
Figure 1.9: Figure 1.9: Wetting behavior of polystyrene (PS) thin films on a layer of PS-g-SiO ₂ . PS MW= 44,200 g/mol (left) 92,000 g/mol (middle) 252,000 g/mol (right).....	28
Figure 1.10: Experimentally determined morphology diagram of PS-g-SiO ₂ in PS matrix (right) and transmission electron micrographs (left) of PS-g-SiO ₂ of varying MW and σ in PS matrix (MW=142 kg/mol).....	29
Figure 1.11: Evolution of polymer grafted nanofillers from simple to complex...	31
Figure 2.1: Representative SEM images of polyHIPE foams (a) before surface polymerization, low magnification (b) after surface polymerization, low magnification, (c) before surface polymerization, high magnification, (d) after surface polymerization,	

high magnification. (Scale bars are 20 μm in images a and b, scale bars are 1 μm in images c and d).	58
Figure 2.2: Pu loading curves for foam and Reillex [®] HPQ columns (left) and Pu elution curves for foam and Reillex [®] HPQ columns (right)	60
Figure 2.3: Gravimetric comparison of Pu loading between foam columns and Reillex [®] HPQ resin.....	61
Figure 3.1: Image of prepared polyHIPE column prototypes. (Total length of the column assemblies is approximately 9 cm).....	77
Figure 3.2: Image of the flow-testing set up used to conduct controlled flow testing of Reillex HPQ and assembled polyHIPE column prototypes. (1) Programmable syringe pump (2) ~4 g/L Pu(IV) feed solution in syringe (3) “quick connect” hose connectors (4) polyHIPE column prototype.....	79
Figure 3.3: Illustration of J. L. Shepherd Model 484 Co-60 Irradiator.....	81
Figure 3.4: Dynamic mechanical analysis of polyHIPE foams before surface polymerization (A-D) and after surface grafting with P4VP (E-H). Testing was conducted at a series of static pressures (A and E = 60psi 1 hr, B and F = 80 psi 1 hr, C and G = 100 psi 1 hr, D and H = 60 psi 12 hr). Strain recovery was observed for 15 min in each experiment	83
Figure 3.5: (a) Kinetic plot and (b) dependence of the GPC molecular weight, theoretical molecular weight, and dispersity on the conversion for the polymerization of 4-vinylpyridine (4-VP) initiated by (3.2). ([4-VP]:[(3.2)] = 200:1, and 4-VP/n-butanol = 30/70 v/v)	87
Figure 3.6: Representative SEM images of polyHIPE foams (A-B) after curing and (C-D) after the surface-initiated polymerization of P4VP. (Scale bars are 20 μm in images A and C, and 1 μm in images B and D).....	88
Figure 3.7: Plutonium breakthrough curves of Reillex HPQ and tested polyHIPE materials. (Labels A-F refer to the polyHIPE foam samples described in Table 3.2)	90
Figure 3.8: Correlation between Pu capacity and percent N due to grafted P4VP on polyHIPE foam samples	91
Figure 3.9: Elution curves of Reillex HPQ and tested polyHIPE materials. (Labels A-F refer to the polyHIPE foam samples described in Table 3.2)	92

Figure 3.10: Bulk Pu capacity of each ion-exchange (IX) material on a volumetric basis (a) and gravimetric basis (b).....	94
Figure 3.11: Loading and elution curves for polyHIPE sample G over four Pu anion-exchange cycles.....	95
Figure 3.12: Bulk Pu capacity of polyHIPE sample G across four loading/elution cycles.....	96
Figure 3.13: Photos of polyHIPEs (top) after soaking in 8 M nitric acid for approx. 7 weeks and (bottom) after soaking in 8 M nitric acid with gamma irradiation for approx. 7 weeks (total dose $\sim 7.8 \times 10^7$ rads). Samples were placed in the glass holders to keep the foam submerged in acid during the soaking.....	97
Figure 3.14: Colormap of radiation dose within irradiator vessel (side view).....	98
Figure 4.1: NMR spectra of monomer conversion of (a) $t=0$ min, solution polymerization (b) $t=5$ min, solution polymerization (c) $t=0$ min, surface-initiated polymerization and (d) $t=5$ min, surface-initiated polymerization. $[M]:[catalyst] = [200]:[1]$, $[cis\text{-cyclooctene}] = 1$ M in THF	121
Figure 4.2: DLS curves and TEM images of PCO-g-SiO ₂ synthesized with (a-c) 0.8 eq. catalyst with respect to norbornyl silane, (d-f) 1.0 eq. catalyst with respect to norbornyl silane, (g-i) 1.15 eq. catalyst with respect to norbornyl silane	122
Figure 4.3: DLS curves for samples A-G and bare silica nanoparticles	123
Figure 4.4: DSC curves before hydrogenation (black), after hydrogenation (red), after second hydrogenation (blue). Displayed curves represent the first cooling and second heating cycle. Labels A-G refer to the samples detailed in Table 4.1.....	125
Figure A.1: ¹ H NMR (300 MHz, CDCl ₃) spectrum of compound 3.1	138
Figure A.2: ¹ H NMR (300 MHz, CDCl ₃) spectrum of compound 3.2	139
Figure B.1: Permission to reprint Scheme 1.2B	141
Figure B.2: Permission to reprint Scheme 1.2C	142
Figure B.3: Permission to reprint Figure 1.5.....	143

Figure B.4: Permission to reprint Figure 1.6.....	144
Figure B.5: Permission to reprint Figure 1.8.....	145
Figure B.6: Permission to reprint Figure 1.9.....	146
Figure B.7: Permission to reprint Figure 1.10.....	147
Figure B.8: Permission to reprint Scheme 1.5.....	148
Figure B.9: Permission to reprint Figure 1.11.....	149
Figure B.10: Permission to reprint Chapter 2.....	150

LIST OF SCHEMES

Scheme 1.1: General outline of polyHIPE synthesis.....	7
Scheme 1.2: (A) polyHIPE prepared from Suzuki-Miyaura coupling (idealized structure) (adapted with permission from ref [28]) (B) Preparation of thiol-acrylate polyHIPE (reproduced with permission from ref [29]) (C) PolyHIPE prepared by ROMP (adapted with permission from ref [30]).....	11
Scheme 1.3: Mechanisms of monomer addition for NMP, ATRP, and RAFT polymerizations and some common NMP agents (inset) Initiation and termination steps have been excluded for brevity	24
Scheme 1.4: Synthesis of attachment of RAFT agent attachment and surface-initiated polymerization	27
Scheme 1.5: Generalized synthesis of bimodal brush nanoparticles (Reproduced with permission from ref [13]).....	30
Scheme 2.1: Synthetic route to prepare HIPE foams with surface-grafted chains of poly(4-vinyl pyridine) (P4VP) and monolithic column prepared for testing (inset)	57
Scheme 3.1: Synthesis of polyHIPE foams with surface grafted chains of P4VP via a dormant alkoxyamine-containing co-monomer (3.1).....	82
Scheme 3.2: Solution-based kinetic study of the polymerization of P4VP using (3.2).	87
Scheme 3.3: Outline of the Pu sorption/elution flow testing performed on prepared polyHIPE column prototypes	89
Scheme 4.1: Mechanism of Ziegler-Natta polymerization of polyethylene (simplified for clarity), and structure of isotactic polypropylene (inset).....	109

Scheme 4.2: Synthetic approach toward nanosilica grafted with well-defined polyethylene..... 119

LIST OF ABBREVIATIONS

CRP	controlled radical polymerization
ROP	ring-opening polymerization
ROMP	ring-opening metathesis polymerization
MW	molecular weight
HIPE.....	high internal-phase emulsion
polyHIPE.....	polymerized high internal-phase emulsion
VBC.....	4-vinylbenzylchloride
ATRP	atom-transfer radical polymerization
RAFT.....	reversible addition/fragmentation chain transfer polymerization
NMP.....	nitroxide-mediated polymerization
NCA.....	N-carboxyanhydride
HMW	high molecular weight
UHMW	ultra high molecular weight
TPE.....	thermoplastic elastomer
DBS	dielectric breakdown strength
P4VP	poly(4-vinylpyridine)
AIBN.....	azobisisobutyronitrile
SEM.....	scanning electron microscopy
IX.....	ion-exchange

GPC..... gel-permeation chromatography
TEMPO (2,2,6,6-tetramethylpiperidin-1-yl)oxidanyl
PE polyethylene
HDPE..... high density polyethylene
LDPE..... low density polyethylene
LLDPE linear low density polyethylene
PEO..... poly(ethylene oxide)
TGA thermogravimetric analysis
DSC..... differential scanning calorimetry
TEM transmission electron microscopy
SI-ROMP..... surface-initiated ring opening metathesis polymerization
PCO..... polycyclooctene

CHAPTER 1
INTRODUCTION

1.1 Polymer Brushes

Modification of surfaces with polymer brushes has become an intense area of focus since the discovery of synthetic techniques which allow for controlled synthesis of macromolecules.¹ These methods include controlled radical polymerization (CRP), ring-opening polymerization (ROP), ring-opening metathesis polymerization (ROMP), etc. Polymer brushes are thin films which consist of a population of polymer chains physically or chemically associated with a solid surface. Depending on the number of chains per unit area (graft density, σ) and the molecular weight (MW) of the chains, polymer brushes can assume a range of conformations described in the literature as “pancake”, “mushroom”, or “brush” (Figure 1.1).² Formally, the term “brush” only applies when the polymer chains are so densely tethered that they are forced to stretch away from the surface due to the steric interactions between chains (the high graft density regime, Figure 1.1 C) rather than having the spatial freedom to exist as random coils. Colloquially, and throughout this work, the term “brush” is used simply to describe a population of polymer chains tethered to a surface.

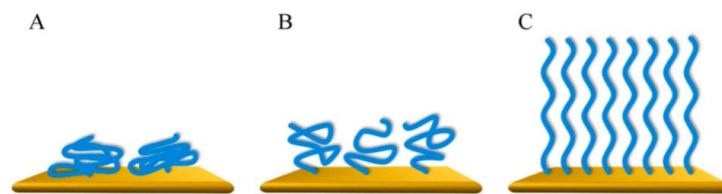


Figure 1.1: Illustration of polymer brush conformations (A) “pancake” (B) “mushroom” and (C) “brush” (reprinted from ref [2], not subject to US copyright)

Synthesis of polymer brushes is generally achieved by one of the four following methods; physisorption, grafting-to, grafting-from, or grafting-through (Figure 1.2). Each approach has some advantages and disadvantages. When physisorption (a physical linkage between the polymer and surface) or grafting-to (a chemical coupling between the polymer and surface) is used, resulting graft densities are typically limited to the “pancake” or “mushroom” regime. Once one chain is attached, it limits subsequent chains from diffusing to and linking with the surface in the immediate vicinity. Higher graft densities can be achieved with grafting-from or grafting-through techniques. In a grafting-from approach, small molecules are added to the surface one-by-one, and a growing polymer brush may not impede the diffusion of further small molecules to the surface. In grafting-through, the situation is nominally different in that the polymerization is not initiated at the surface, but polymerizable functional groups on the surface are quickly incorporated into the growing polymer, resulting in a tethered chain (also having the potential to reach medium and high graft densities).

Physisorption and grafting-to methods have the advantage of attaining a polymer brush in as little as one step. Grafting-from and grafting-through strategies require more synthetic steps but exert much better control over the density of grafted chains, and this level of control allows for the synthesis of any brush morphology which may be desired.

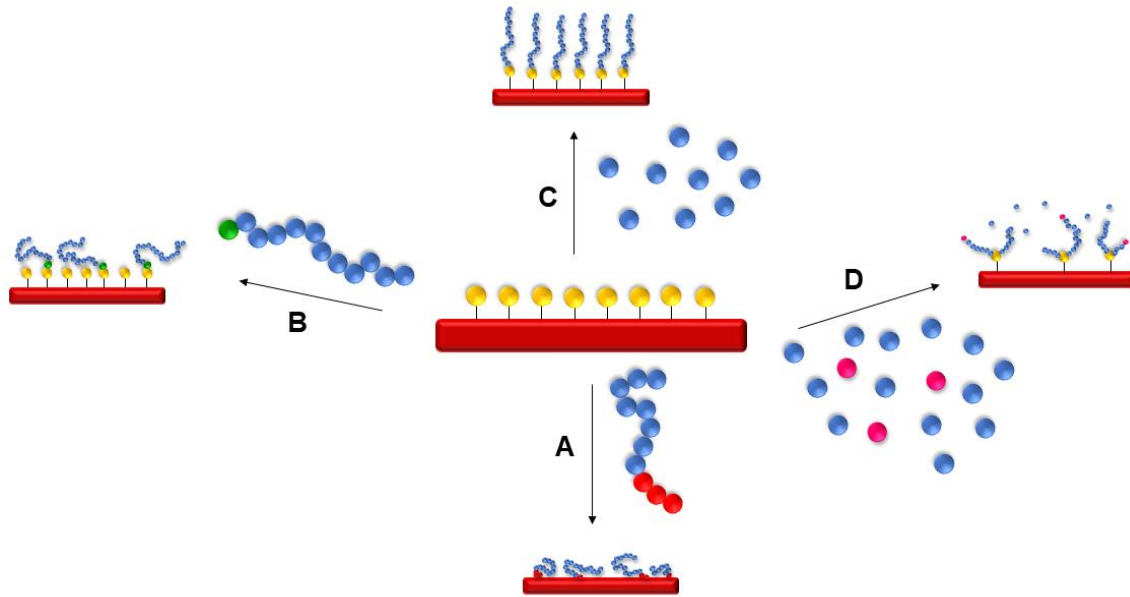


Figure 1.2: Polymer brush grafting techniques (A) physisorption (B) grafting-to (C) grafting-from (D) grafting-through

Polymer brushes prepared using the above methods have recently been used to produce many different types of advanced materials including stimuli-responsive surfaces,³ nanocomposites,⁴⁻⁶ bio-compatible and non-fouling surfaces,⁷ catalytic supports,⁸ surfaces with improved adhesion and wettability,⁹⁻¹⁰ self-assembling nanomaterials,¹¹ bioconjugates,¹² etc. The high level of synthetic control over polymer chemistry and macromolecular weight afforded by advanced polymer synthesis techniques has also allowed for a variety of polymer brush architectures to be prepared which are summarized in Figure 1.3. Brush architecture can have a profound effect on the macroscopic properties of a material, and some of the most elegant examples from the literature using

controlled radical techniques include bimodal brush (either mixed chemistry or molecular weight),¹³ grafted block copolymer,¹⁴ and Janus nanoparticles.¹⁵

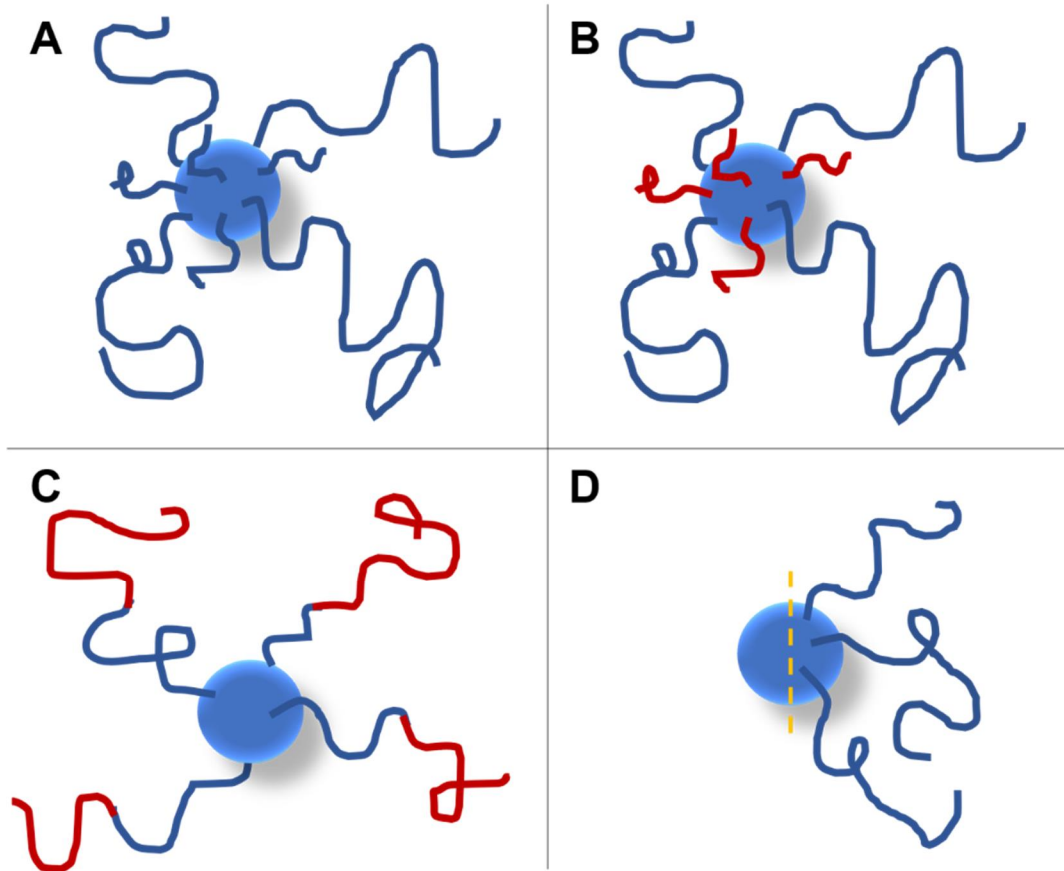


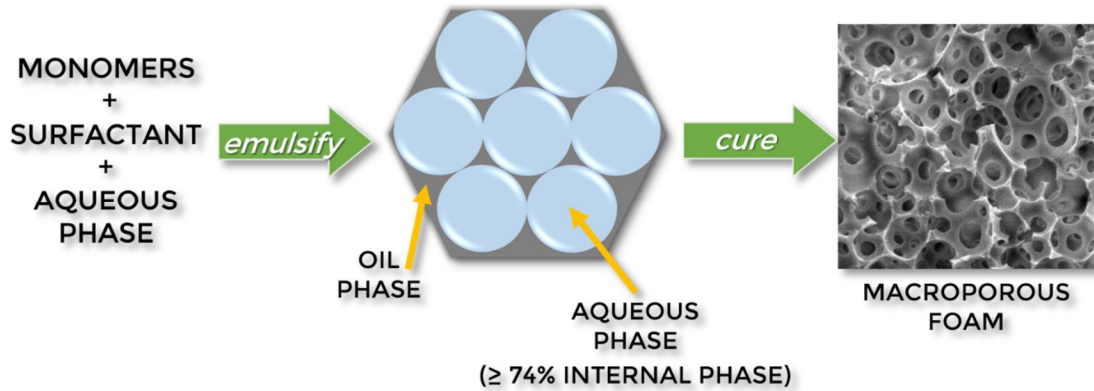
Figure 1.3: Polymer brush architectures (A) bimodal (molecular weight) (B) mixed-bimodal (different chemistries) (C) block copolymer (D) Janus (two faces, or “patchy”)

Combining the brush synthesis approaches with unique architectures enabled by advanced polymer chemistry forms a synthetic “toolbox” which is the basis for designing materials which have properties greater than the sum of their parts, and this motif was the foundation for the new work discussed herein.

1.2 Polymeric High Internal-Phase Emulsion (polyHIPE) Foams

1.2.1 Discovery, Properties, and General Use

PolyHIPE foams are crosslinked porous polymeric materials templated from high internal-phase emulsions (HIPEs). The synthesis of materials now known as polyHIPEs with a characteristic interconnected pore structure was first disclosed in a 1982 patent from Unilever,¹⁶ though the concept of a polymeric foam templated from an emulsion existed earlier.¹⁷⁻¹⁸ This was the first reported method to reliably generate polymeric foams with an interconnected pore structure rather than a closed-cell morphology. To be classified as a HIPE, the emulsion must have greater than or equal to 74% internal phase by volume.¹⁹ In contrast to conventional emulsions, HIPEs have a continuous oil phase and dispersed aqueous phase, and when the oil phase consists of polymerizable small molecules a polymerization initiator can be added to cure the continuous phase to “cure” the oil phase (thus the resulting foam is templated from the emulsion structure). Slow addition of the aqueous phase to the oil phase with constant stirring or applied shear is essential to generate the desired inverse emulsion. All HIPEs also contain some sort of stabilizer (surfactant, nanoparticles, macromolecule, etc.) to help form the emulsion as well as to preserve the structure during curing. A general scheme which outlines the emulsification and curing process is shown in Scheme 1.1.



Scheme 1.1: General outline of polyHIPE synthesis

When the volume fraction of the aqueous phase is sufficiently high (≥ 74 vol %), the dispersed droplets are only separated by a thin monomer film, regions which generate “windows” (holes between voids where the discrete droplets existed in the initial emulsion) upon curing and removal of the aqueous phase. Careful work conducted on polyHIPEs during the late 1980s by Williams and co-workers established the relationship between the cured polyHIPE microstructure and the effects of surfactant concentration, aqueous phase volume fraction, locus of curing initiation (aqueous or organic phase), cross-linker weight fraction, and the corresponding mechanical properties (elastic modulus and yield strength).²⁰⁻²¹ Each of these parameters can be tuned independently of the rest and changes can result in vast differences in the microstructure (closed-cell versus open-cell, dimension of pores and windows) and mechanical properties (very flexible and elastic to very stiff and brittle). Generally, the surface area of conventional polyHIPEs made from the most commonly-used

styrene/divinylbenzene system is fairly low ($20\text{-}50\text{ m}^2\text{ g}^{-1}$),²³ but addition of a porogenic solvent (commonly toluene or chlorobenzene) to the oil phase can increase the surface area dramatically (up to an order of magnitude increase is common) without negatively impacting the interconnected macropore structure.²⁴

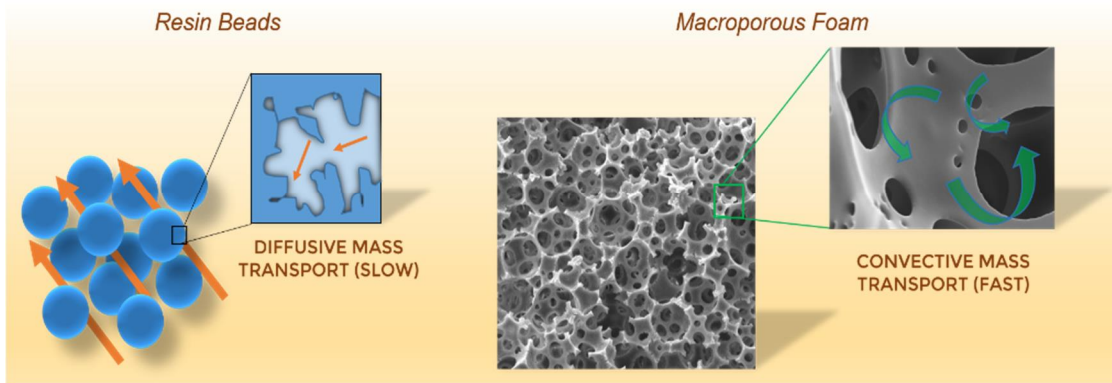


Figure 1.4: Diffusive mass transfer versus convective mass transfer

Early polyHIPEs were explored as bulk sorbents for liquids and gases but quickly attracted the attention of those studying resin-based separations and chemical transformations.²⁵ The interconnected macropore structure lends itself to convective mass-transfer which is a kinetically faster transfer mechanism than diffusion (Figure 1.4). Resin-based materials generally have much higher surface areas than polyHIPE materials and may be endowed with a high degree of chemical functionality which enables the separation or chemical transformation of interest. Liquid flows easily in the interstitial space between spherical resin beads, and bulk liquid flow for these systems is predictable and easy to control. However, the bulk of active sites are located deep within micro- or mesopores on

the resin bead's surface. Inside these pores, the liquid flow is essentially stagnant, and diffusion becomes the dominant mass-transfer mechanism.

In resin systems, long contact times may be necessary to achieve quality separations or a high yield in catalytic reactions. The structural continuity and macroporosity of a polyHIPE foam minimizes the diffusion necessary for the liquid flowing through the structure to contact the surface where chemical residues lie. This results in fast and quantitative contact of the solution with the surface of the foam. For separations, this means better efficiency and little chromatographic overlap and for chemical transformations it means higher yield in a shorter amount of time. It is simple to envision how a polyHIPE might directly replace a resin, especially since polyHIPEs can be formed and cured into any shape or size; constructing columns or other devices where a resin might be used is straightforward. PolyHIPEs are versatile materials whose physical properties (like mechanical strength, or pore structure) can be easily tailored to fit an application. Much more recently, research efforts have focused on tailoring their chemical properties for specific applications.

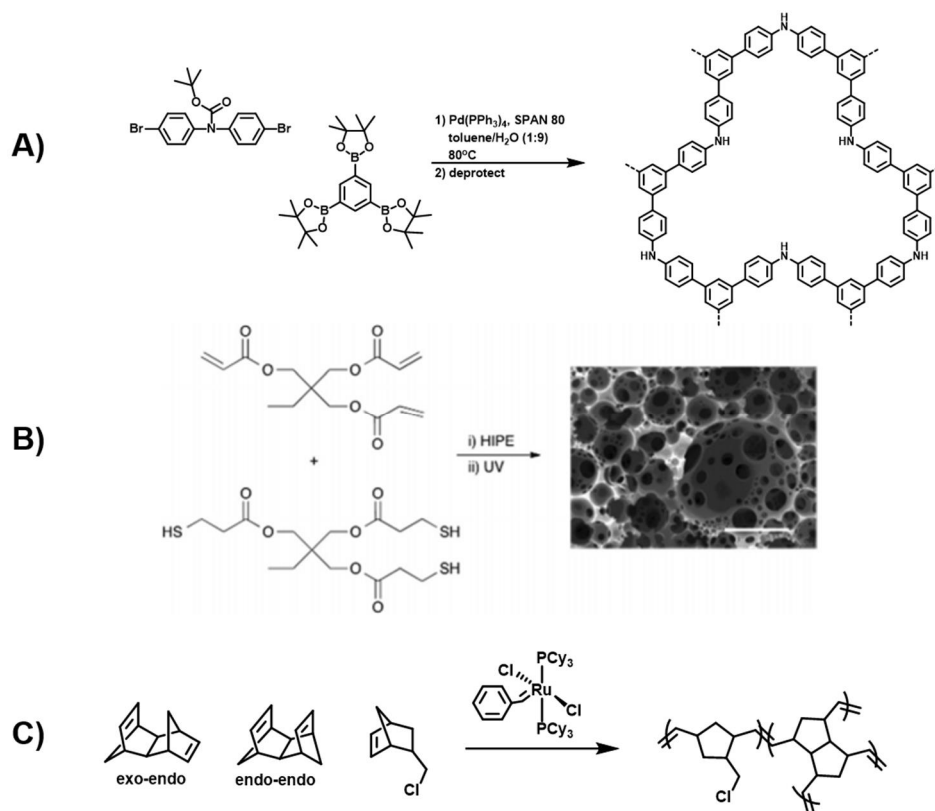
1.2.2 Synthesis and Surface Functionalization Techniques

PolyHIPEs made from comonomers styrene and divinylbenzene in the oil phase are by far the most ubiquitous in the polyHIPE literature, no doubt due to the low cost and abundance of those monomers. Also, styrene and

divinylbenzene strongly segregate from the aqueous phase so it is possible to use very little surfactant to stabilize the HIPE which results in the often-desired interconnected pore morphology and good mechanical properties (more hydrophilic monomers can cause HIPE destabilization, so a higher fraction of stabilizer may be required which may affect mechanical properties).²¹ PolyHIPEs made from other monomer systems have been explored in detail including acrylates, methacrylates, acrylamides, and maleimides.²⁶⁻²⁷ Conveniently, each of these systems can be polymerized via free-radical polymerization, a method for which both organic and water-soluble initiators are cheaply and readily available. Some exotic polyHIPEs have been prepared by Suzuki-Miyaura cross-coupling polymerization, ring-opening metathesis polymerization (ROMP), and thiol-ene/ thiol-yne reactions (Scheme 1.2).²⁸⁻³⁰

The most commonly used emulsion stabilizer is the non-ionic surfactant SPAN 80 (sorbitan monooleate), but many types of stabilizers have been investigated for polyHIPE synthesis including ionic surfactants,³¹ nanoparticles,³²⁻³³ and amphiphilic macromolecules.³⁴ In general, higher fractions of surfactants cause smaller windows and pores so to achieve the typical open-celled morphology, the HIPE should contain less than ~30 wt. % SPAN 80. High weight fractions of small molecule surfactants (>60%) can lead to closed-cell morphologies and poor mechanical properties.¹⁹ Poor polyHIPE mechanical

properties at high surfactant loadings are attributed to inclusion of the surfactant molecules in the organic phase even after curing and removal of the internal phase, lowering the effective cross-link density.^{19,34} HIPEs stabilized with



Scheme 1.2: (A) polyHIPE prepared from Suzuki-Miyaura coupling (idealized structure) (adapted from ref [28], not subject to US copyright) (B) Preparation of thiol-acrylate polyHIPE (reproduced with permission from ref [29]) (C) PolyHIPE prepared by ROMP (adapted with permission from ref [30])

amphiphilic particles (known as Pickering emulsions) have been extensively studied, especially to overcome the detrimental effects that high loadings of small molecule surfactants can impose.³⁵ The amphiphilic particles preferentially migrate to and assemble at the oil/water interface creating very stable emulsions which are resistant to Ostwald ripening (small drop coalescence favoring the

formation of large droplets). The reason for the enhanced stability of Pickering-stabilized HIPEs is that the desorption energy of a particle can be up to three orders of magnitude greater than the desorption energy of a small surfactant molecule. Pickering-stabilized HIPEs have a much narrower void size distribution because of this resistance to coalescence, and some particles remain at the water/oil interface where they can be a valuable synthetic handle for post-curing modification. More recently, high-modulus polyHIPEs with an interconnected pore structure were synthesized with just 0.5 wt.% amphipathic hyperbranched macromolecules.³⁴

PolyHIPEs decorated with surface functionality have been prepared in several different ways. Incorporation of a functional comonomer in the HIPE has been common since the early days of polyHIPEs. For example, 4-vinylbenzyl chloride (VBC) or acrylic acid are a popular comonomers to include in polyHIPEs because the chloro/acid groups are good synthetic handles to further functionalize polyHIPEs post-curing.³⁶⁻³⁷ Presence of hydrophobic comonomers (e.g. VBC) does not significantly disrupt the stability of the HIPE and these can be used a high weight fractions in the HIPE. Incorporation of hydrophilic/polar comonomers (i.e. acrylic acid or vinylpyridine) can be problematic at high loadings because there is the potential they could destabilize the emulsion, so stabilizer content must be optimized for each new formulation.³⁸ Post-curing

sulfonation of surface aromatic rings can be quite exhaustive and is useful for improving the hydrophilicity of polyHIPEs.³⁹ Click chemistry, specifically the Huisgen 1,3-dipolar cycloaddition, has also been used to affix small molecules to the surface of polyHIPEs.⁴⁰

In instances where a high degree of surface functionality is desired, polyHIPEs with surface-bound polymer brushes have been prepared. Polymer brushes have been prepared from surface-initiated free radical polymerization,³⁶ but often more control of grafted polymer MW is desired. PolyHIPEs with surface-grafted polymer brushes prepared by atom-transfer radical polymerization (ATRP) were first prepared in 2003.⁴¹ PolyHIPEs with surface-bound ATRP initiators are generally prepared by incorporating a comonomer with a pendant bromoester group (an ATRP initiator) which does not participate in the foam curing polymerization. After curing, these groups can be activated in the presence of a copper catalyst to initiate polymerization from the surface of the foam. Because ATRP is a versatile CRP technique, many classes of monomers are compatible with this type of polymerization method, so monomers with a wide range of chemical functionality can be implemented.⁴²⁻⁴⁴

Reversible addition-fragmentation chain transfer (RAFT) polymerization has also been used to prepare polyHIPEs with surface-grafted polymer brushes.⁴⁵⁻⁴⁶ RAFT has much of the same versatility of ATRP as a CRP technique

without the need for metal catalysts but using RAFT polymerization to grow a brush from the surface is not as straightforward as ATRP. A RAFT agent incorporated into the initial emulsion will unavoidably participate in the radical polymerization used to cure the polyHIPE. Incorporation of a RAFT agent into the initial HIPE was successful in grafting polymer chains from the polyHIPE surface (essentially a chain-extension reaction), but varying concentrations of RAFT agent in the emulsion were found to have a significant impact on the pore morphology and flow characteristics of the resulting monoliths.⁴⁶ Also, it is difficult to predict and analyze what fraction of RAFT agents end up on the surface of the foam to perform the surface-initiated RAFT polymerization. RAFT agents have also been attached to the polyHIPE surface as a post-curing modification step via EDC (1-ethyl-3-(3-dimethylaminopropyl)carbodiimide) coupling which allowed for better characterization of the grafted RAFT agent content and resulted in polyHIPEs with a dense covering of poly(N-isopropylacrylamide) which had excellent water uptake properties.⁴⁷

Polymer-grafted PolyHIPEs have also been prepared by ring-opening polymerization of N-carboxyanhydride (NCA) derivatives initiated from surface-bound amino groups,⁴⁸ surface-initiated ROMP,⁴⁹ and by surface-initiated nitroxide-mediated polymerization (NMP) which is discussed in detail in Chapter 3 of this work. Heise and co-workers reported a clever approach for

incorporating a polymer brush onto the surface of polyHIPEs by tethering polymer-grafted nanoparticles to the surface of polyHIPEs via click chemistry or electrostatic interaction.⁵⁰ Polymer-grafted particles are much more straightforward to prepare which adds a high degree of adaptability to this approach. Surprisingly, the authors demonstrated uniform surface coverage of the polyHIPE with the polymer-grafted nanoparticles. Cameron, Battaglia, and co-workers described what may be the most robust, yet simple synthesis of polymer grafted polyHIPEs.⁵¹ Amphiphilic block copolymers were used to stabilize the HIPE, and after curing, the hydrophobic block becomes physically entangled within the cured matrix, leaving the hydrophilic block exposed on the polyHIPE surface. In principle, this approach could be used to make functional polymer-grafted polyHIPEs in one step.

1.2.3 Applied PolyHIPEs

Foundational work on polyHIPEs over the past three decades has enabled the rich development of functional polyHIPEs which have been applied in many different areas. Specifically, polyHIPEs have excelled as scaffolds for separations and catalysis because of their mass transfer properties and ease of incorporating chemical functionality as described above. Research towards developing these materials has accelerated since the principles of Green Chemistry were delineated by Anastas and Warner in 1998.⁵² Chief among these principles where

advanced polyHIPE materials can contribute are: designing processes for efficiency, using catalytic reagents rather than stoichiometric reagents, reducing derivatization steps (e.g. installing protecting groups), and designing chemicals which are safe to use and minimally toxic. A brief summary of recent advances of polyHIPEs used for separations and chemical transformations, as well as some interesting developments of polyHIPEs for 3D printing and biological scaffolds is offered here in light of these principles.

PolyHIPEs have been investigated for heavy metal removal from water by way of metal complexation or ion-exchange. As stated before, early reports of separations using polyHIPEs relied on foams with small molecules tethered to the surface (e.g. phosphonic or sulfonic acid groups) and were used to demonstrate successful uptake of ions like Eu(III), Fe(III), Cu(II), and Pb(II).⁵³ As expected, the foams had higher uptake kinetics than a resin with similar chemical functionality, but simple acid groups lack selectivity. A later study focused on incorporating chelating ligands rather than acid groups on the surface of the polyHIPE to take advantage of the fast uptake kinetics while perhaps improving selectivity of chelating sites.⁵⁴ PolyHIPEs with ion-exchange sites were also shown to have excellent uptake kinetics compared to commercial resins for a variety of ion-exchange separations (Fe(III), Pu(IV), Pb(II), As(V), Ni(II), Cr(VI), NO₃⁻).^{36,55-58} PolyHIPEs have been developed as stationary phases for size-

exclusion chromatography of nanoparticles⁵⁹ as well as for protein purification⁶⁰ based on the incorporation of weak ion-exchange sites. Highly oleophilic polyHIPEs have shown promise for oil/water separations as illustrated in Figure 1.5.⁶¹

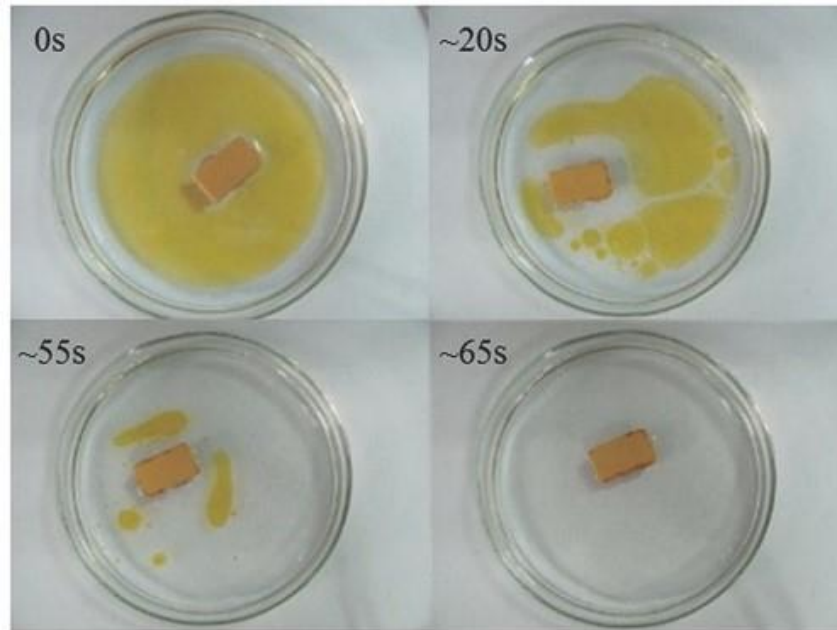


Figure 1.5: PolyHIPE absorption of n-hexane (dyed with Sudan 1) over time. Reproduced with permission from ref [61].

The same mass transfer properties which make polyHIPEs desirable scaffolds for separations also apply to chemical transformations performed by supported catalysts. There are many excellent reviews about the development of heterogenous catalysis,⁶²⁻⁶⁴ but within those there are relatively few reports of polyHIPEs as catalytic supports. Foam materials retain many of the same desirable features as other catalysts supports (i.e. soluble polymer chains, microporous resins, etc.) with the added benefit that the cross-linked foams

require no precipitation step, or in the case of a monolith, no filtration to recover and reuse the supported catalyst. These features make polyHIPEs a nearly ideal substrate to investigate for the development of “green” syntheses.

Much of the existing literature on polyHIPEs as catalyst supports focuses on supported metal nanoparticles. Metal nanoparticles have interesting physicochemical properties due to their small size and catalyze a wide variety of chemical reactions. The main challenge in using nanoparticles as catalysts is preventing agglomeration, which destroys much of the desired catalytic activity. Also, this makes them difficult to recover and recycle effectively. Palladium nanoparticles have been prepared *in situ* within polyHIPEs (Pd@polyHIPE) and were found to be excellent catalysts for hydrogenation, and Suzuki-Miyaura and Mizoroki-Heck cross-couplings.⁶⁵⁻⁶⁷ PolyHIPE-supported gold nanoparticles prepared similarly to the Pd@polyHIPE systems were efficient oxidation catalysts.⁶⁸ In most cases, the supported nanoparticles catalyzed the desired reactions just as efficiently as commercial catalysts, but could be used in flow-through set-ups, or were more easily recycled than the commercial supported catalysts.

Enzymes, nature’s most selective catalysts, were supported on polyHIPEs to study whether the enzymes could be used more efficiently and recycled.⁶⁹ Specifically, the activity of immobilized lipases *Candida rugosa* and *Thermomyces*

lanuginosus were studied for esterification and hydrolysis reactions. Typically, reactions catalyzed by free enzymes are slow due to slow diffusion of the cumbersome enzyme molecule in solution and recovery/reuse of the enzyme can be challenging. In this study, the immobilized enzymes performed esterification and hydrolysis reactions with greater efficiency and good recyclability was demonstrated.

Lately, the leading edge of polyHIPE research has focused on injecting polyHIPEs (figuratively and literally) into the field of medicine and regenerative therapy. In this sphere, polyHIPEs have been investigated as shape memory materials, 3D cell-growth media, and HIPEs as “emulsion inks” for 3D printing. Shape memory polyHIPEs were prepared from acrylate and methacrylate monomers bearing long alkyl side chains.⁷⁰ The crosslinker incorporated into HIPE sets the permanent shape, and the temporary shape is reversibly held by crystallization of the alkyl sidechains incorporated (Figure 1.6). In principle, this type of system could be used to install implants of a small dimension into a patient, and then the implant would return to its permanent shape upon heating (or reaching physiological temperature). PolyHIPEs which are completely biodegradable and biocompatible were developed by Cameron and co-workers based on poly(caprolactone) derivatives which may also find uses in implants.⁷¹ A study from the same group demonstrated successful culturing of human

endometrial cells on a polyHIPE scaffold.⁷² The benefit of a 3D cell scaffold is two-fold. First, the 3D shape helps to approximate the structure of human tissue much better than conventional 2D monolayer cultures, closely imitating the microenvironment which cells experience in real tissue. This is a target for medical researchers wanting to study cell/tissue systems in vitro. Second, 2D cultures limit the number of cells which can be propagated within a certain area, and the 2D configuration is not conducive to maintaining the native function of the cell. A 3D scaffold overcomes both of those issues.

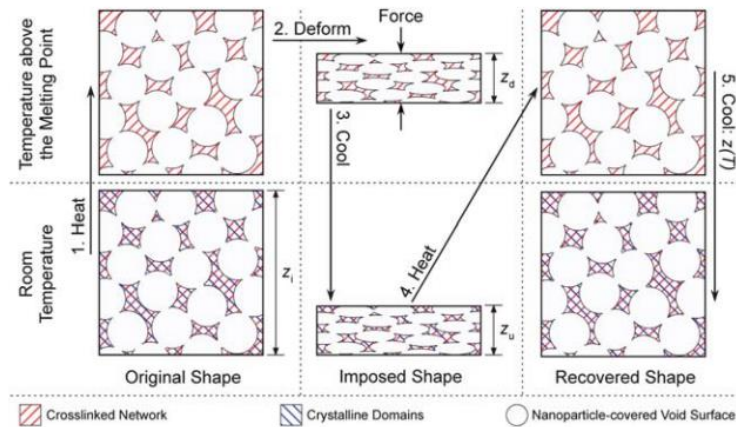


Figure 1.6: Illustration of thermomechanical deformation and recovery in shape memory polyHIPEs (reproduced with permission from ref [70]).

Photocurable emulsion “inks” for 3D printing were developed by Cosgriff-Hernandez and co-workers as the first part in a series of elegant work aimed at developing printable bone implants and wound dressings. In the first iteration of this work, rheologically-tuned polyHIPEs were prepared from low-viscosity poly(propylene glycol) dimethacrylate (PPGDMA) and high-viscosity

diurethane dimethacrylate (DUDMA).⁷³ Understanding how to tune the emulsion viscosity to avoid spreading or deformation of the extruded emulsion before curing was vital to forming hierarchically porous structures. An extension of this work saw the incorporation of calcium phosphate nanoparticles into a printable HIPE with a propylene fumarate dimethacrylate (PFDMA) backbone.⁷⁴ The resulting polyHIPEs retained the injectable (biocompatible) and quick-curing aspects of the previously described system and the incorporated calcium nanoparticles rendered the printed polyHIPE osteoinductive. A similar polyHIPE system was developed for printable advanced wound dressings doped with kaolin which are hemostatic and absorbent.⁷⁵

1.3 Polymer Nanocomposites

Nano-sized fillers blended with polymers comprise what are known as polymer nanocomposites. When properly compatibilized with the polymer matrix, the incorporated sub-micron sized fillers bestow properties onto the nanocomposite which are not realized by the incorporation of larger fillers, even those of identical chemical composition.⁷⁶ A classic example of these disparate properties is the comparison between graphite and carbon nanotubes. Though they are chemically identical, the nanotubes have a Young's modulus nearly an order of magnitude greater than graphitic carbon fibers attributed to their unique shape and dimension.⁷⁷ Simply mixing a nanofiller with a polymer matrix is not

sufficient to obtain homogenous dispersion of the nanofiller throughout the polymer in most cases (Figure 1.7). When there is interfacial incompatibility between the filler and matrix, large agglomerates which have a deleterious effect on the composite properties are the dominant morphology. These agglomerates are unlikely to be overcome by more intensive processing, especially at high loadings.⁷⁸ Grafting a matrix-compatible polymer brush on the nanofiller surface can overcome these challenges.

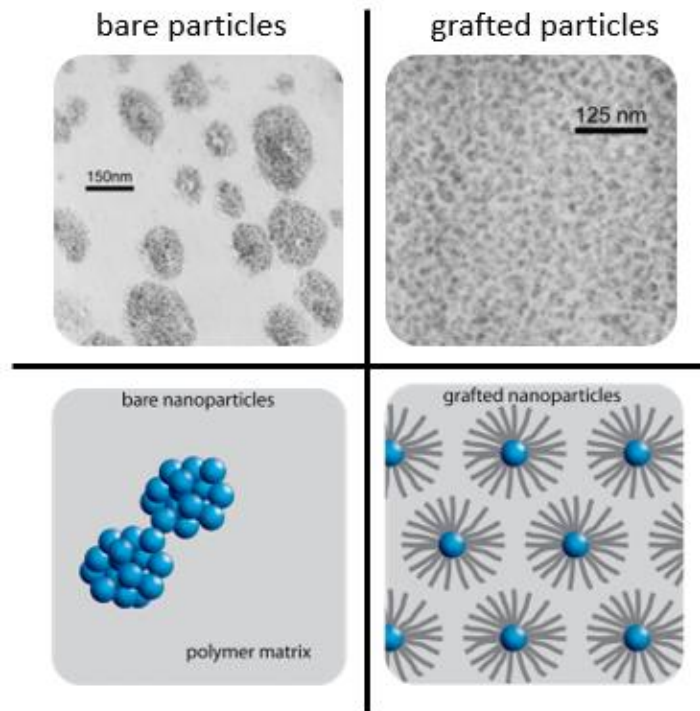


Figure 1.7: Dispersion states of bare nanoparticles versus polymer-grafted nanoparticles in a polymer matrix (in gray)

Often, the aim when synthesizing polymer nanocomposites is to achieve homogenous dispersion of the nanofiller throughout the matrix. Property enhancements are most pronounced when there is a large interfacial volume

between the polymer matrix and the filler (Figure 1.8). This is because load transfer (i.e. thermal, mechanical) between the bulk polymer and filler happens at this interface. So, in addition to any innate properties possessed by the nanofiller, the small size guarantees a large filler surface area where load transfer can occur. Resulting nanocomposites thus retain the processability of the polymer while gaining the robust properties of the filler.

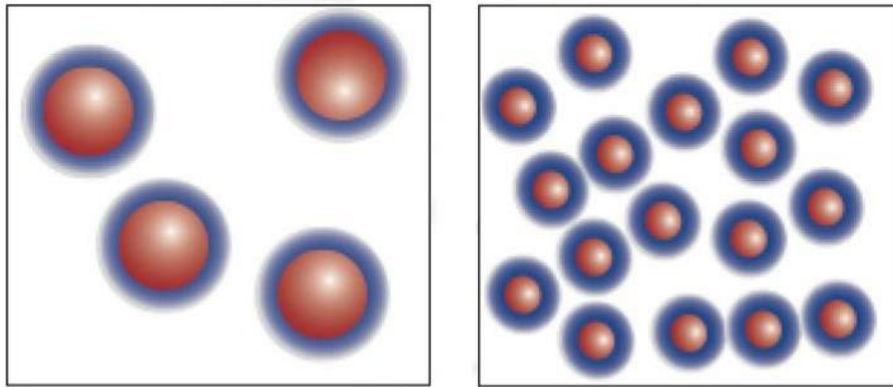
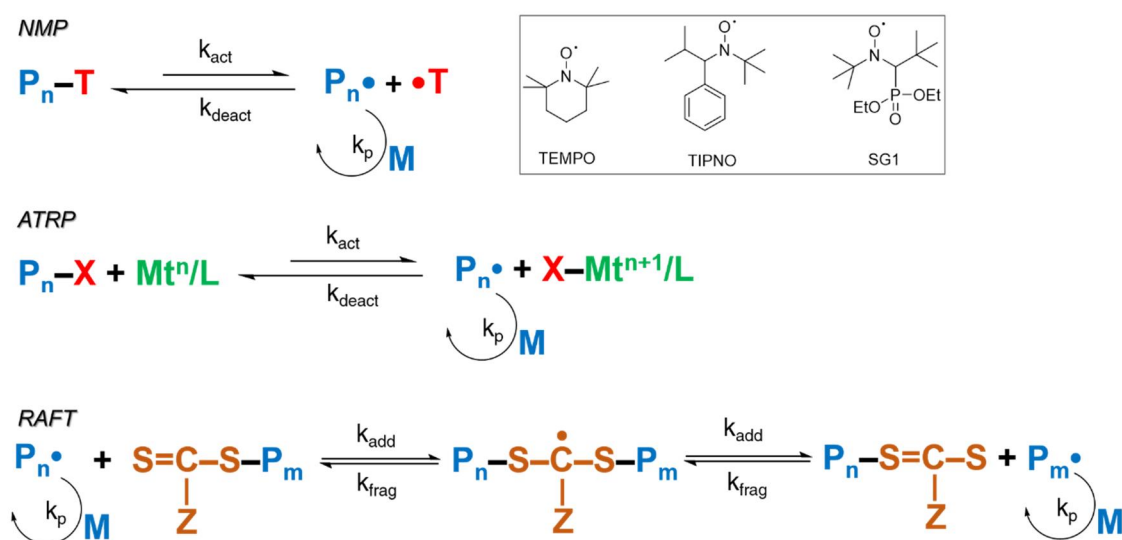


Figure. 1.8: Illustration of relative interfacial volume (in blue) between larger and smaller fillers in a polymer matrix (reproduced with permission from ref [76]).

Recent synthetic efforts to create thermodynamically benign interactions between nanofiller surfaces and polymer matrices has seen the development of synthetic strategies which exert a high degree of control over nanofiller dispersion state. This synthetic control has allowed for the development of nanocomposites with excellent mechanical, thermal, optical, dielectric, etc. properties.

1.3.1 Synthesis of Polymer Brushes via Controlled Radical Polymerization

Many methods of polymer attachment to nanofillers have been investigated and are briefly discussed here. By far the most popular class of polymerization methods is the controlled radical polymerization techniques which include nitroxide-mediated polymerization (NMP), atom transfer radical polymerization (ATRP) and reversible addition-fragmentation chain transfer polymerization (RAFT). Each of these techniques can emulate the characteristics of a living polymerization, leading to polymers with narrow dispersity (\mathcal{D}) and predictable molecular weight by virtue of controlled polymerization kinetics. Though each technique shares these traits, the mechanisms and synthetic conditions for each are quite different.



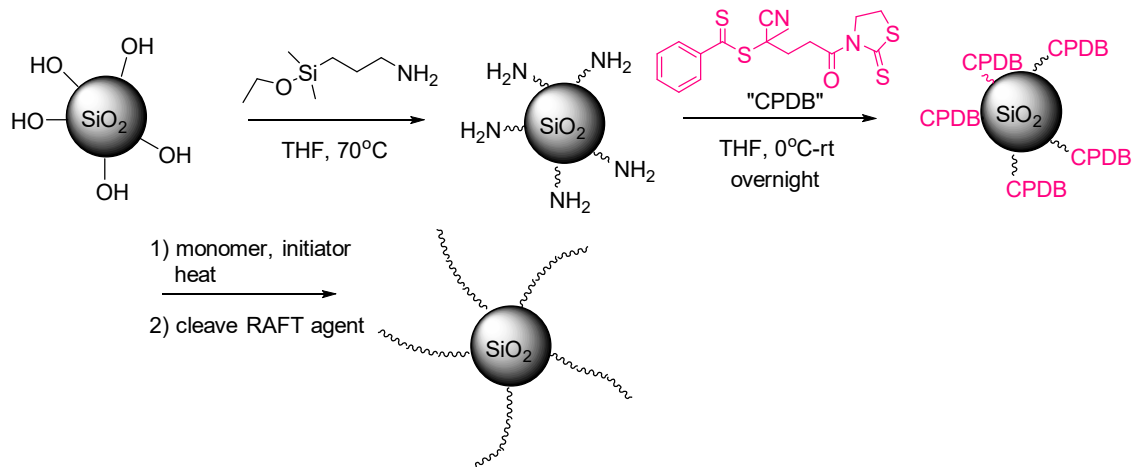
Scheme 1.3: Mechanisms of monomer addition for NMP, ATRP, and RAFT polymerizations and some common NMP agents (inset) Initiation and termination steps have been excluded for brevity.

NMP gains its ability to mediate a “living” polymerization from a thermally labile alkoxyamine which is reversibly and homolytically cleaved from the polymer chain end at high temperature.^{79,80} In good systems, the rate of deactivation is faster than the rate of homolysis which allows for each growing chain to grow at approximately the same rate (Scheme 1.3, top). This is the basis for the narrow Đ which can be achieved. Early NMP work when (2,2,6,6-tetramethylpiperidin-1-yl)oxyl (TEMPO) was the nitroxide of choice was limited to styrenic monomers because of the relative stability of the styrenic radical compared to acrylic or methacrylic monomers (where faster, uncontrolled polymer growth could occur).⁸¹ More recently, alkoxyamines such as N-tert-butyl-1-diethoxyphosphoryl-N'-oxidanyl-2,2-dimethylpropan-1-amine (SG1) and 2,2,5-Trimethyl-4-phenyl-3-azahexane-3-nitroxide (TIPNO) have allowed for controlled polymerization of some acrylic and methacrylic monomers. NMP is a valuable grafting technique because of its temperature orthogonality to ATRP and RAFT.⁸²⁻⁸³

ATRP was discovered by Matyjaszewski and co-workers in the mid-1990s and has since been one of the most versatile polymer synthesis techniques.⁸⁴ The controlled nature of the polymerization comes from a reversible oxidation of a metal catalyst which activates or deactivates the propagating species (Scheme 1.3). Similarly to NMP, the deactivation step is much faster than the activation

step which ensures that each growing polymer chain has the same statistical probability to add a repeat unit. Because of ATRP's ability to polymerize many different classes of monomers, it has been extensively investigated for surface modification.⁸⁵⁻⁸⁶

RAFT has much of the same versatility as ATRP including the ability to polymerize many different classes of monomers, mild reaction conditions, and the added benefit that no metal catalyst is required. The mechanism harnesses the chain transfer ability of dithioesters or trithiocarbonates (most commonly) to establish an equilibrium which exerts excellent control over the polymerization because the rate of chain transfer is much greater than the rate of propagation, giving each growing chain a statistically equal probability of growing.⁸⁷ In nanocomposites, RAFT has an advantage for making very well-defined grafted surfaces. RAFT agents are typically highly-colored (usually orange, yellow, or pink), which makes characterizing the surface density via UV-Visible spectroscopy (UV-Vis) very simple. A method of RAFT agent attachment to silica nanoparticles developed in our group (Scheme 1.4) has seen widespread use throughout the past decade.⁸⁸ The ability to carefully tune the number of chains per unit area as well as to precisely control the MW of the grafted polymer has allowed for very careful investigation of nanocomposite properties which are discussed in detail below.



Scheme 1.4: Synthesis of attachment of RAFT agent attachment and surface-initiated polymerization

1.3.2 Nanofiller Dispersion and Nanocomposite Properties

To achieve predictable and well-controlled dispersion of nanofiller throughout a polymer matrix, having control over the grafted chain MW and graft density is essential. Intuitively, it seems that if a nanofiller is coated in a polymer brush that is chemically identical to that of the desired matrix polymer, one might expect that it would be thermodynamically favorable for the nanofiller to mix with the matrix, as there should be no energetic penalty for a polymer mixing with itself. However, it has been demonstrated that when $N^{\text{graft}} \ll N^{\text{matrix}}$ and $\sigma^2 N^{\text{matrix}} \gg 1$ (where N is the chain length and σ is the brush graft density), the matrix polymer chains cannot wet the brush interface. This behavior, known as autophobic dewetting, is caused by a high osmotic pressure cost of high MW polymers infiltrating a dense brush (Figure 1.9).⁸⁹ By controlling the brush density and MW it is possible to overcome this effect, and the surface-initiated

RAFT technique developed in our group allows for exquisite control over the wetting behavior, and consequently, nanofiller dispersion.

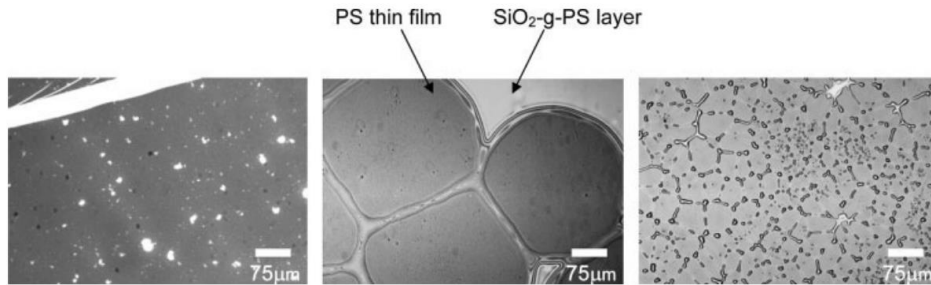


Figure 1.9: Wetting behavior of polystyrene (PS) thin films on a layer of PS-g-SiO₂. PS MW= 44,200 g/mol (left) 92,000 g/mol (middle) 252,000 g/mol (right) (Reproduced with permission from ref [89])

By manipulating the graft density and MW with respect to the polymer matrix of interest, it is possible not only to have the brush of the nanofiller entangle with the matrix, but to reliably and predictably obtain a variety of self-assembled filler morphologies (Figure 1.10).⁹⁰ A morphology diagram of these findings was constructed, and the observed morphologies (sheets, strings, clusters, homogeneous dispersion) represent an exciting advance in self-assembled nanocomposite anisotropy on the nanoscale. Some limitations to this approach arise when the MW of the matrix of interest is sufficiently high that CRP techniques may not facilitate the controlled growth of polymers in the high MW (HMW) or ultra-high MW (UHMW) regimes. As seen in Figure 1.10, fine control of the grafted chain MW ($\bar{D} \approx 1$) is critically important to achieving the desired dispersion state.

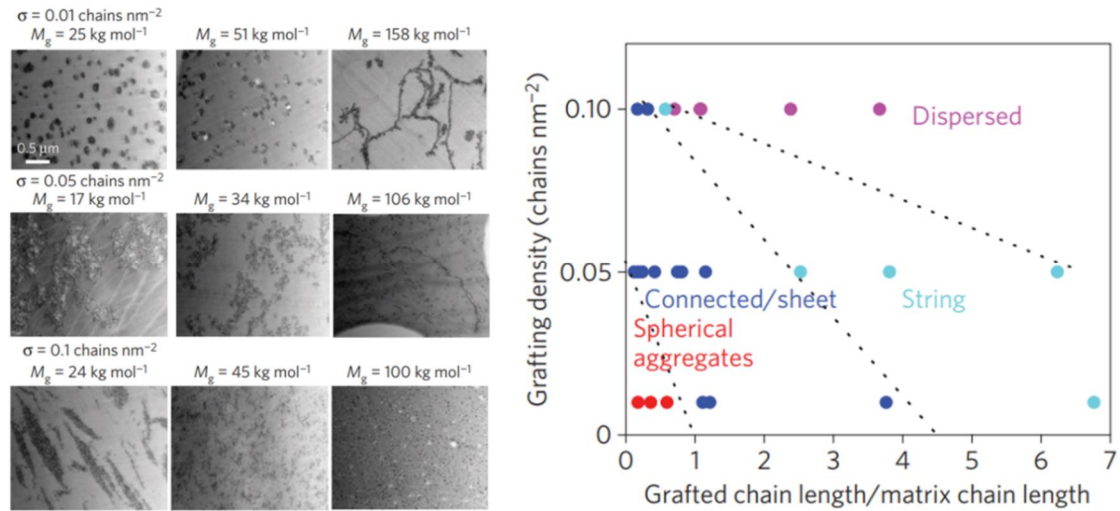
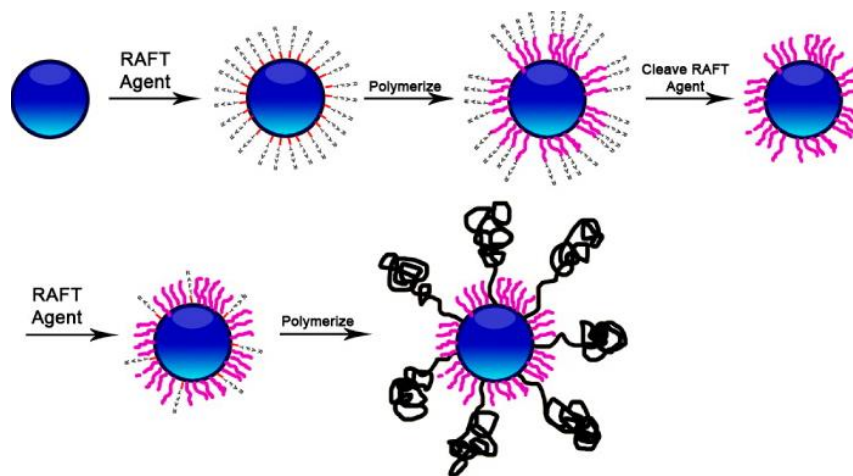


Figure 1.10: Experimentally determined morphology diagram of PS-g-SiO₂ in PS matrix (right) and transmission electron micrographs (left) of PS-g-SiO₂ of varying MW and σ in PS matrix (MW=142 kg/mol) (Reproduced with permission from ref [90]).

RAFT polymerization enables the synthesis of advanced polymer architectures which translates to advanced brush architectures in polymer nanocomposites. To overcome the issue of dispersing nanoparticles in HMW matrices, a bimodal brush synthesis approach was developed.¹³ A densely-tethered “short brush” has the effect of screening core-core van der Waals attractions which are the driving force for particle agglomeration. A sparsely tethered “long brush” provides matrix compatibility, and the ability to use relatively dilute brushes means that the autophobic dewetting observed when nanocomposites are made with densely tethered brushes is overcome. In essence, this approach decouples the entropic and enthalpic interfacial interactions which jointly dictate nanofiller dispersion.



Scheme 1.5: Generalized synthesis of bimodal brush nanoparticles (Reproduced with permission from ref [13])

The first examples of bimodal brushes were “bimodal” in the sense that there were two distinct polymer brushes which differed in molecular weight, but bimodal brushes in which the two brushes are different chemistries are possible to synthesize and use in nanocomposites without having a negative effect on the dispersion state.⁹¹ From a design standpoint, this opens up many possibilities for incorporating functional ligands into the short brush which also serves to screen core van der Waals attractions while the long brush provides matrix compatibility. This synthetic toolbox has created a thriving discovery space for advanced nanocomposites.⁹²

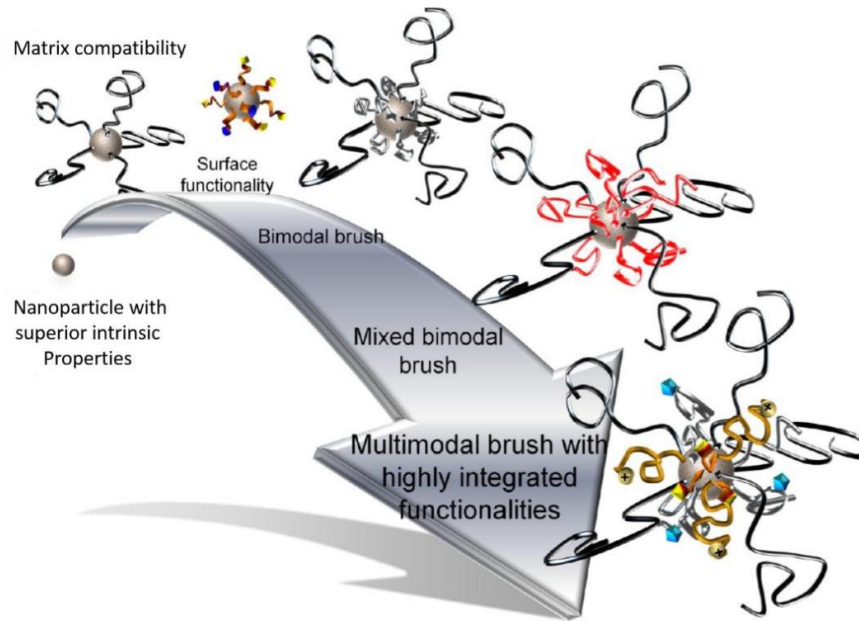


Figure 1.11: Evolution of polymer grafted nanofillers from simple to complex (reproduced with permission from ref [92])

Recently, many types of nanoparticle substrates have been investigated in addition to silica including other metal oxides,⁹³⁻⁹⁶ CdSe quantum dots,⁹⁷ gold,⁹⁸⁻⁹⁹ carbon materials including graphene oxide and carbon black,¹⁰⁰⁻¹⁰¹ bionanoparticles,¹⁰²⁻¹⁰³ and polymers.¹⁰⁴⁻¹⁰⁵ The ability to synthesize well-defined polymer brushes on a variety of nanomaterials has promoted tremendous growth in this field throughout the past decade. Some examples of exceptional material properties derived from polymer-grafted nanomaterials are offered here.

An attractive feature of commodity glassy polymers is their mechanical sturdiness. With the discovery that bimodal brushes could facilitate improved dispersion of nanosilica compared to a monomodal system,¹³ the mechanical

properties of so-prepared nanocomposites were studied and had improved glassy-state storage moduli (measured by dynamic mechanical analysis) and elastic moduli (measured by nanoindentation) attributed to better matrix/brush entanglement.¹⁰⁶ Thermoplastic-elastomer (TPE) films formed from silica nanoparticles grafted with a block copolymer of poly(butylacrylate-*b*-styrene) where butyl acrylate formed the rubbery block and styrene the glass block exhibited an tensile strength $\sim 1.4x$ that of a conventional TPE.¹⁰⁷

Nanocomposites with superior optical properties were prepared by dispersing TiO₂ nanoparticles in an epoxy matrix.⁹³ The resulting composites showed an increase of 0.3 in the refractive index while minimizing scattering by good dispersion of the nanoparticles. A similar study was conducted with indium tin oxide demonstrated up to 90% transparency in the visible region while improving UV absorption of the composite.⁹⁴ More recently, photonic films with tunable reflected colors and cross-linked silica layers were prepared from block copolymers.¹⁰⁸

Bimodal grafted nanoparticles with enhanced dielectric breakdown strength (DBS) were prepared with surface ligands of anthracene, thiophene, and terthiophene combined with a poly(glycidyl methacrylate) matrix-compatible brush.¹⁰⁹ AC dielectric breakdown strength of the composite was improved up to 35% by simply tuning the surface ligands and modifying the silica volume

percent in the composite. A similar study also investigated the effect of ferrocene as the electron-trapping moiety.⁹¹

Looking forward, the next major advancements in composite systems are likely to come from a combination of the arrangements of particles within a nanocomposite in addition to their physicochemical properties. Already, there are a few examples in the literature which support the idea that where particles are (or aren't) located in a composite can have major implications for the bulk properties of the material. Polymer films prepared from poly(methyl acrylate) (PMA) grafted on silica NPs were tested for their ability to separate a mixture of CO₂ and CH₄, a common separation of interest.¹¹⁰ By controlling the graft density and MW of the grafted polymer (and ensuring the absence of any free polymer), the free volume of the composite could be tuned. Simulations suggested that the ordering of particles in the composite created regions of low polymer density in the interstitial spaces between particles. The resulting changes in free volume in the composite had a sizable impact on the permeability of the membrane and represents the ability to tune the permeability in a unique way.

Templating nanoparticle ordering by polymer crystallization represents another recent advance which leverages the arrangement of nanoparticles within a composite.¹¹ Poly(methyl methacrylate) grafted SiO₂ NPs were dispersed in poly(ethylene oxide) which was then isothermally crystallized. In the resulting

composite, the grafted NPs ended up in the interlamellar regions in the semicrystalline polymer. Interestingly, the modulus difference between a composite where the particles were randomly dispersed versus the ordered composite (at the same silica loading) was nearly an order of magnitude. This work begins to fill a void in the nanoscience community which ultimately aims to have nanomaterials elegantly self-assemble within a hierarchy of scales which may result in materials with exquisite properties.

1.4 Dissertation Outline

This dissertation focuses on the design, synthesis, and characterization of polymer brushes on foam and nanoparticle substrates for two purposes, respectively; plutonium purification and nanofiller compatibility in polyethylene matrices. The principles discussed here in Chapter 1 guided the design of the polymer brush materials discussed in Chapters 2-4 and new understanding of how to synthesize polymer brushes which act as functional interfaces was realized.

Chapter 2 focuses on understanding the mass-transfer differences between a polyHIPE and resin material and whether a polyHIPE system may be a viable material for plutonium separations. PolyHIPE foam monoliths with grafted poly(4-vinylpyridine) (P4VP) made from a simple UV-initiated free radical polymerization were prepared and tested for their plutonium sorption and

elution characteristics in comparison to a commercial resin. The foam materials exhibited very narrow elution profiles but had low plutonium capacities. The low capacity was attributed to a penetration gradient of the UV-light used to initiate the surface polymerization into the opaque monoliths.

Chapter 3 expanded on the work from Chapter 2, but a new synthetic approach to make polyHIPE foams with much more uniformly grafted P4VP brushes was developed. The capacities of the polyHIPE monoliths prepared using this new approach exceeded the capacity of the commercial resin based on both mass and volume (an exciting result due to the low density of the polyHIPEs). The narrow elution profiles were maintained, and the polyHIPE materials were investigated for their recyclability and stability, an important parameter because of the cost and harsh conditions of the plutonium separation. The polyHIPEs proved stable over multiple plutonium purification cycles, indicating that the polyHIPEs represented an efficient alternative to the commercial resin currently used for the separation.

Chapter 4 is a departure from the polyHIPE foam materials, but an extension of the pioneering nanocomposites work done in our group. Much of the earlier nanocomposites work was done in materials synthesized by radical polymerization. One of the biggest classes of commodity materials which has been somewhat underexplored in the field of nanocomposites is polyethylene.

This is because of the synthetic challenge of synthesizing well-defined polyethylene as well as polyethylene polymer brushes. As a result, there are only a few examples reported in the literature of polyethylene nanocomposites. We have developed an approach using surface-initiated ROMP to prepare well-defined linear polyethylene/silica nanocomposites. The synthesis, control of synthetic parameters, and characterization of these materials are discussed in detail.

1.5 References

- [1] Barbey, R.; Lavanant, L.; Paripovic, D.; Schuwer, N.; Sugnaux, C.; Tugulu, S.; Klok, H.-A. Polymer brushes via surface-initiated controlled radical polymerization: synthesis, characterization, properties, and applications. *Chem. Rev.* **2009**, *109*, 5437–5527.
- [2] Zoppe, J. O.; Ataman, N. C.; Mocny, P.; Wang, J.; Morales, J.; Klok, H.-A. Surface-initiated controlled radical polymerization: state-of-the-art, opportunities, and challenges in surface and interface engineering with polymer brushes. *Chem. Rev.* **2017**, *117*, 1105–1318.
- [3] Zhai, L. Stimuli-responsive polymer films. *Chem. Soc. Rev.* **2013**, *42*, 7148–7160.
- [4] Kumar, S. K.; Jouault, N.; Benicewicz, B. C.; Neely, T. Nanocomposites with grafted nanoparticles. *Macromolecules* **2013**, *46*, 3199–3214.
- [5] Tao, P.; Li, Y.; Rungta, A.; Viswanath, A.; Gao, J.; Benicewicz, B. C.; Siegel, R.; Schadler, L. S. TiO₂ nanocomposites with high refractive index and transparency. *J. Mater. Chem.* **2011**, *21*, 18623–18629.
- [6] Qiao, Y.; Islam, M. S.; Wang, L.; Yan, Y.; Zhang, J.; Benicewicz, B. C.; Ploehn, H. J.; Tang, C. Thiophene polymer-grafted barium titanate nanoparticles toward nanodielectric composites. *Chem. Mater.* **2014**, *26*, 5319–5326.

- [7] Bernards, M. T.; Cheng, G.; Zhang, Z.; Chen, S.; Jiang, S. Nonfouling polymer brushes via surface-initiated, two-component atom transfer radical polymerization. *Macromolecules* **2008**, *41*, 4216–4219.
- [8] Truong, T. N. P.; Randriamahazaka, H.; Ghilane, J. Polymer brushes ionic liquid as a catalyst for oxygen reduction and oxygen evolution reactions. *ACS Catal.* **2018**, *8*, 869–875.
- [9] Landherr, L. J. T.; Cohen, C.; Agarwal, P.; Archer, L. A. Interfacial friction and adhesion of polymer brushes. *Langmuir* **2011**, *27*, 9387–9395.
- [10] Kobayashi, M.; Terayama, Y.; Yamaguchi, H.; Terada, M.; Murakami, D.; Ishihara, K.; Takahara, A. Wettability and antifouling behavior on the surfaces of superhydrophilic polymer brushes. *Langmuir* **2012**, *28*, 7212–7222.
- [11] Zhao, D.; Gimenez-Pinto, V.; Jimenez, A. M.; Zhao, L.; Jestin, J.; Kumar, S. K.; Kuei, B.; Gomez, E. D.; Prasad, A. S.; Schadler, L. S.; Khani, M. M.; Benicewicz, B. C. Tunable multiscale nanoparticle ordering by polymer crystallization. *ACS Cent. Sci.* **2017**, *3*, 751–758.
- [12] Navarro, L. A.; French, D. L.; Zauscher, S. Synthesis of modular brush polymer-protein hybrids using diazotransfer and copper click chemistry. *Bioconjugate Chem.* **2018**, *29*, 2594–2605.
- [13] Rungta, A.; Natarajan, B.; Neely, T.; Dukes, D.; Schadler, L. S.; Benicewicz, B. C. Grafting bimodal polymer brushes on nanoparticles using controlled radical polymerization. *Macromolecules* **2012**, *45*, 9303–9311.
- [14] Huang, Y.; Zheng, Y.; Sarkar, A.; Xu, Y.; Stefik, M.; Benicewicz, B. C. Matrix-free polymer nanocomposite thermoplastic elastomers. *Macromolecules* **2017**, *50*, 4742–4753.
- [15] Li, J.; Wang, L.; Benicewicz, B. C. Synthesis of Janus nanoparticles via combination of reversible click reaction and “grafting-to” strategies. *Langmuir* **2013**, *29*, 11547–11553.
- [16] Barby, D. and Haq, Z. (1982) *Low density porous cross-linked polymeric materials and their preparation*. US4522953A.
- [17] Bartl, V. H.; Von Bonin, W. Uber die polymerization in umgekehrter emulsion (On the polymerization in reversed emulsions). *Macromol. Chem.* **1962**, *57*, 74–95.

- [18] Bartl, V. H.; Von Bonin, W. Uber die polymerization in umgekehrter emulsion (On the polymerization in reversed emulsions). *Macromol. Chem.* **1963**, *66*, 151–156.
- [19] Silverstein, M. S. PolyHIPEs: recent advances in emulsion-templated porous polymers. *Prog. Polym. Sci.* **2014**, *39*, 199–234.
- [20] Williams, J. M.; Wroblewski, D. A. Spatial distribution of the phases in water-in-oil emulsions. Open and closed microcellular foams from cross-linked polystyrene. *Langmuir* **1988**, *4*, 656–662.
- [21] Williams, J. M.; Gray, A. J.; Wilkerson, M. H. Emulsion stability and rigid foams from styrene or divinylbenzene water-in-oil emulsions. *Langmuir* **1990**, *6*, 437–444.
- [22] Barbetta, A.; Cameron, N. R. Morphology and surface area of emulsion-derived (polyHIPE) solid foams prepared with oil-phase soluble porogenic solvents: Span 80 as surfactant. *Macromolecules* **2004**, *37*, 3188–3201.
- [23] Silverstein, M. S. Emulsion-templated porous polymers: a retrospective perspective. *Polymer* **2014**, *55*, 304–320.
- [24] Cameron, N. R. High internal phase emulsion templating as a route to well-defined porous polymers. *Polymer* **2005**, *46*, 1439–1449.
- [25] Choudhury, S.; Connolly, D.; White, B. Supermacroporous polyHIPE and cryogel monolithic materials as stationary phases in separation science: a review. *Anal. Methods* **2015**, *7*, 6967–6982.
- [26] Kimmins, S. D.; Cameron, N. R. Functional porous polymers by emulsion templating: recent advances. *Adv. Func. Mater.* **2011**, *21*, 211–225.
- [27] Pulko, I.; Krajnc, P. High internal phase emulsions templating—a path to hierarchically porous functional polymers. *Macromol. Rapid Commun.* **2012**, *33*, 1731–1746.
- [28] Wang, Z. J.; Ghasimi, S.; Landfester, K.; Zhang, K. A. I. Highly porous conjugated polymers for selective oxidation of organic sulfides under visible light. *Chem. Commun.* **2014**, *50*, 8177–8180.
- [29] Langford, C. R.; Johnson, D. W.; Cameron, N. R. Chemical functionalization of emulsion-templated porous polymer by thiol-ene “click” chemistry. *Polym. Chem.* **2014**, *5*, 6200–6206.

- [30] Deleuze, H.; Faivre, R.; Harroquez, V. Preparation of emulsion-derived microcellular polymeric foams (polyHIPEs) by ring-opening metathesis polymerization (ROMP). *Chem. Commun.* **2002**, *0*, 2822–2823.
- [31] Zhang, S.; Chen, J.; Perchyonok, V. T. Stability of high internal phase emulsions with sole cationic surfactant and its tailoring morphology of porous polymers based on emulsions. *Polymer* **2009**, *50*, 1723–1731.
- [32] Menner, A.; Ikem, V.; Salgueiro, M.; Shaffer, M. S. P. Bismarck, A. High internal phase emulsion templates solely stabilized by functionalized titania nanoparticles. *Chem. Commun.* **2007**, *0*, 4274–4276.
- [33] Ikem, V. O.; Menner, A.; Bismarck, A. High internal phase emulsions stabilized solely by functionalized silica particles. *Angew. Chem. Int. Ed.* **2008**, *47*, 8277–8279.
- [34] Wang, S.; Li, J.; Qi, M.; Gao, X.; Wang, W.-J. Toward maximizing the mechanical property of interconnected macroporous polystyrenes made from high internal phase emulsions. *Langmuir* **2017**, *33*, 14294–14303.
- [35] Chevalier, Y.; Bozinger, M.-A. Emulsions stabilized with solid nanoparticles: Pickering emulsions. *Colloids Surf. A Physicochem. Eng. Asp.* **2013**, *439*, 23–34.
- [36] Benicewicz, B. C.; Jarvinen, G. D.; Kathios, D. J.; Jorgenson, B. S. Open-celled polymeric foam monoliths for heavy metal separations study. *J. Radioanal. Nuc. Chem.* **1998**, *235*, 31–35.
- [37] Luo, Y.; Wang, A.-N.; Gao, X. One-pot interfacial polymerization to prepare polyHIPEs with functional surface. *Colloid Polym. Sci.* **2015**, *293*, 1767–1779.
- [38] Koler, A.; Paljevac, M.; Cmager, N.; Iskra, J.; Kolar, M.; Krajnc, P. Poly(4-vinylpyridine) polyHIPEs as catalysts for cycloaddition click reaction. *Polymer* **2017**, *126*, 402–407.
- [39] Ottens, M.; Leene, G. Beenackers, A. A. C. M.; Cameron, N.; Sherrington, D. C. PolyHIPE: a new polymeric support for heterogeneous catalytic reactions: kinetics of hydration of cyclohexene in two-and three-phase systems over a strongly acidic sulfonated polyHIPE. *Ind. Eng. Chem. Res.* **2000**, *39*, 259–266.

- [40] Cummins, D.; Duxbury, C. J.; Quaedflieg, P. J. L. M.; Magusin, P. C. M. M.; Koning, C. E.; Heise, A. Click chemistry as a means to functionalize macroporous polyHIPE. *Soft Matter* **2009**, *5*, 804–811.
- [41] Moine, L.; Deleuze, H.; Degueil, M.; Maillard, B. Copper-mediated polymerization on a microcellular monolith surface. *J. Polym. Sci. A Polym. Chem.* **2004**, *42*, 1216–1226.
- [42] Cummins, D. M.; Magusin, P. C. M. M.; Heise, A. Functionalization of polyHIPE materials by ATRP surface grafting. In *Controlled/Living Radical Polymerization: Progress in ATRP*; ACS Symposium Series 1023; American Chemical Society: Washington, DC, 2009; pp 327–341.
- [43] Cummins, D.; Wyman, P.; Duxbury, C. J.; Thies, J.; Koning, C. E.; Heise, A. Synthesis of functional photopolymerized macroporous polyHIPEs by atom transfer radical polymerization surface grafting. *Chem. Mater.* **2007**, *19*, 5285–5292.
- [44] Audouin, F.; Larragy, R.; Fox, M.; O'Connor, B.; Heise, A. Protein immobilization onto poly(acrylic acid) functional macroporous polyHIPE obtained by surface-initiated ARGET ATRP. *Biomacromolecules* **2012**, *13*, 3787–3794.
- [45] Anderson, K. L.; Nazarov, W.; Musgrave, C. S. A.; Bazin, N.; Faith, D. Synthesis and characterization of low density porous polymers by reversible addition-fragmentation chain transfer (RAFT). *J. Radioanal. Nucl. Chem.* **2014**, *299*, 969–975.
- [46] Barlow, K. J.; Hao, X.; Hughes, T. C.; Hutt, O. E.; Polyzos, A.; Turner, K. A.; Moad, G. Porous, functional, poly(styrene-co-divinylbenzene) monoliths by RAFT polymerization. *Polym. Chem.* **2014**, *5*, 722–732.
- [47] Audouin, F.; Heise, A. Surface-initiated RAFT polymerization of NIPAM from monolithic macroporous polyHIPE. *Eur. Polym. J.* **2013**, *49*, 1073–1079.
- [48] Audouin, F.; Fox, M.; Larragy, R.; Clarke, P.; Huang, J.; O'Connor, B.; Heise, A. Polypeptide-grafted macroporous polyHIPE by surface-initiated *N*-carboxyanhydride (NCA) polymerization as a platform for bioconjugation. *Macromolecules* **2012**, *45*, 6127–6135.

- [49] Unnu, V. S.; Cetinkaya, S. Synthesis and catalytic activity of polyHIPE-supported NHC-bearing ruthenium initiator for ROMP. *Catal. Lett.* **2018**, *148*, 2432–2445.
- [50] Iacono, M.; Connolly, D.; Heise, A. Polymer brush decorated nanoparticles immobilized on polymer monoliths for enhanced biopolymer elution. *RSC Adv.* **2017**, *7*, 19976–19981.
- [51] Viswanathan, P.; Johnson, D. W.; Hurley, C.; Cameron, N. R.; Battaglia, G. 3D surface functionalization of emulsion-templated polymeric foams. *Macromolecules* **2014**, *47*, 7091–7098.
- [52] Anastas, P. T.; Warner, J. C. *Green Chemistry: Theory and Practice*, Oxford University Press: New York, 1998, p.30.
- [53] Alexandratos, S. D.; Beauvais, R.; Duke, J. R.; Jorgenson, B. S. Functionalized polymer foams as metal ion chelating agents with rapid complexation kinetics. *J. Appl. Polym. Sci.* **1998**, *68*, 1911–1916.
- [54] Hus, S.; Kolar, M.; Krajnc, P. Separation of heavy metals from water by functionalized glycidyl methacrylate poly(high internal phase emulsions). *J. Chromatogr. A* **2016**, *1437*, 168–175.
- [55] Katsoyiannis, I. A.; Zouboulis, A. I. Removal of arsenic from contaminated water sources by sorption onto iron oxide-coated polymeric materials. *Water Res.* **2002**, *36*, 5141–5155.
- [56] Wakeman, R. J.; Bhungara, Z. G.; Akay, G. Ion exchange modules formed from polyHIPE foam precursors. *Chem. Eng. J.* **1998**, *70*, 133–141.
- [57] Barlik, N.; Keskinler, B.; Kocakerim, M. M.; Akay, G. Surface modification of monolithic polyHIPE polymers for anionic functionality and their ion exchange behavior. *J. Appl. Polym. Sci.* **2015**, *132*, 42286.
- [58] Alikhani, M.; Moghbeli, M. R. Ion-exchange polyHIPE type membrane for removing nitrate ions: preparation, characterization, kinetics and adsorption studies. *Chem. Eng. J.* **2014**, *239*, 93–104.
- [59] Hughes, J. M.; Budd, P. M.; Tiede, K.; Lewis, J. Polymerized high internal phase emulsion monoliths for the chromatographic separation of engineered nanoparticles. *J. Appl. Polym. Sci.* **2015**, *132*, 41229.

- [60] Yao, C.; Qi, L.; Jia, H.; Xin, P.; Yang, G.; Chen, Y. A novel glycidyl methacrylate-based monolith with sub-micron skeletons and well-defined macropores. *J. Mater. Chem.* **2009**, *19*, 767–772.
- [61] Yang, X.; Tan, L.; Xia, L.; Wood, C. D.; Tan, B. Hierarchical porous polystyrene monoliths from polyHIPE. *Macromol. Rapid Commun.* **2015**, *36*, 1553–1558.
- [62] Kobayashi, S.; Akiyama, R. Renaissance of immobilized catalysts. New types of polymer-supported catalysts, ‘microencapsulated catalysts’, which enable environmentally benign and powerful high-throughput organic synthesis. *Chem. Commun.* **2003**, *4*, 449–460.
- [63] Lu, J.; Toy, P. H. Organic polymer supports for synthesis and for reagent and catalyst immobilization. *Chem. Rev.* **2009**, *109*, 815–838.
- [64] Zhang, Y.; Riduan, S. N. Functional porous organic polymers for heterogeneous catalysis. *Chem. Soc. Rev.* **2012**, *41*, 2083–2094.
- [65] Desforges, A.; Deleuze, H.; Mondain-Monval, O.; Backov, A. Palladium nanoparticle generation within microcellular polymeric foam and size dependence under synthetic conditions. *Ind. Eng. Chem. Res.* **2005**, *44*, 8521–8529.
- [66] Desforges, A.; Backov, R.; Deleuze, H.; Mondain-Monval, O. Generation of palladium nanoparticles within microcellular polymeric supports: application to heterogeneous catalysis of the Suzuki-Miyaura coupling reaction. *Adv. Funct. Mater.* **2005**, *15*, 1689–1695.
- [67] Ungureanu, S.; Deleuze, H.; Sanchez, C.; Popa, M. I.; Backov, R. First Pd@Organo-Si(HIPE) open-cell hybrid monoliths generation offering cycling Heck catalysis reactions. *Chem. Mater.* **2008**, *20*, 6494–6500.
- [68] Liu, X.; Li, Y.; Xing, Z.; Zhao, X.; Liu, N.; Chen, F. Monolithic carbon foam-supported Au nanoparticles with excellent catalytic performance in a fixed-bed system. *New J. Chem.* **2017**, *41*, 15027–15032.
- [69] Brun, N.; Garcia, A. B.; Deleuze, H.; Achard, M.-F.; Sanchez, C.; Durand, F.; Oestreicher, V.; Backov, R. Enzyme-based hybrid macroporous foams as highly efficient biocatalysts obtained through integrative chemistry. *Chem. Mater.* **2010**, *22*, 4555–4562.

- [70] Gurevitch, I.; Silverstein, M. S. Shape memory polymer foams from emulsion templating. *Soft Matter* **2012**, *8*, 10378–10387.
- [71] Johnson, D. W.; Langford, C. R.; Didsbury, M. P.; Lipp, B.; Przyborski, S. A.; Cameron, N. R. Fully biodegradable and biocompatible emulsion templated polymer scaffolds by thiol-acrylated polymerization of polycaprolactone macromonomers. *Polym. Chem.* **2015**, *6*, 7256–7263.
- [72] Eissa, A. M.; Barros, F. S. V. Vrljicak, P.; Brosens, J. J.; Cameron, N. R. Enhanced differentiation potential of primary human endometrial cells cultured on 3D scaffolds. *Biomacromolecules* **2018**, *19*, 3343–3350.
- [73] Sears, N. A.; Dhavalikar, P. S.; Cosgriff-Hernandez, E. M. Emulsion inks for 3D printing of high porosity materials. *Macromol. Rapid Commun.* **2016**, *37*, 1369–1374.
- [74] Robinson, J. L. McEnery, M. A. P.; Pearce, H.; Whitely, M. E.; Munoz-Pinto, D. J.; Hahn, M. S.; Li, H.; Sears, N. A.; Cosgriff-Hernandez, E. Osteoinductive polyHIPE foams as injectable bone grafts. *Tissue Eng. Part A* **2016**, *22*, 403–414.
- [75] Streifel, B. C.; Lundin, J. G.; Sanders, A. M.; Gold, K. A.; Wilems, T. S.; Williams, S. J.; Cosgriff-Hernandez, E.; Wynne, J. H. Hemostatic and absorbent polyHIPE-kaolin composites for 3D printable wound dressing materials. *Macromol. Biosci.* **2018**, *18*, 1700414.
- [76] Schadler, L. S.; Kumar, S. K.; Benicewicz, B. C.; Lewis, S. L.; Harton, S. E. Designed interfaces in polymer nanocomposites: a fundamental viewpoint. *MRS Bull.* **2007**, *32*, 335–340.
- [77] Treacy, M. M. J.; Ebbesen, T. W.; Gibson, J. M. Exceptionally high Young's modulus observed for individual carbon nanotubes. *Nature* **1996**, *381*, 678–680.
- [78] Calebrese, C.; Hui, L.; Schadler, L. S.; Nelson, J. K. A review on the importance of nanocomposite processing to enhance electrical insulation. *IEEE T. Dielect. Electr. Insul.* **2011**, *18*, 938–945.
- [79] Greszta, D.; Mardare, D.; Matyjaszewski, K. "Living" radical polymerization. 1. Possibilities and limitations. *Macromolecules* **1994**, *27*, 638–644.

- [80] Hawker, C. J. Molecular weight control by a “living” free-radical polymerization process. *J. Am. Chem. Soc.* **1994**, *116*, 11185–11186.
- [81] Lee, N. S.; Li, Y.; Ruda, C. M.; Wooley, K. L. Aqueous-only, pH-induced nanoassembly of dual pK_a-driven contraphilic block copolymers. *Chem. Commun.* **2008**, *42*, 5339–5341.
- [82] Blas, H.; Save, M.; Boisseiere, C.; Sanchez, C.; Charleux, B. Surface-initiated nitroxide-mediated polymerization from ordered mesoporous silica. *Macromolecules* **2011**, *44*, 2577–2588.
- [83] St. Thomas, C.; Cabello-Romero, J. N.; Garcia-Valdez, O.; Jimenez-Regalado, E. J.; Maldonado-Textle, H.; Guerrero-Santos, R. Surface-initiated nitroxide-mediated polymerization of sodium 4-styrene sulfonate from latex particles. *J. Polym. Sci. A Polym. Chem.* **2017**, *55*, 437–444.
- [84] Wang, J. S.; Matyjaszewski, K. Controlled/“living” radical polymerization. Atom transfer radical polymerization in the presence of transition-metal complexes. *J. Am. Chem. Soc.* **1995**, *117*, 5614–5615.
- [85] Pyun, J.; Jia, S.; Kowalewski, T.; Patterson, G. D.; Matyjaszewski, K. Synthesis and characterization of organic/inorganic hybrid nanoparticles: kinetics of surface-initiated atom transfer radical polymerization and morphology of hybrid nanoparticle ultrathin films. *Macromolecules* **2003**, *36*, 5094–5104.
- [86] Matyjaszewski, K.; Dong, H.; Jakubowski, W.; Pietrasik, J.; Kusumo, A. Grafting from surfaces for “everyone”: ARGET ATRP in the presence of air. *Langmuir* **2007**, *23*, 4528–4531.
- [87] Chiefari, J.; Chong, Y. K.; Ercole, F.; Krstina, J.; Jeffery, J.; Le, T. P. T.; Mayadunne, R. T. A.; Meijs, G. F.; Moad, C. L.; Moad, G.; Rizzardo, E.; Thang, S. H. Living free-radical polymerization by reversible addition-fragmentation chain transfer: The RAFT process. *Macromolecules* **1998**, *31*, 5559–5562.
- [88] Li, C.; Han, J.; Ryu, C. Y.; Benicewicz, B. C. A versatile method to prepare RAFT agent anchored substrates and the preparation of PMMA grafted nanoparticles. *Macromolecules* **2006**, *39*, 3175–3183.
- [89] Bansal, A.; Yang, H.; Li, C.; Benicewicz, B. C.; Kumar, S. K.; Schadler, L. S. Controlling the thermomechanical properties of polymer nanocomposites

- by tailoring the polymer-particle interface. *J. Polym. Sci. B Polym. Phys.* **2006**, *44*, 2944–2950.
- [90] Akcora, P.; Liu, H.; Kumar, S. K.; Moll, J.; Li, Y.; Benicewicz, B. C.; Schadler, L. S.; Acehan, D.; Panagiotopoulos, A. Z.; Pryamitsyn, V.; Ganesan, V.; Ilavsky, J.; Thiyagarajan, P.; Colby, R. H.; Douglas, J. F. Anisotropic self-assembly of spherical polymer-grafted nanoparticles. *Nature Mater.* **2009**, *8*, 354–359.
- [91] Viranen, S.; Krentz, T. M.; Nelson, J. K.; Schadler, L. S.; Bell, M.; Benicewicz, B. C.; Hillborg, H.; Zhao, S. Dielectric breakdown strength of epoxy bimodal-polymer-brush-grafted core functionalized silica nanocomposites. *IEEE Trans. Dielectr. Electr. Insul.* **2014**, *21*, 563–570.
- [92] Li, Y.; Krentz, T. M.; Wang, L.; Benicewicz, B. C.; Schadler, L. S. Ligand engineering of polymer nanocomposites: from the simple to the complex. *ACS Appl. Mater. Interfaces*, **2014**, *6*, 6005–6021.
- [93] Tao, P.; Li, Y.; Rungta, A.; Viswanath, A.; Gao, J.; Benicewicz, B. C.; Siegel, R. W.; Schadler, L. S. TiO₂ nanocomposites with high refractive index and transparency. *J. Mater. Chem.* **2011**, *21*, 18623–18629.
- [94] Tao, P.; Viswanath, A.; Schadler, L. S.; Benicewicz, B. C.; Siegel, R. W. Preparation and optical properties of indium tin oxide/epoxy nanocomposites with polyglycidyl methacrylate grafted nanoparticles. *ACS Appl. Mater. Interfaces*, **2011**, *3*, 3638–3645.
- [95] Qiao, Y.; Islam, M. S.; Wang, L.; Yan, Y.; Zhang, J.; Benicewicz, B. C.; Ploehn, H. J.; Tang, C. Thiophene polymer-grafted barium titanate nanoparticles toward nanodielectric composites. *Chem. Mater.* **2014**, *26*, 5319–5326.
- [96] Wang, L.; Cole, M.; Li, J.; Chen, Y. P.; Zheng, Y.; Miller, K. P.; Decho, A. W.; Benicewicz, B. C. Polymer grafted recyclable magnetic nanoparticles. *Polym. Chem.* **2014**, *6*, 248–255.
- [97] Viswanath, A.; Shen, Y.; Green, A. N.; Tan, R.; Greytak, A. B.; Benicewicz, B. C. Copolymerization and synthesis of multiple binding histamine ligands for the robust functionalization of quantum dots. *Macromolecules* **2014**, *47*, 8137–8144.

- [98] Dong, H.; Zhu, M.; Yoon, J. A.; Gao, H.; Jin, R.; Matyjaszewski, K. One pot synthesis of robust core/shell gold nanoparticles. *J. Am. Chem. Soc.* **2008**, *130*, 12852–12853.
- [99] Yang, W.; Ella-Menye, J. R.; Liu, S.; Bai, T.; Wang, D.; Yu, Q.; Li, Y.; Jiang, S. Cross-linked carboxybetaine SAMs enable nanoparticles with remarkable stability in complex media. *Langmuir* **2014**, *30*, 2522–2529.
- [100] Zhang, B.; Chen, Y.; Xu, L.; Zeng, L.; He, Y.; Kang, E.-T.; Zhang, J. Growing poly(*N*-vinylcarbazole) from the surface of graphene oxide via RAFT polymerization. *J. Polym. Chem. A Polym. Chem.* **2011**, *49*, 2043–2050.
- [101] Yang, Q.; Wang, L.; Xiang, W.-D.; Zhou, J.-F.; Tan, Q.-H. Preparation of polymer-grafted carbon black nanoparticles by surface-initiated atom transfer radical polymerization. *J. Poly. Sci. Part A Polym. Chem.* **2007**, *45*, 3451–3459.
- [102] Cobo, I.; Li, M.; Sumerlin, B. S.; Perrier, S. Smart hybrid materials by conjugation of responsive polymers to biomacromolecules. *Nat. Mater.* **2015**, *15*, 143–159.
- [103] Cummings, C.; Murata, H.; Koepsel, R.; Russell, A. J. Dramatically increased pH and temperature stability of chymotrypsin using dual block polymer-based protein engineering. *Biomacromolecules* **2014**, *15*, 763–771.
- [104] Ragupathy, L.; Ziener, U.; Graf, R.; Landfester, K. Grafting polyacrylates on natural rubber latex by miniemulsion polymerization. *Colloid Polym. Sci.* **2011**, *289*, 229–235.
- [105] Liu, Y.; Klep, V.; Zdyrko, B.; Luzinov, I. Synthesis of high-density grafted polymer layers with thickness and grafting density gradients. *Langmuir* **2005**, *21*, 11806–11813.
- [106] Natarajan, B.; Neely, T.; Rungta, A.; Benicewicz, B. C.; Schadler, L. S. Thermomechanical properties of bimodal brush modified nanoparticle composites. *Macromolecules*, **2013**, *46*, 4909–4918.
- [107] Huang, Y.; Zheng, Y.; Sarkar, A.; Xu, Y.; Stefik, M.; Benicewicz, B. C. Matrix-free nanocomposite thermoplastic elastomers. *Macromolecules* **2017**, *50*, 4742–4753.
- [108] Huang, Y.; Zheng, Y.; Pribyl, J.; Benicewicz, B. C. A versatile approach to different colored photonic films generated from block copolymers and

- their conversion into polymer-grafted nanoplatelets. *J. Mater. Chem. C* **2017**, *5*, 9873–9878.
- [109] Bell, M.; Krentz, T.; Nelson, J. K.; Schadler, L. S.; Wu, K.; Breneman, C.; Zhao, S.; Hillborg, H.; Benicewicz, B. C. Investigation of dielectric breakdown in silica-epoxy nanocomposites using designed interfaces. *J. Colloid Interface Sci.* **2017**, *495*, 130–139.
- [110] Bilchak, C. R.; Buenning, E.; Asai, M.; Kai Zhang, K.; Durning, C. J.; Kumar, S. K.; Huang, Y.; Benicewicz, B. C.; Gidley, D. W.; Cheng, S.; Sokolov, A. P.; Minelli, M.; Doghieri, F. Polymer-grafted nanoparticle membranes with controllable free volume. *Macromolecules* **2017**, *50*, 7111–7120.

CHAPTER 2

PHOTOINITIATED POLYMERIZATION OF 4-VINYLPYRIDINE ON POLYHIPE FOAM SURFACE TOWARDS IMPROVED PLUTONIUM SEPARATIONS¹

¹ Pribyl, J.; Fletcher, B.; Steckle, W.; Taylor-Pashow, K.; Shehee, T.; Benicewicz, B.
Anal. Chem. **2017**, *89*, 5174–5178.

Reprinted here with permission of the publisher.

2.1 Abstract

The separation of hazardous metals from contaminated sources is commonly achieved with ion-exchange resins. The resins have a high surface area decorated with many ion-exchange sites and thus a high sorption capacity for the analyte of interest. However, these sites are primarily accessed by diffusion which limits the throughput and quality of the separation. Reported herein is a study of monolithic polyHIPE foam columns surface-grafted with a brush of polymer containing ion-exchange functionality for the separation of Pu. It was found that the loading curves of the foam material are steeper than a similarly scaled resin-based column, and the elution profiles of the foams were narrower than the resin, generating more concentrated eluate relative to the amount of Pu loaded onto the foam columns. On a gravimetric basis, the foams had a similar or greater Pu capacity than the resin with fewer ion-exchange sites per unit mass. These characteristics are mainly due to the convective mass transport which dominates the separation in the polyHIPE materials, suggesting that these materials may be useful for more efficient hazardous metal separations.

2.2 Introduction

Due to their versatility, polymeric high internal-phase emulsion (polyHIPE) foams have garnered attention for many diverse applications

including flow-through chemistry,¹⁻³ separation media and supports for biomolecules,⁴⁻⁶ sequestration of small organic molecules,⁷ and ion-exchange supports to separate metals⁸⁻¹³ and other ions.¹⁴⁻¹⁶ Materials known as polyHIPE foams are macroporous, emulsion-templated polymeric materials formed from an emulsion with an internally dispersed phase which is greater than or equal to 74% of the total emulsion by volume.¹⁷ Upon curing, an interconnected pore morphology can be formed with pore sizes on the order of 10-250 μm .¹⁷⁻²⁰ By virtue of the synthetic process used to make polyHIPE foams, structural parameters such as pore volume fraction, pore connectivity, pore size, and surface functionality are each highly tunable.²¹⁻²² In addition to the synthetic ease of modifying these parameters, polyHIPE foams are particularly well-appointed for separations processes because of the ability to incorporate chemical functionality on the surface of the macropores which has the effect of minimizing diffusional path lengths and allowing for almost no chromatographic overlap as a result of convective mass transport.²³

Ion-exchange processes used to remove hazardous metals from contaminated sources commonly rely on the use of polymeric resins which have been extensively studied and produced commercially.⁸⁻⁹ The bulk of ion-exchange sites contained within the resin beads are accessed by diffusion into small pores on the surface. The use of smaller beads has the benefit of shorter ion

diffusion path lengths; however, in a packed-bed column the use of small beads results in high column backpressures.²⁴ In applications where high backpressure is undesirable or impractical, larger beads are used at the expense of longer ion diffusion path lengths which creates the need for longer contact times with the resin to complete the ion-exchange process.²⁴ Ideally, ion-exchange materials should rely minimally on diffusional mass transport and instead employ a primarily convective mechanism of mass transport to maximize throughput and separation efficiency.²⁴

A promising alternative to ion-exchange resins are polyHIPE foams surface-functionalized with ion-exchange sites on the surface of the macropores.²⁴ To date, most functionalized polyHIPE foams synthesized and tested for ion-exchange applications have monomeric ion-exchange or other functionality tethered or coated onto the foam surface to perform the separation.⁸⁻¹⁶ Described herein is an approach which takes advantage of the convective mass transport offered by the polyHIPE foams and introduces ion-exchange functionality onto the surface of the foam by growing a “brush” of polymer chains from surface initiating sites in a similar manner to previous reports.^{12, 25-27} Use of a functional monomer endows each repeat unit of the grafted chains with ion-exchange functionality. The aim of this work is to better understand the parameters which will result in a more efficient ion-exchange

process and to gain an understanding of the separation characteristics under flow conditions of this type of material. The specific application being studied is the purification of plutonium by anion-exchange utilizing a quaternary amine functional group.

2.3 Experimental

2.3.1 Materials and Instrumentation

All materials were purchased from either Sigma-Aldrich or McMaster-Carr and were used as received unless otherwise specified. Prior to use, styrene, 4-vinyl benzyl chloride, and divinyl benzene (mixed isomers) were each passed through a column of basic alumina to remove the inhibitor.

Azobisisobutyronitrile (AIBN) was recrystallized twice from methanol and stored at -30 °C prior to use. 4-Vinylpyridine was distilled under reduced pressure and stored under nitrogen prior to use. Scanning electron microscopy (SEM) images of the foams were observed with a Zeiss Ultraplus thermal field emission SEM using an acceleration voltage of 8 kV. Prior to SEM imaging, the foam samples were rendered conductive via sputter coating using a Pd/Au target. Elemental analysis was performed at Midwest Microlab, Indianapolis, IN. Pu concentration was determined by gamma spectroscopy using either a Canberra or Ortec high purity germanium detector instrument.

2.3.2 Preparation of PolyHIPE Foam Monoliths

The general procedure for the synthesis of each polyHIPE foam monolith is as follows. The components of the oil phase including styrene (0.68 g, 45 wt.%), divinyl benzene (0.378 g, 25 wt.%), 4-vinyl benzyl chloride (0.453 g, 30 wt.%), sorbitan monooleate (SPAN 80, 0.288 g, 20 wt.% relative to monomers) and AIBN (0.010 g) as initiator were weighed out and combined in a small resin kettle equipped with a glass paddle stirrer. The aqueous phase (comprised only of distilled water, 15 g) was placed in a dropwise addition funnel and was added slowly to the stirring oil phase (350 rpm) over the course of 15 minutes. After complete addition of the aqueous phase, the resulting emulsion was allowed to stir 5 additional minutes to ensure even mixing. The resulting emulsion was deposited via syringe into thin glass tubing and cured overnight at 70 °C. The monoliths were removed from the glass tubes by breaking the glass and were washed for 24 h in a Soxhlet extractor with ethanol as the extraction solvent. The monoliths were dried overnight in an 80 °C oven prior to further use.

2.3.3 Reaction of Surface Chloromethyl Groups with Sodium Thiosulfate

Approximately 0.5 g of polyHIPE foam monoliths were added to a 250 mL round bottom flask equipped with a 1-inch magnetic stir bar. To the flask was added 100 mL of a 50/50 (%v/v) mixture of distilled water and N,N'-dimethylformamide and 1.6 g (excess) anhydrous sodium thiosulfate. The

contents of the flask were allowed to stir slowly overnight at 70 °C. The resulting thiosulfate modified foams were washed for 24 h in a Soxhlet extractor with ethanol as the extraction solvent, then dried in an 80 °C oven overnight prior to further use. Successful thiosulfate modification was confirmed via elemental analysis (Table 2.1).

2.3.4 UV-Initiated Surface Polymerization of P4VP

A monolith of thiosulfate-functionalized polyHIPE was placed into a 25 mL Schlenk flask equipped with a rubber septum and a glass stopcock. The foam was deoxygenated by 3 cycles of evacuating and backfilling with nitrogen. Freshly distilled 4-vinylpyridine (~3 mL) was added via gas-tight syringe to saturate the prepared monolith. The flask was sealed under nitrogen then placed 10 cm from a high intensity UV lamp for varying time intervals. After the surface polymerization was complete, the monoliths were washed for 24 h in a Soxhlet extractor with ethanol as the extraction solvent. The homogeneity of the photoinitiated graft polymerization was investigated for a polyHIPE foam column of diameter=6mm. A sample from the exterior of the foam had a nitrogen content of 4.49% and a sample from the interior of the same foam had a nitrogen content of 4.69% (these values are within experimental error), indicating that the surface grafted polymer is uniform throughout the sample. Each of the polyHIPE monoliths tested in this work were of equal dimension to this test case.

2.3.5 Assembly of Column Prototypes

The column prototypes were prepared using the following procedure. The foam monolith was first wrapped in a layer of PTFE tape, encapsulated in one layer of PVDF heat-shrink tubing, then one layer of high-strength heat-shrink tubing. PVDF hose connectors were attached to the end of the column and secured with one additional layer of high-strength heat shrink tubing. Specific column dimensions for each sample are shown in Table 2.1.

Table 2.1: Dimensions of materials tested and elemental analysis data for synthesized polyHIPE foams.

Sample	Length (mm)	Diameter (mm)	Volume ^a (mL)	Mass (g)	% Cl in Unmodified polyHIPE	%S After Na ₂ S ₂ O ₃ Modification
A	45	6	1.272	0.0975	7.08	-
B	44	6	1.244	0.1385	7.08	0.87
C	52	6	1.470	0.1998	5.60	1.05
D	50	6	1.413	0.2150	6.80	2.97
Reillex HPQ	-	-	2.75	2.4475	-	-

^aCalculated from column length and diameter

2.3.6 Pu Uptake and Elution Studies.

Plutonium sorption capacity and elution characteristics of the synthesized materials were studied using a feed solution of 3.28 g/L Pu solution in 8 M nitric acid which approximates the conditions for this separation process at the Savannah River Site. The feed solution was treated with ascorbic acid prior to use to reduce any Pu(VI) to Pu(III). Upon adjusting the acid concentration to 8

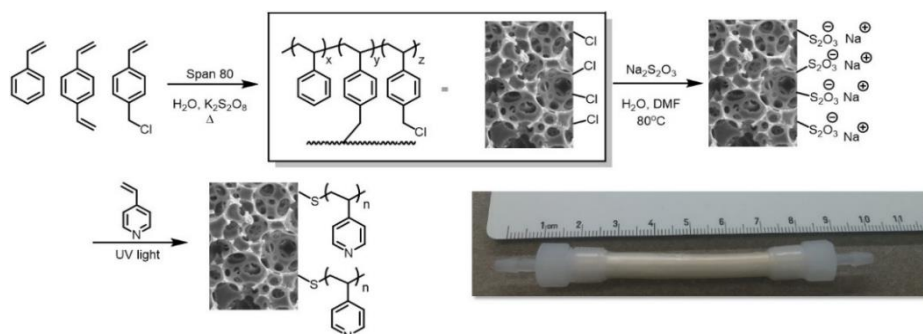
M, the Pu(III) was oxidized to Pu(IV), forming the $[\text{Pu}(\text{NO}_3)_6]^{2-}$ complex which readily loads onto the anion exchange sites. Each prepared column was first conditioned with approximately 10 mL of 8 M nitric acid using a syringe pump at a flow rate of 0.75 mL/min to protonate the pyridine groups and to flush any water or dilute acid from the material. The Pu feed solution was then fed at 0.5 mL/min and 1 mL aliquots were collected until break-through was observed visually, followed by a 10 mL wash of 8 M nitric acid at a flow rate of 0.75 mL/min to remove any impure solution, in effect purifying the loaded Pu. The sorbed Pu was then eluted by flowing 0.35 M nitric acid through the column at a flow rate of 0.5 mL/min with 1 mL aliquots taken until elution was complete. The low nitrate concentration allowed the Pu complex to desorb from the anion exchange sites to be collected in a purified form. The sorption and elution results of these experiments were compared to a similarly-scaled glass column packed with Reillex[®] HPQ ion-exchange resin which was also tested using the procedure described above.

2.4 Results and Discussion

To study the sorption and elution properties of the P4VP-grafted polyHIPE foams, a series of P4VP-grafted polyHIPE foam columns with differing nitrogen contents were prepared according to Scheme 2.1. The physical and

chemical characteristics of the synthesized materials are shown in Table 2.2.

Differing nitrogen content between samples correlates to the amount of grafted



Scheme 2.1: Synthetic route to prepare HIPE foams with surface-grafted chains of poly(4-vinyl pyridine) (P4VP) and monolithic column prepared for testing (inset)

P4VP, since there was no nitrogen present in the unmodified material. The typical open-celled morphology of the polyHIPE foams pre- and post- surface polymerization are shown in Figure 2.1 (images a and b). Surface modification of the polyHIPE with grafted P4VP appeared to slightly smooth the surface texture which was observed by scanning electron microscopy (Figure 2.1, images c and d) and the open celled morphology generated by nearly 90% internal phase in the initial emulsion was amenable to flow testing.

Table 2.2: Chemical and physical characteristics of synthesized polyHIPE foam columns and Reillex® HPQ

Sample	Internal Phase (vol.%)	Crosslinker Content (wt.%)	Weight Gain (%)	Polymerization Time (hr)	%N	Density ^b (g/mL)
A	89	25	0	0	0	0.077
B	89	25	34	6	3.58	0.111
C	89	25	70	10.5	5.54	0.136
D	89	25	77.2	10.5	6.24	0.152
Reillex® HPQ	-	25	-	-	8.75 ^a	0.890

^aCalculated theoretical value for nitrogen content

^bCalculated from column dimensions listed in Table 2.1

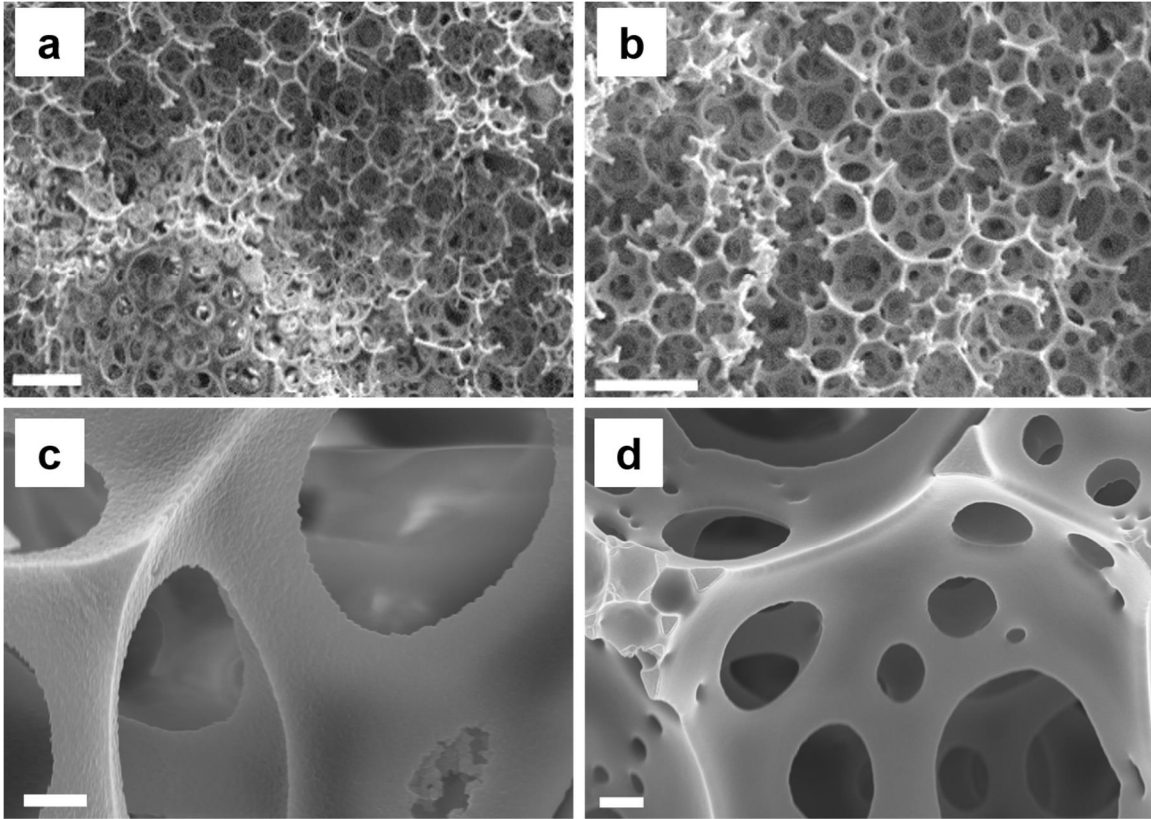


Figure 2.1: Representative SEM images of polyHIPE foams (a) before surface polymerization, low magnification (b) after surface polymerization, low magnification, (c) before surface polymerization, high magnification, (d) after surface polymerization, high magnification. (Scale bars are 20 μm in images a and b, scale bars are 1 μm in images c and d).

The loading and elution characteristics of the grafted polyHIPE foam columns were tested using prepared columns which were subjected to a similar procedure used for the ion-exchange separation of Pu at the Savannah River Site. These results were compared to the same testing of a similarly scaled column of the ion-exchange resin currently used for this separation, Reillex[®] HPQ (an N-methylated cross-linked P4VP resin). Due to the similarity in functionality between the resin and the grafted P4VP chains, the reactivity of the resin and the

grafted chains was expected to be very similar (the grafted P4VP became quaternized under the strongly acidic conditions of the feed solution). It has been previously demonstrated that this type of material demonstrates faster uptake kinetics than resin materials bearing similar functionality.¹² The loading and elution data for the synthesized columns are shown in Figure 2.2 (left). Due to a large difference in density between the foam materials and the resin (Table 2.2), both loading and elution characteristics were plotted as a function of bed volume so that the materials were compared on a volumetric basis.

In general, as the nitrogen content of the foam samples increased (indicative of larger amounts of grafted P4VP), the number of bed volumes until breakthrough also increased which indicates that the amount of grafted P4VP is correlated with the capacity of the material. In this case, % Breakthrough is defined as the concentration of Pu detected in the collected eluate divided by the initial concentration of the feed. Compared to the Reillex® HPQ, which has a theoretical nitrogen content of 8.75%, the volumetric capacity of the polyHIPE with the largest amount of grafted P4VP (Sample D, Figure 2.2, left) was about half the volumetric Pu capacity of the resin, and the breakthrough curves of the foams are noticeably steeper than the resin. The steepness of the curves is likely an artifact of the difference in mass transport between the materials. Because of the convective mass transport employed by the foams, the ion-exchange sites

were efficiently used until no more existed. This process caused a steep breakthrough curve for the foam samples once all sites were used while the resin had more of a gradient breakthrough trend due to diffusional mass transport. The elution profiles (Figure 2, right) more clearly demonstrate the advantage of the foam over the resin. The complete elution of adsorbed Pu was completed in less than two bed volumes on average for the P4VP-grafted polyHIPE foams compared to nearly 4 bed volumes for the resin. The demonstrated narrow elution profiles are a substantial improvement in the efficiency of the separation because the separated material is obtained in a more concentrated form relative to the Pu eluted from the resin (which shows an elution tail, diluting the eluate).

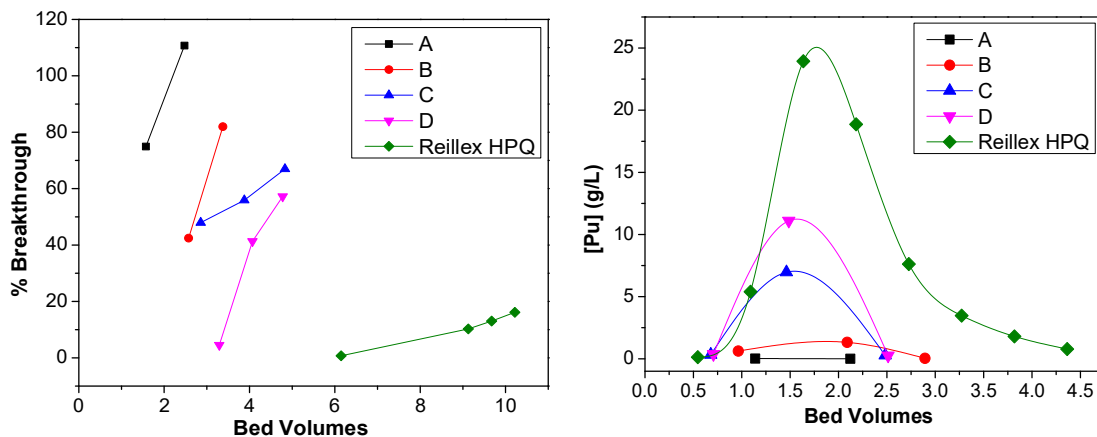


Figure 2.2: Pu loading curves for foam and Reillex[®] HPQ columns (left) and Pu elution curves for foam and Reillex[®] HPQ columns (right)

When these two types of materials were compared on a gravimetric basis (the mass of Pu sorbed per gram of material), the foam demonstrated a higher Pu capacity than the resin even with relatively modest amounts of grafted P4VP

(Figure 2.3). In applications such as capture and storage, the mass fraction capability is important to consider in minimizing the amount of hazardous material which must be sequestered. Because the Pu is sorbed by the grafted chains which are in a solution-like environment, all ion-exchange sites are more freely accessible which helps explain why the foam, despite having modest levels of grafted P4VP (and fewer ion exchange sites per unit mass) compared to the resin, exceeded the sorption capacity of the resin on a gravimetric basis.

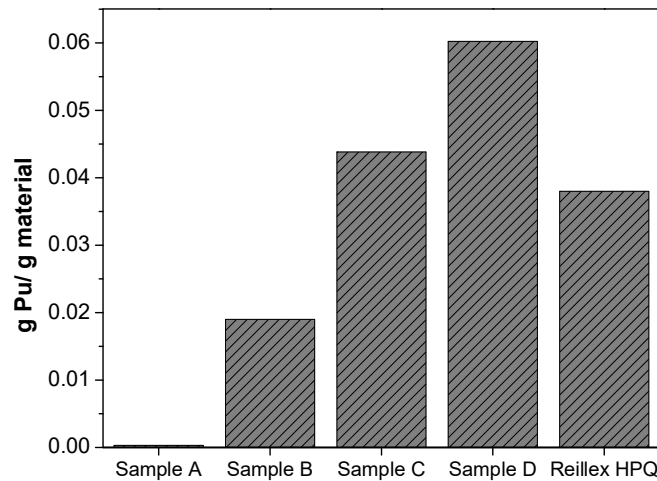


Figure 2.3: Gravimetric comparison of Pu loading between foam columns and Reillex® HPQ resin

2.5 Conclusion

This work demonstrated the potential for polyHIPE foams surface-grafted with polymers containing ion-exchange functionality to improve the efficiency of the current resin-based ion-exchange separation of Pu from contaminated sources. Because of the convective mass transport afforded by the macroporous

structure of the polyHIPE materials tested, the loading curves were steep, and the elution profiles were narrow relative to the resin material currently used for this separation. The Pu sorption capacity of the polyHIPE foam increased as the nitrogen content of the foam increased, suggesting that sorption capacity and amount of grafted polymer are correlated. On a gravimetric basis, the polyHIPE foams demonstrated a higher Pu capacity than the resin which could prove useful for capture and storage applications of hazardous materials. Further inquiry into the synthesis of these materials with the goal of incorporating more functionality (either higher density of surface chains or higher chain molecular weights) could give materials with equal or greater volumetric sorption capacity with the advantage of recovering more concentrated Pu during the elution step compared to the resin. It is also possible that tailoring the chemistry of the grafted polymer for other types of separations could render this material useful for other separation processes.

2.6 References

- [1] Moine, L.; Deleuze, H.; Maillard, B. Preparation of high loading PolyHIPE monoliths as scavengers for organic chemistry. *Tetrahedron Letters* **2003**, *44*, 7813–7816.
- [2] Ottens, M.; Leene, G.; Beenackers, A. A. C. M.; Cameron, N. PolyHIPE: A new polymeric support for heterogeneous catalytic reactions: kinetics of hydration of cyclohexene in two- and three-phase systems over a strongly acidic sulfonated polyHIPE. *Ind. Eng. Chem. Res.* **2000**, *39*, 259–266.

- [3] Small, P. W.; Sherrington, D. C. Design and application of a new rigid support for high-efficiency continuous-flow peptide synthesis. *J. Chem. Soc.* **1989**, *21*, 1589–1591.
- [4] Krajnc, P.; Leber, N.; Stefanec, D.; Kontrec, S.; Podgornik, A. Preparation and characterisation of poly(high internal phase emulsion) methacrylate monoliths and their application as separation media. *J. Chromatogr. A* **2005**, *1065*, 69–73.
- [5] Yao, C.; Qi, L.; Yang, G.; Wang, F. Preparation of sub-micron skeletal monoliths with high capacity for liquid chromatography. *J. Sep. Sci.* **2010**, *33*, 475–483.
- [6] Hayman, M. W.; Smith, K. H.; Cameron, N. R.; Przyborski, S. A. Enhanced neurite outgrowth by human neurons grown on solid three-dimensional scaffolds. *Biochem. Biophys. Res. Commun.* **2004**, *314*, 483–488.
- [7] Pulko, I.; Kolar, M.; Krajnc, P. Atrazine removal by covalent bonding to piperazine functionalized PolyHIPEs. *Sci. Total Environ.* **2007**, *386*, 114–123.
- [8] Beatty, S. T.; Fischer, R. J.; Hagers, D. L.; Rosenberg, E. A comparative study of the removal of heavy metal ions from water using a silica–polyamine composite and a polystyrene chelator resin. *Ind. Eng. Chem. Res.* **1999**, *38*, 4402–4408.
- [9] Xiong, C.; Yao, C. Synthesis, characterization, and application of triethylenetetramine modified polystyrene resin in removal of mercury, cadmium, and lead from aqueous solutions. *Chem. Eng. J.* **2009**, *155*, 844–850.
- [10] Mert, E. H.; Kaya, M. A.; Yildirim, H. Preparation and characterization of polyester–glycidyl methacrylate polyHIPE monoliths to use in heavy metal removal. *Des. Monomers Polym.* **2012**, *15*, 113–126.
- [11] Katsoyiannis, I. A.; Zouboulis, A. I. Removal of arsenic from contaminated water sources by sorption onto iron-oxide-coated polymeric materials. *Water Res.* **2002**, *36*, 5141–5155.

- [12] Benicewicz, B. C.; Jarvinen, G. D.; Kathios, D. J.; Jorgensen, B. S. Open-celled polymeric foam monoliths for heavy metal separations study. *J. Radioanal. Nucl. Chem.* **1998**, *235*, 31–35.
- [13] Hus, S.; Kolar, M.; Krajnc, P. Separation of heavy metals from water by functionalized glycidyl methacrylate poly (high internal phase emulsions). *J. Chromatogr. A* **2016**, *1437*, 168–175.
- [14] Inoue, H.; Yamanaka, K.; Yoshida, A.; Aoki, T.; Teraguchi, M.; Kaneko, T. Synthesis and cation exchange properties of a new porous cation exchange resin having an open-celled monolith structure. *Polymer* **2004**, *45*, 3–7.
- [15] Barlik, N.; Keskinler, B.; Kocakerim, M. M.; Akay, G. Surface modification of monolithic PolyHIPE polymers for anionic functionality and their ion exchange behavior. *J. Appl. Polym. Sci.* **2015**, *132*, 42286.
- [16] Barlik, N.; Keskinler, B.; Kocakerim, M. M.; Akay, G. Functionalized PolyHIPE polymer monoliths as an anion-exchange media for removal of nitrate ions from aqueous solutions. *Desalin. Water. Treat.* **2016**, *57*, 26440–26447.
- [17] Silverstein, M. S. PolyHIPEs: Recent advances in emulsion-templated porous polymers. *Prog. Polym. Sci.* **2014**, *39*, 199–234.
- [18] Barbetta, A.; Cameron, N. R. Morphology and surface area of emulsion-derived (polyHIPE) solid foams prepared with oil-phase soluble porogenic solvents: Span 80 as surfactant. *Macromolecules* **2004**, *37*, 3188–3201.
- [19] Cameron, N. R. High internal phase emulsion templating as a route to well-defined porous polymers. *Polymer* **2005**, *46*, 1439–1449.
- [20] Zhang, T.; Xu, Z.; Guo, Q. Closed-cell and open-cell porous polymers from ionomer-stabilized high internal phase emulsions. *Polym. Chem.* **2016**, *7*, 7469–7476.
- [21] Williams, J. M.; Wroblewski, D. A. Spatial distribution of the phases in water-in-oil emulsions. Open and closed microcellular foams from cross-linked polystyrene. *Langmuir* **1988**, *4*, 656–662.

- [22] Williams, J. M.; Gray, A. J.; Wilkerson, M. H. Emulsion stability and rigid foams from styrene or divinylbenzene water-in-oil emulsions. *Langmuir* **1990**, *6*, 437–444.
- [23] Miller, S. Product Review: Separations in a monolith. *Anal. Chem.* **2004**, *76*, 99A–101A.
- [24] Choudhury, S.; Connolly, D.; White, B. Supermacroporous polyHIPE and cryogel monolithic materials as stationary phases in separation science: a review. *Anal. Methods* **2015**, *7*, 6967–6982.
- [25] Yao, C.; Li, X.; Neoh, K. G.; Shi, Z.; Kang, E. T. Surface modification and antibacterial activity of electrospun polyurethane fibrous membranes with quaternary ammonium moieties *J. Membr. Sci.* **2008**, *320*, 259–267.
- [26] Wang, W. C.; Vora, R. H.; Kang, E. T.; Neoh, K. G. Electroless plating of copper on fluorinated polyimide films modified by surface graft copolymerization with 1-vinylimidazole and 4-vinylpyridine. *Polym. Eng. Sci.* **2004**, *44*, 362–375.
- [27] Tsunooka, M.; Ando, N.; Tanaka, M. Photochemical reactions of high polymers. XIII. Photografting of methyl methacrylate onto the polymers bearing thiosulfate groups. *Appl. Polym. Sci.* **1974**, *18*, 1197–1211.

CHAPTER 3

HIGH-CAPACITY POLY(4-VINYLPYRIDINE) GRAFTED POLYHIPE FOAMS FOR EFFICIENT PLUTONIUM SEPARATION AND PURIFICATION²

² Pribyl, J. G., Taylor-Pashow, K. M. L.; Shehee, T. C.; Benicewicz, B. C. *ACS Omega* **2018**, *3*, 8181–8189.

Open-access article. Not subject to US copyright.

3.1 Abstract

The use of anion-exchange resins to separate and purify plutonium from various sources represents a major bottleneck in the throughput that can be achieved when this step is part of a larger separation scheme. Slow sorption kinetics and broad elution profiles necessitate long contact times with the resin, and the recovered Pu is relatively dilute, requiring the handling of large volumes of hazardous material. In this work, high internal-phase emulsion (HIPE) foams were prepared with a comonomer containing a dormant nitroxide. Using surface-initiated nitroxide-mediated polymerization, the foam surface was decorated with a brush of poly(4-vinylpyridine), and the resulting materials were tested under controlled flow conditions as anion-exchange media for plutonium separations. It was found that the grafted foams demonstrated greater ion-exchange capacity per unit volume than a commercial resin commonly used for Pu separations and had narrower elution profiles. The ion-exchange sites (quaternized pyridine) were exposed on the surface of the large pores of the foam, resulting in convective mass transfer, the driving force for the excellent separation properties exhibited by the synthesized polyHIPE foams.

3.2 Introduction

Past decades have seen pointed inquiry into improving the processes for recovering and purifying valuable fissile material from spent nuclear fuel

(reprocessing), legacy materials, mixed waste streams, etc.¹⁻¹¹ Despite these efforts, seasoned technologies such as organophosphorus-based solvent extraction (e.g., the PUREX process) and ion-exchange (IX) resins persist as the dominant techniques for separation and purification of fissile materials used independently or as part of a larger separation scheme. For plutonium, an anion-exchange resin purification conducted in nitric acid is the preferred technique for recovery from a variety of sources. Pu(IV) strongly adsorbs onto anion-exchange sites (quaternized pyridine) as the 12-coordinate hexanitrate complex in concentrated nitric acid (7–9 M).¹ Once the resin is loaded, it is generally washed with concentrated nitric acid to remove weakly bound or unbound impurities; then, the Pu(IV) is eluted from the column in dilute (0.35 M) nitric acid. The Pu(IV) recovered from this process is generally obtained in a highly pure form.² A popular resin used for this process is Reillex HPQ, a resin of partially methylated poly(4-vinylpyridine) (P4VP) cross-linked with divinylbenzene (25 wt %), which exhibits excellent stability in the harsh radiation and concentrated nitric acid conditions, hence its dominance as a Pu separation tool for the past three decades.⁴ Though Reillex HPQ is an excellent ion-exchange material from a capacity and stability point-of-view, it is not without disadvantages. The chief mechanism of mass transport in resin chromatography is diffusion into the small pores on a resin bead's surface. This slow process has important implications for

separation efficiency, including slow sorption kinetics and broad profiles during elution, leading to relatively dilute solutions of recovered Pu that must be handled. Processing actinides is a risky and expensive endeavor because of the radioactivity and toxicity characteristic of each actinide element; efforts to minimize the amount of hazardous material that must be handled are an important element of actinide separation process intensification.¹² The resin-based separation of Pu used as part of the HB-line process (a facility originally dedicated to the production of Pu-238 and now used for the recovery of valuable legacy fissile materials) at the Savannah River Site in Aiken, SC offers an opportunity to not only develop a material that has the strengths of an anion-exchange resin but also improve the mass transfer properties that may lead to more efficient separations. A scaffold that offers the potential to meet both needs lies in polymerized high internal-phase emulsion (polyHIPE) foams. PolyHIPEs are generally formed from water-in-oil emulsions in which the oil phase contains radically polymerizable monomer and cross-linker that are cured by a thermal radical initiator.¹³

Recent years have seen robust development of these porous polymers as solid supports for various separations and chemical transformations.¹⁴⁻²⁶ Specifically, polyHIPEs with surface-grafted chains of P4VP prepared via photoinitiated polymerization have been studied as a potential replacement for

columns of Reillex HPQ for the Pu purification process at the Savannah River Site.^{27,28} Conveniently, the backbone of the polyHIPE foam is polystyrene cross-linked with divinylbenzene (a similar chemical composition to the Reillex resin), which is known to have fairly good stability under the harsh acid and radiation conditions used for testing.⁴ In batch testing experiments, the foam samples were found to have faster uptake kinetics than the resin.²⁷ Testing of similarly prepared P4VP-grafted monoliths under controlled flow conditions showed that the Pu could be eluted from the columns much more efficiently than the resin and despite having a lower anion-exchange capacity (based on nitrogen content due to P4VP), some of the tested foams could adsorb more Pu per unit mass than the resin.²⁸ These performance improvements are likely owed to the convective mass transport made possible by the large open pore structure afforded by the polyHIPEs. Grafting the chains from the foam surface ensures all ion-exchange functionality is freely available on the surface of the foam, rather than hidden in the bulk of the material (like a resin bead). However, preparation of surface-grafted foams using a surface-photoinitiation approach limited the size of columns that could be produced and the amount of grafted P4VP was somewhat unpredictable.²⁸ To be a viable replacement for anion-exchange resins, the ion-exchange capacity of the foam materials needed improvement. Reported herein is a new approach to the synthesis of P4VP-grafted polyHIPE foams prepared

using a dormant nitroxide, which is incorporated into the foam backbone as a comonomer. The use of this functional comonomer allows for excellent control over the amount of nitroxide-mediated polymerization (NMP) sites available for surface-grafting chains of P4VP. Using this new approach to P4VP-grafted polyHIPE foams, monolithic columns were prepared with a much higher degree of P4VP functionalization than with the photoinitiated approach, also allowing for monoliths of any size to be prepared since the mode of initiation of the surface polymerization is thermal rather than light activated. Surface-grafted polyHIPE foam monoliths prepared in this manner were also tested for their Pu separation capabilities and were found to have excellent capacity and elution characteristics compared with the Reillex HPQ resin.

3.3 Experimental

3.3.1 Materials and Instrumentation.

All materials were purchased from Alfa Aesar, Acros Organics, Millipore Sigma, or McMaster-Carr and were used as received unless otherwise specified. Inhibitor was removed from styrene and divinyl benzene (mixed isomers) by passing each through a column of basic alumina. 4-Vinylpyridine was distilled under reduced pressure and stored under nitrogen at -30 °C prior to use. ¹H NMR spectroscopy was conducted on a Bruker Avance III-HD 300 MHz NMR spectrometer using CDCl₃ as a solvent. Molecular weight and dispersity of the

solution-based polymers were analyzed by gel-permeation chromatography (GPC). GPC was performed in HPLC grade N,N'-dimethylformamide (DMF) at a flow rate of 0.8 mL/min at 50 °C on a Varian system equipped with a ProStar 210 pump and a Varian 356-LC RI detector and three 5 µm phenogel columns (Phenomenex Co.). Samples were analyzed in comparison to narrow dispersity polystyrene standards. Scanning electron microscopy (SEM) images of the foams were observed with a Zeiss Ultraplus thermal field emission SEM at an acceleration voltage of 8kV. Prior to SEM imaging, the foam samples were rendered conductive via sputter coating for 60 seconds using a Pd/Au target. Foam compression experiments were performed at 25 °C using a parallel plate test fixture made of PTFE coated stainless steel on a dynamic mechanical analyzer (DMA) (TA Instruments, model RSAIII). Elemental analysis was performed at Midwest Microlab, Indianapolis, IN. Pu concentrations were determined by gamma spectroscopy using either a Canberra or Ortec high-purity germanium detector instrument.

3.3.2 General Procedure for the Synthesis of 1-[(4-Ethenylphenyl)methoxy]-2,2,6,6-tetramethyl-piperidine (3.1) and 2,2,6,6-Tetramethyl-1-(phenylmethoxy)-piperidine (3.2).

Compounds (3.1) and (3.2) were synthesized according to a modified literature procedure.²⁹ A solution of sodium ascorbate (4 g, 20 mmol) in 40 mL distilled water was shaken with (2,2,6,6-tetramethylpiperidin-1-yl)oxyl (TEMPO)

(1.9 g, 12.16 mmol) for 30 minutes until the TEMPO crystals were pale yellow in color. The suspension was extracted with 80 mL diethyl ether, and the organic layer was washed with water, brine, then dried over anhydrous MgSO_4 and concentrated on a rotary evaporator, yielding an orange oil. Sodium hydride (NaH, 60 % dispersion in mineral oil, 1.05g, 26 mmol) was added to an oven-dried 100 mL round bottom flask equipped with a magnetic stir bar. The NaH was washed 3x with hexanes under nitrogen flow to remove the mineral oil, then dried briefly under a high flow of nitrogen. Dry DMF (15 mL) was added to the NaH, forming a slurry. The reduced TEMPO was dissolved in dry DMF and added slowly to the NaH slurry. This mixture was stirred at room temperature for 1 hour, then 4-vinylbenzyl chloride (1.15 mL, 8.16 mmol) or benzyl chloride (0.939 mL, 8.16 mmol) was added via syringe and the reaction mix was stirred overnight under nitrogen protection. The mixture was slowly quenched with water, then extracted 2x with diethyl ether (40 mL). The organic layer was washed 3x with water to remove excess DMF, then brine, then dried over anhydrous MgSO_4 , and concentrated on a rotary evaporator. The product was purified by column chromatography (100% hexanes).

1-[(4-Ethenylphenyl)methoxy]-2,2,6,6-tetramethyl-piperidine (3.1).

Obtained as a colorless oil (1.025 g, 55% yield). ¹H NMR (300 MHz, CDCl₃) δ 1.14-1.35 (m, 12H), 1.47-1.61 (m, 6H), 4.81 (s, 2H), 5.22 (d, 1H), 5.73 (d, 1H), 6.71 (dd, 1H), 7.30-7.40 (m, 4H).

2,2,6,6-Tetramethyl-1-(phenylmethoxy)-piperidine (3.2).

Obtained as a colorless oil (1.23 g, 61% yield). ¹H NMR (300 MHz, CDCl₃) δ 7.26-7.39 (m, 5H), 4.83 (s, 2H), 1.36-1.68 (m, 6H), 1.26 (s, 6H), 1.15 (s, 6H).

3.3.3 Preparation of PolyHIPE Foam Monoliths.

The following is a general procedure for the synthesis of each polyHIPE foam monolith. Compound (3.1) (varying weight percent), styrene (varying weight percent), and divinyl benzene (0.275 g, 25 wt %) were combined to arrive at a total monomer mass of 1.1 g (specific formulations of each sample are detailed in Table 3.1). The monomers and sorbitan monooleate (SPAN 80, 0.4 g, 36 wt % relative to monomers) were combined in a small resin kettle equipped with a glass paddle stirrer. The aqueous phase, which consisted of distilled water (11 g) and potassium persulfate (K₂S₂O₈, 0.15 g) was added to a dropwise addition funnel. The aqueous phase was slowly added to the stirring oil phase (350 rpm) over the course of 15 min. After complete addition of the aqueous phase, the resulting emulsion was allowed to stir 5 additional minutes. The prepared emulsion was carefully deposited via syringe into thin glass tubing

(sealed on one end) and cured in an oven overnight at 70 °C. The foam monoliths were removed from the glass tubes by carefully breaking the glass, then washed for 24 h in a Soxhlet extractor (ethanol was used as the extraction solvent.) The monoliths were dried in a 70 °C oven overnight, and stored in plastic for further use.

3.3.4 Surface-Initiated Nitroxide-Mediated Polymerization of P4VP on PolyHIPE Monoliths.

A foam monolith weighing approximately 0.05 g was placed into a 50 mL Schlenk flask along with a small magnetic stir bar. The flask was sealed with a rubber septum (secured with copper wire), and the foam monolith was deoxygenated by evacuating and backfilling the flask with nitrogen five times. In a separate 50 mL Schlenk flask, 4-vinylpyridine (7.5 mL, 30 vol %) and n-butanol (17.5 mL, 70 vol %) were combined and degassed by 3 freeze-pump-thaw cycles. On the last cycle, the flask was back-filled with nitrogen. The thawed liquid mixture was transferred via gas-tight syringe to the flask containing the foam monolith (the foam readily soaks up the monomer mixture). The reaction mixture was heated at 130 °C for varying time intervals while stirring. The resulting polymer-grafted polyHIPE monolith was washed for 24 h in a Soxhlet extractor (ethanol was used as the extraction solvent), then dried in a 70 °C oven.

3.3.5 Assembly of polyHIPE anion-exchange column prototypes.

Small column prototypes used for testing under flow conditions were prepared according to the following procedure. The prepared polyHIPE monolith was coated in Devcon HP250 (a chemically resistant, high strength epoxy) and immediately encased in a layer of high-strength heat shrink tubing. The tubing was shrunk, and the epoxy was cured overnight. This process sealed the tubing to the monolith, minimizing the possibility of channeling around the monolith. Any excess epoxy was sliced off the ends of the monolith with a pristine razor blade so that liquid flow was not inhibited through the foam. Two more layers of heat shrink tubing were added so that the encased monolith fit snugly into the end of hose connectors which were attached with more Devcon HP250 epoxy. The assembly was tested by flowing water through to ensure there were no leaks prior to testing. Specific column dimensions for each sample are shown in Table 3.1 and an image of some of the prepared prototypes is shown in Figure 3.1.

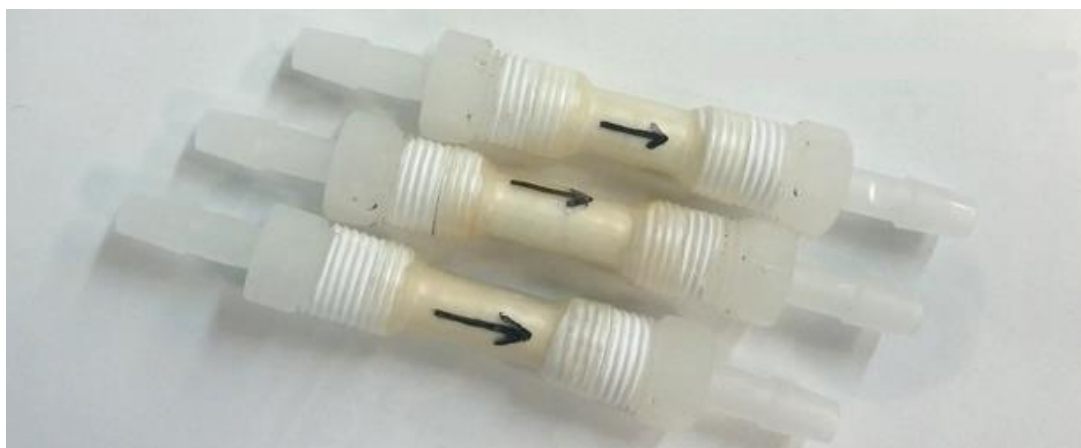


Figure 3.1: Image of prepared polyHIPE column prototypes. (Total length of the column assemblies is approximately 9 cm)

Table 3.1: Dimensions and formulation information of materials tested

Sample	Length (mm)	Diameter (mm)	Volume ^a (mL)	Mass (g)	% Styrene in Initial Emulsion (wt %)
A	40	8	2.01	0.3092	52
B	35	8	1.76	0.3665	40
C	32	8	1.61	0.2875	45
D	33	8	1.66	0.3032	52
E	35	9	2.23	0.4078	40
F	33	7	1.27	0.2089	40
G	35	8	1.76	0.3321	45
Reillex HPQ	-	-	2.75	2.4475	-

^aCalculated from column length and diameter

3.3.6 Plutonium Adsorption and Elution Studies.

Pu sorption and elution properties of the prepared polyHIPE foam column prototypes were studied using a feed solution of ~4 g/ L Pu in 8 M nitric acid (data for each sample is normalized for the precisely determined feed concentration for comparison between samples). These conditions approximate

the conditions of the Pu separation of the HB-line process at the Savannah River Site. The feed solution was prepared by treating stock Pu solution with ascorbic acid to reduce all Pu(IV) to Pu(III). The acid concentration was then adjusted to 8 M, and the Pu(III) was oxidized to Pu(IV), forming the $[\text{Pu}(\text{NO}_3)_6]^{2-}$ complex which readily loads onto quaternized pyridine anion-exchange sites (for the purposes of this testing, the feed solution contained only Pu and no other major contaminants). Each prepared column was conditioned with approximately 10 mL of 8 M nitric acid at a flow rate of 0.75 mL/min (using a programmable syringe pump) to protonate the pyridine groups and to remove any water or dilute nitric acid from the column. The prepared Pu feed solution was then fed at 0.5 mL/min and 1 mL aliquots were collected until breakthrough of the Pu feed was visually observed. The columns were washed with 10 mL of 8 M nitric acid at 0.75 mL/min to remove any unbound impurities, and the adsorbed Pu was eluted with 0.35 M nitric acid at a flow rate of 0.5 mL/min, collecting 1 mL aliquots until elution was complete. The results of the tested polyHIPE materials were compared to the results of a similarly-scaled glass column packed with Reillex HPQ resin which was tested according to the procedure detailed above. An image of the testing set-up is shown in Figure 3.2.

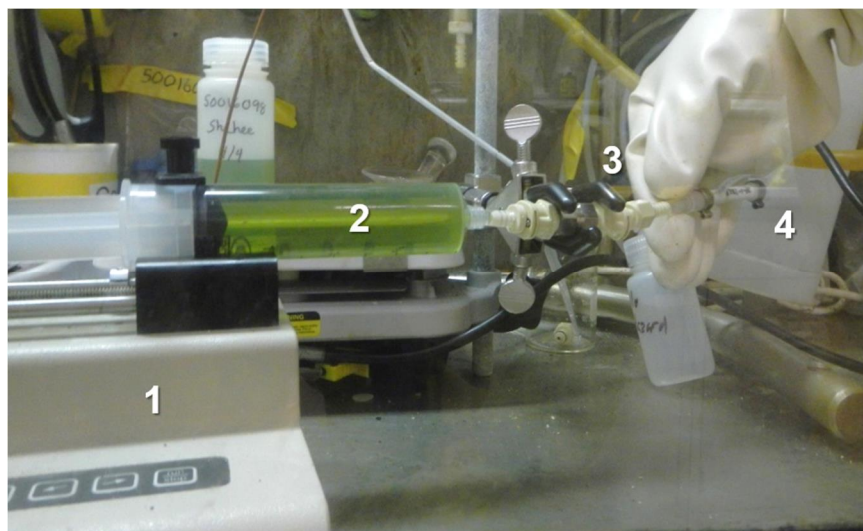


Figure 3.2: Image of the flow-testing set up used to conduct controlled flow testing of Reillex HPQ and assembled polyHIPE column prototypes. (1) Programmable syringe pump (2) ~4 g/L Pu(IV) feed solution in syringe (3) “quick connect” hose connectors (4) polyHIPE column prototype

3.3.7 DMA Compression Testing of PolyHIPEs.

In a typical experiment, a predetermined compressive force (pounds per square inch, psi) was applied to a small section of foam for varying duration (see Figure 3.4) during which sample thickness (% Strain) was measured as a function of time. This was followed by removal of the force and observation of the strain recovery for 15 min.

3.3.8 Solution-Based Kinetic Study of (3.2).

Compound (3.2) (0.1 g, 1 eq.), 4-vinylpyridine (8.7 mL, 200 eq.), and n-butanol (20.3 mL) were added to a 50 mL Schlenk flask equipped with a 1 inch stir bar, a glass stopcock, and rubber septum. The flask was sealed and the reaction mix was degassed by three freeze-pump-thaw cycles, then backfilled

with nitrogen. The flask was heated to 130 °C while stirring, and aliquots of the reaction solution were taken at varying time intervals and analyzed by ^1H NMR for reaction conversion information. The remainder of the aliquots were precipitated in diethyl ether, and the polymer was recovered by centrifugation. Molecular weight and dispersity characteristics of the polymer samples were determined by GPC analysis in DMF.

3.3.9 Irradiation Testing of PolyHIPE Materials.

Gamma irradiation was performed using a J.L Shepherd Model 484 Co-60 Irradiator (Figure 3.3). This irradiator features two 715 Ci Co-60 source rods in the irradiation chamber and allows users to adjust the target proximity to vary the desired dose rate. For this work, a 1 cm thick steel vessel containing samples submerged in 8M nitric acid was placed as physically near the source rods as allowable and set within a glass beaker for secondary containment. A vent line was attached to the steel vessel to allow any fumes or generated gases to exit the irradiation chamber and into a gas bubbler.

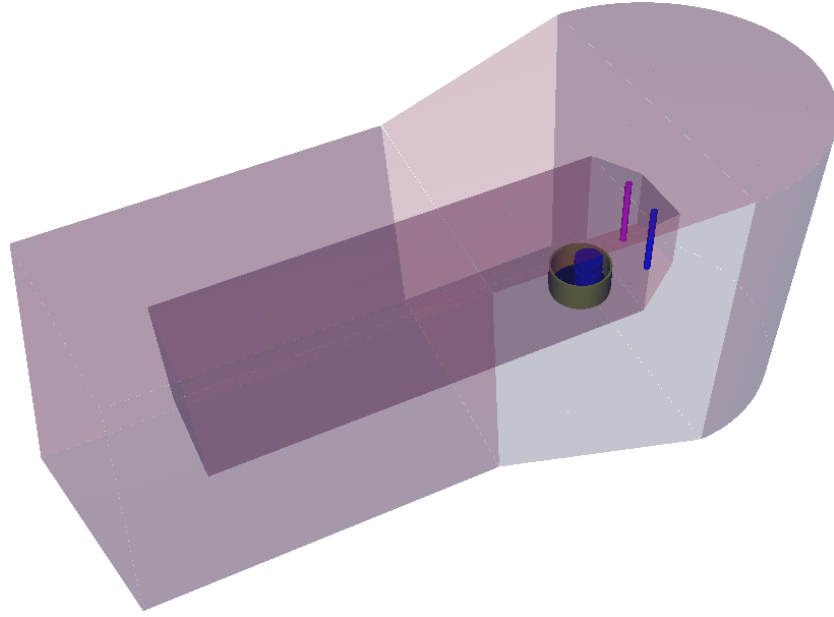
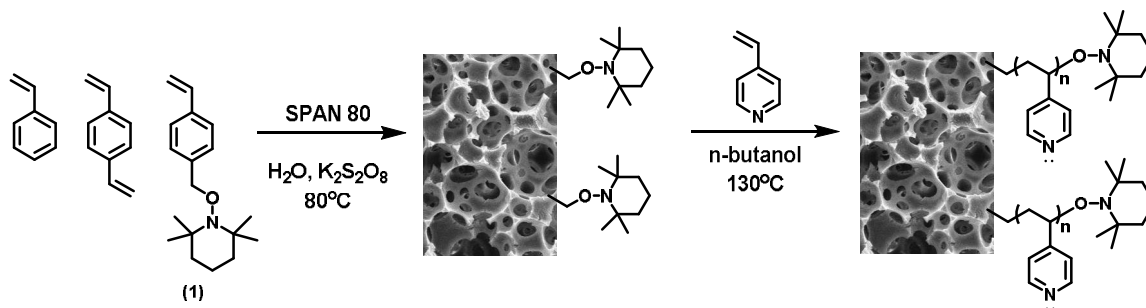


Figure 3.3: Illustration of J.L. Shepherd Model 484 Co-60 Irradiator

Irradiation was performed over a period of 7 weeks, totaling 1173.2 hours of active irradiation time. The samples were removed periodically to ensure appreciable evaporation had not occurred. Accumulated sample dose during this period was determined through a Monte Carlo N-Particle (MCNP) modeling of the irradiator and experiment set up. MCNP6 is a general purpose Monte Carlo code that can be used for neutron, photon, electron, or coupled transport. It is used to calculate position-dependent radiation flux and resultant effective dose rates for any user specified geometry and source definition. Dose rates were calculated using decay corrected source activities throughout the irradiation period.

3.4 Results and Discussion



Scheme 3.1: Synthesis of polyHIPE foams with surface grafted chains of P4VP via a dormant alkoxyamine-containing co-monomer (3.1)

A main aim of this work was to increase the anion exchange capacity of P4VP grafted polyHIPE monoliths. Previous work with these materials showed their promising chromatographic separation behavior owed to an interconnected pore structure and the method of incorporating anion exchange functionality directly on the surface of the foam where it can be freely accessed in solution through convective mass transport.²⁷⁻²⁸ PolyHIPE foams have previously been shown to have very robust mechanical properties (yield strengths of up to 130 psi).^{27,30} PolyHIPE foams representative of those tested in this report (pre- and post-P4VP grafting) were tested for their mechanical properties under a series of compressive forces (60-100 psi) (Figure 3.4). It was found that at each pressure tested, the foams exhibited elastic recovery, even after applying the compressive force for 12 hours. This is evidence that under these pressures the polyHIPE foams do not mechanically degrade. Despite these desirable properties, the

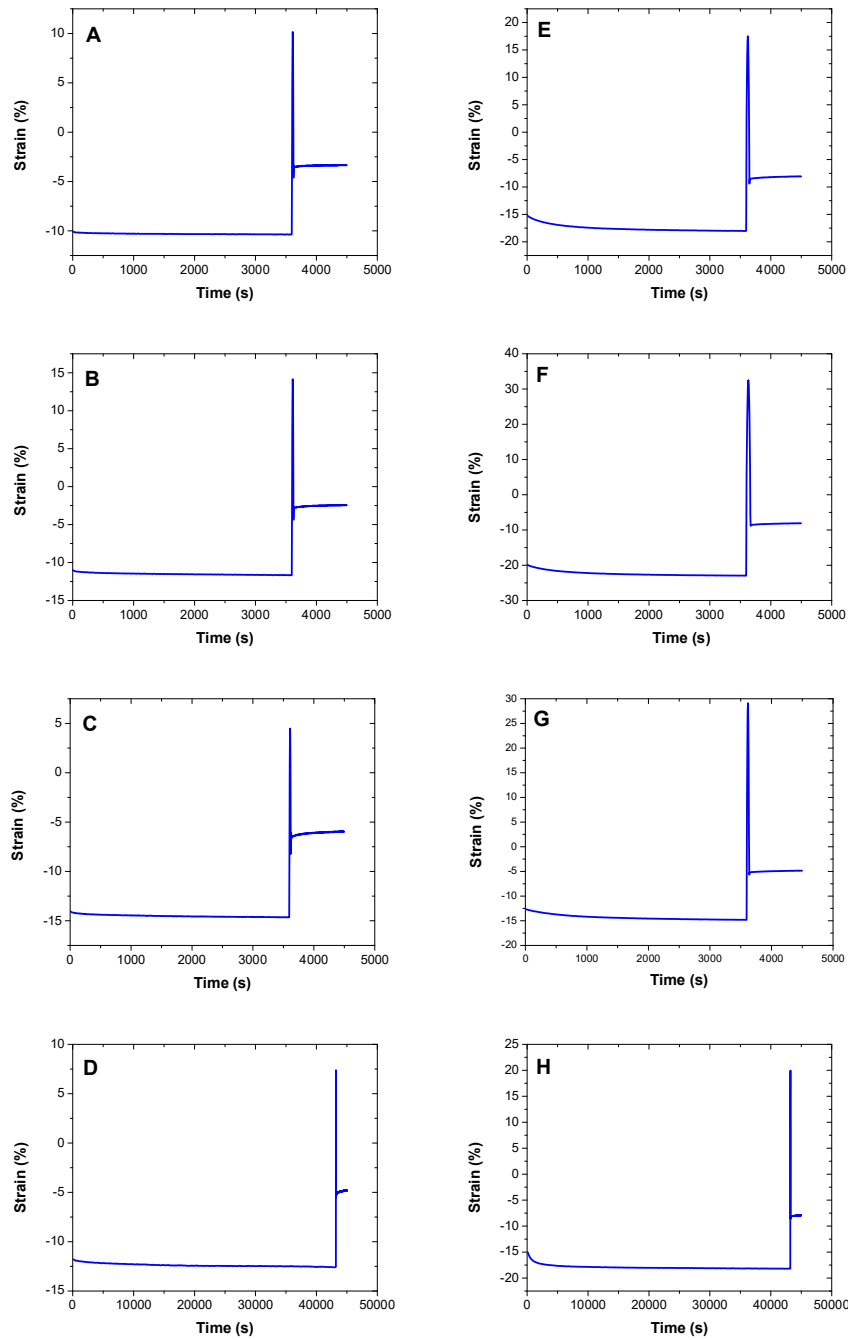


Figure 3.4: Dynamic mechanical analysis of polyHIPE foams before surface polymerization (A-D) and after surface grafting with P4VP (E-H). Testing was conducted at a series of static pressures (A and E = 60psi 1 hr, B and F = 80 psi 1 hr, C and G = 100 psi 1 hr, D and H = 60 psi 12 hr). Strain recovery was observed for 15 min in each experiment.

foams prepared by photoinitiated graft polymerization could not be prepared with comparable ion-exchange capacity to the Reillex HPQ resin on a volumetric basis, an important parameter if these materials should become suitable to directly replace a resin column in a separation scheme, for example.²⁸ To overcome this limitation, a new approach to synthesizing polyHIPE foams with many surface-bound initiating sites was developed (Scheme 3.1). This method borrows a concept from early work done with star and hyperbranched polymers by Hawker and co-workers;³¹⁻³³ the vinyl moiety on the nitroxide containing monomer can be radically polymerized at a lower temperature than that which homolytically activates the carbon-oxygen bond of the alkoxyamine. This allows for the incorporation of the functional co-monomer (3.1) at high weight fractions in the initial high internal-phase emulsion, and the co-monomer content can be tuned more or less independently from the pore structure of the polyHIPE. Some of the dormant nitroxide groups then presumably end up on the surface of the cured foam and are available as surface initiating sites to grow P4VP.

Table 3.2: Physical and chemical characteristics of synthesized polyHIPE foams and Reillex HPQ resin

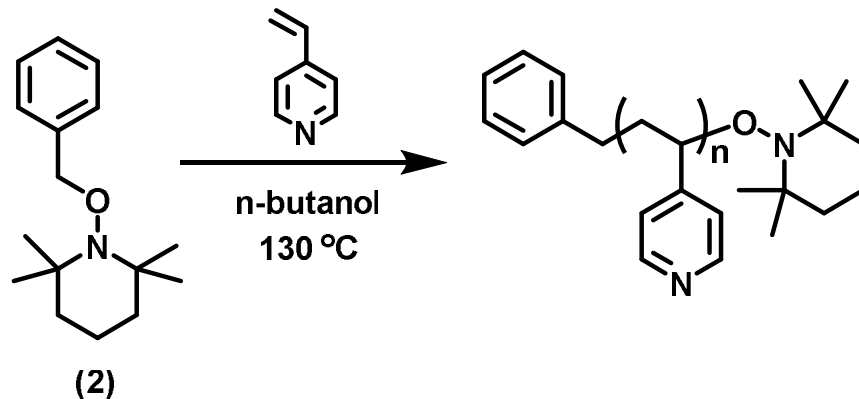
Sample	Cross-linker Content (wt %)	% of Co-monomer 1 in Initial Emulsion (wt %)	%N Before Surface Polymerization	%N After Surface Polymerization	Surface Polymerization Reaction Time (hr)	%N Due to P4VP ^a	Weight Gain (%) ^b	Density (g/cm ³) ^c
A	25	23	1.12	9.81	25	9.56	366	0.153
B	25	35	1.49	11.37	25	11.16	599	0.208
C	25	30	1.23	11.35	25	11.14	490	0.178
D	25	23	1.05	10.65	25	10.46	450	0.183
E	25	35	1.49	11.65	48	11.47	722	0.183
F	25	35	1.49	8.38	6	7.84	272	0.164
G	25	30	1.50	10.89	25	10.44	472	0.188
Reillex HPQ	25	-	--	--	--	8.75 ^d	--	0.890

^aValues represent percent nitrogen only due to P4VP ^bPercent weight gain of the monolith based on the initial and final mass of the monolith ^cCalculated from monolith dimensions and mass ^dCalculated theoretical value

Table 3.2 summarizes the measured characteristics of the polyHIPE foams prepared for testing. The crosslinker content of the polyHIPE foam was kept constant throughout all samples to emulate the backbone structure of the resin (and ideally a similar chemical stability in harsh conditions). The nitrogen content of the polyHIPEs was analyzed before and after the surface polymerization. The nitrogen in the cured polyHIPEs is due to the dormant nitroxide, and the nitrogen present in the samples after the surface-initiated polymerization of P4VP represents the nitrogen due to the combination of nitroxide groups and polymer present. Because the surface-bound initiating

species is a benzyl radical, directly characterizing the grafted P4VP is difficult because there is no straightforward way to cleave the grafted polymer.

A solution analog of the initiating species was synthesized and the kinetics of the polymerization were studied according to Scheme 3.2. The results of the kinetic study are shown in Figure 3.5. An approximately linear relationship between $\ln([M_0]/[M_t])$ and time indicates a pseudo first-order relationship between monomer consumption and reaction time (Figure 3.5a). The evolution of molecular weight with respect to monomer conversion (Figure 3.5b) is fairly linear up to ~30% conversion, with dispersity (\bar{M}_w/\bar{M}_n) values ranging from 1.3-1.55. It is important to note that there are many examples in the literature which demonstrate that rates of polymerization may differ greatly between solution polymerizations and surface-initiated polymerizations.³⁴⁻³⁷ This study was not intended to be used as a direct estimation of the kinetics of the surface-initiated polymerization, but rather to serve as a model for how well-controlled the surface-initiated polymerization may be. Based on the behavior of the polymerization of P4VP in solution initiated by compound (3.2), we hypothesize that the polymerization behavior of P4VP grown from the foam-bound NMP initiating species (which is chemically very similar to the benzyl radical generated in the solution study) is qualitatively similar to the solution study in terms of the initiation and nitroxide-mediated control on the growing polymer.



Scheme 3.2: Solution-based kinetic study of the polymerization of P4VP using (3.2).

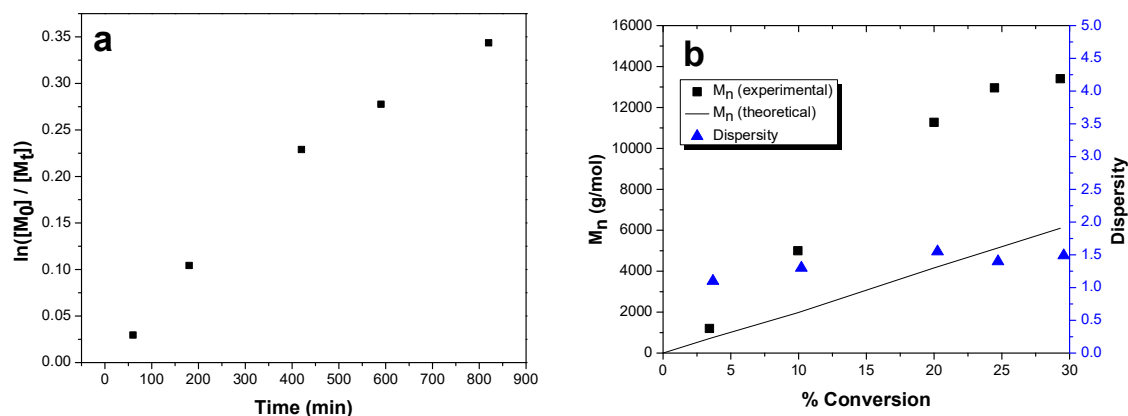


Figure 3.5: (a) Kinetic plot and (b) dependence of the GPC molecular weight, theoretical molecular weight, and dispersity on the conversion for the polymerization of 4-vinylpyridine (4-VP) initiated by (3.2). ($[4\text{-VP}]:[(3.2)] = 200:1$, and $4\text{-VP}/n\text{-butanol} = 30/70$ v/v).

After each surface-initiated polymerization of P4VP on the polyHIPEs, there was an appreciable increase in mass for all samples, indicating that a large amount of ion-exchange functionality was grafted from the foam surface. Figure 3.6 shows the foam morphology after curing (A and B) and after the surface polymerization (C and D), respectively. From images A and C in Figure 3.6, there is not a perceptible difference in the overall morphology of the pore structure

before and after the graft polymerization. There is a marked difference in the surface of the foam before and after the surface polymerization which is observed at high magnification (images B and D). The evolution of a distinctly rougher texture is a visual indication of the grafted polymer brush which extends from the foam surface.

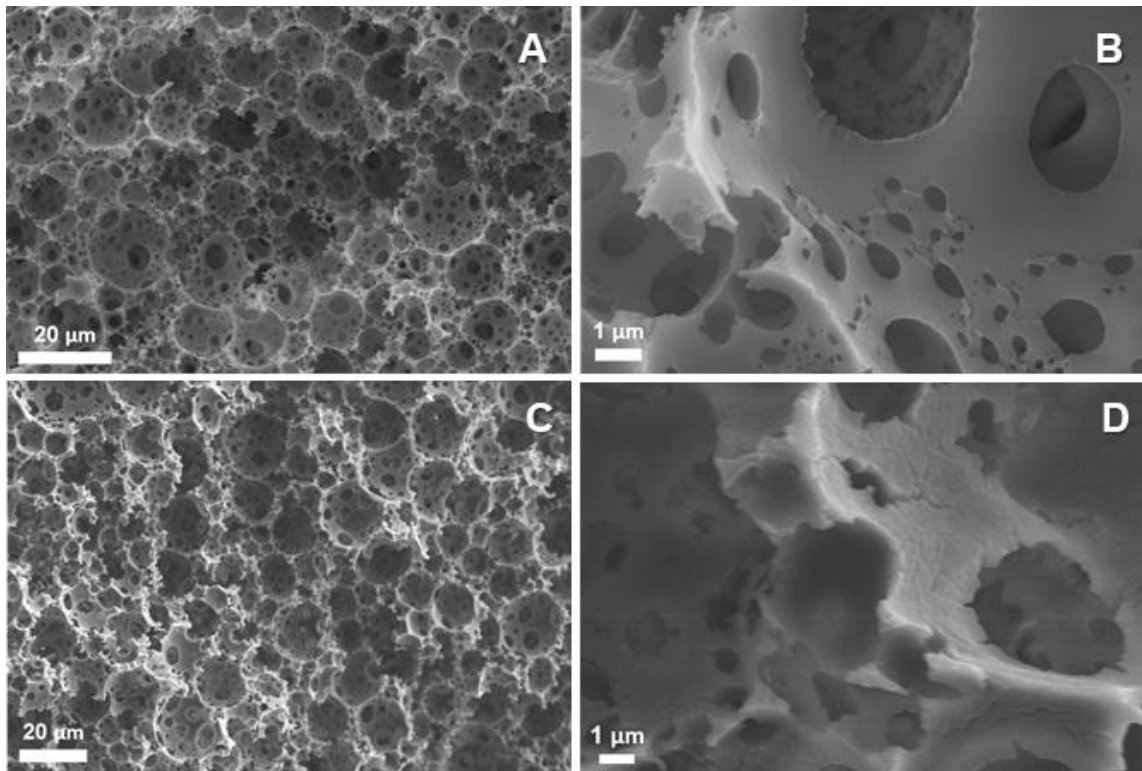
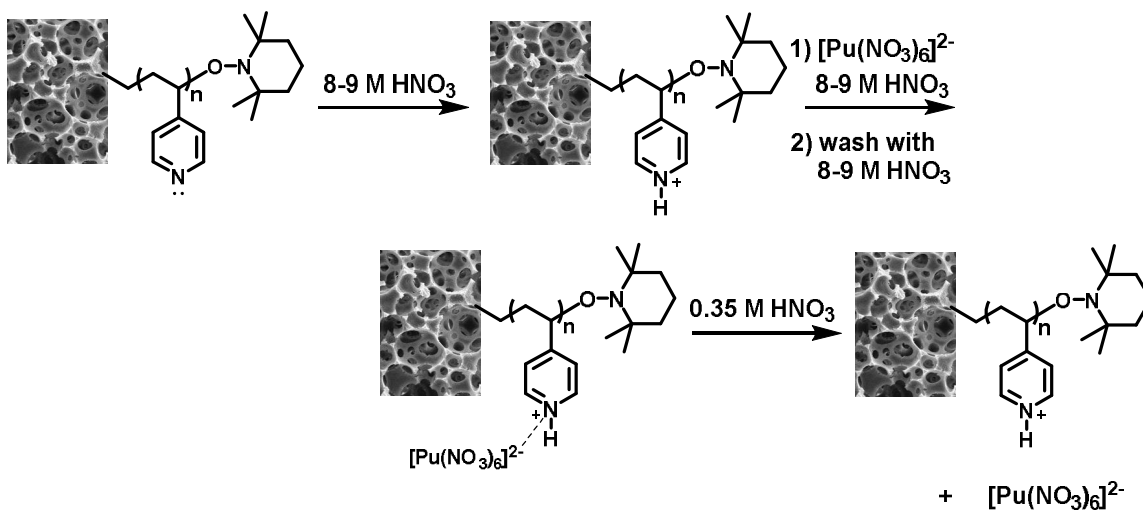


Figure 3.6. Representative SEM images of polyHIPE foams (A-B) after curing and (C-D) after the surface-initiated polymerization of P4VP. (Scale bars are 20 μm in images A and C, and 1 μm in images B and D).

Column prototypes made from the synthesized polyHIPE monoliths were tested under controlled flow conditions for their Pu adsorption capacity and elution characteristics according to Scheme 3.3. In these tests, our aim was to demonstrate that this material efficiently binds and elutes Pu under these test

conditions, so pure Pu solution was used to demonstrate these properties. In the separation scheme used at the HB line facility, the only ion which efficiently binds with the resin at this particular step of the scheme is the $[\text{Pu}(\text{NO}_3)_6]^{2-}$, so



Scheme 3.3: Outline of the Pu sorption/elution flow testing performed on prepared polyHIPE column prototypes

these polyHIPE materials, in principle, should exhibit similar selectivity towards the Pu ions at this step of the separation scheme since the anion exchange group is the same. Figure 3.7 shows the Pu loading curves of each tested material as a function of bed volumes of the ion-exchange material. The resin and foam materials are compared on a volumetric basis (bed volumes) because of the large difference in the density between them. Column bed volumes (defined as the volume of solution required to fully saturate the monolith or resin bed) are normalized values to account for small differences in void volumes between samples. Measured concentrations of Pu are expressed as $[\text{Pu eluate}]/[\text{Pu feed}]$,

where when the ratio is less than 1, the concentration of the collected eluate was less than the feed solution, and when the ratio was greater than 1, concentration of the collected eluate was greater than the feed solution. It was found that the

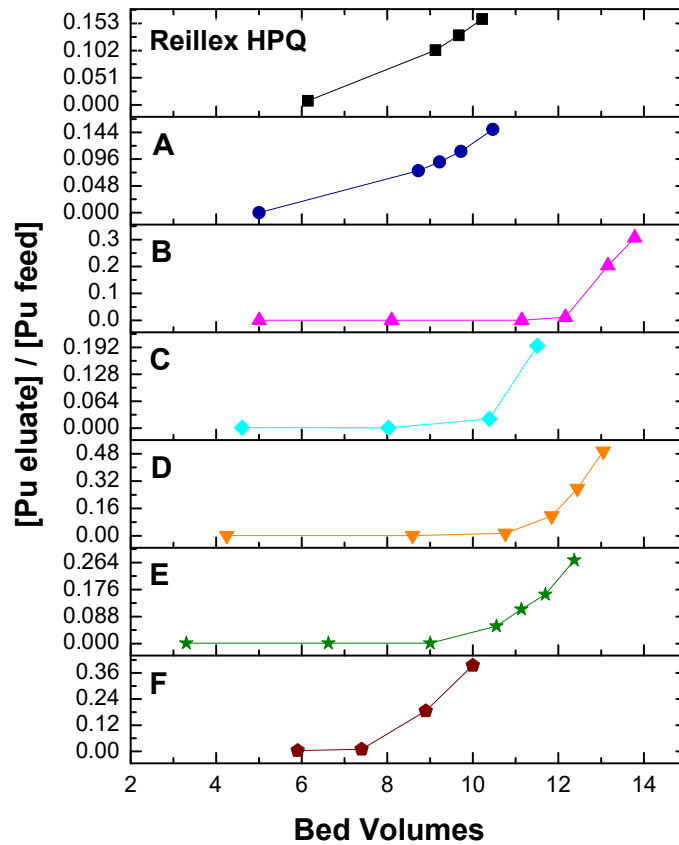


Figure 3.7: Plutonium breakthrough curves of Reillex HPQ and tested polyHIPE materials. (Labels A-F refer to the polyHIPE foam samples described in Table 3.2).

majority of the polyHIPE samples tested equaled or exceeded the capacity of the Reillex HPQ resin as a function of the number of bed volumes until significant (~10%) breakthrough of the feed solution occurred. This confirms that the

procedure developed in this work to incorporate many NMP initiating sites into the foam backbone which are activated thermally is an effective strategy for imparting a large amount of ion-exchange functionality onto the foam surface. Interestingly, there is an approximately linear correlation between the capacity of each of the polyHIPE samples with respect to the amount of nitrogen due to P4VP in the sample (Figure 3.8). This indicates that there is no discernible effect on the Pu capacity from the graft density (chains per unit area) or the molecular weight of the grafted chains.

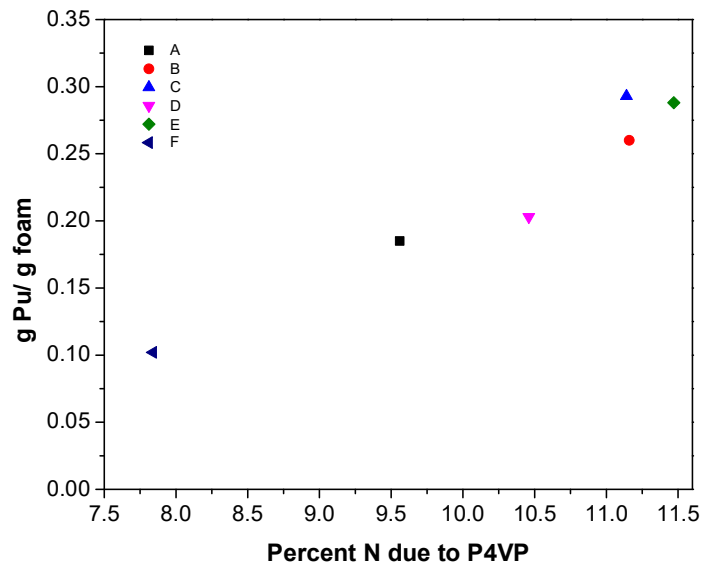


Figure 3.8: Correlation between Pu capacity and percent N due to grafted P4VP on polyHIPE foam samples

The corresponding elution curves for the above-mentioned samples are presented in Figure 3.9. The key benefit of the convective mass transfer resulting from the foam's large interconnected pore structure is realized here. For each of the foam samples, the loaded Pu is fully eluted from the column over the course

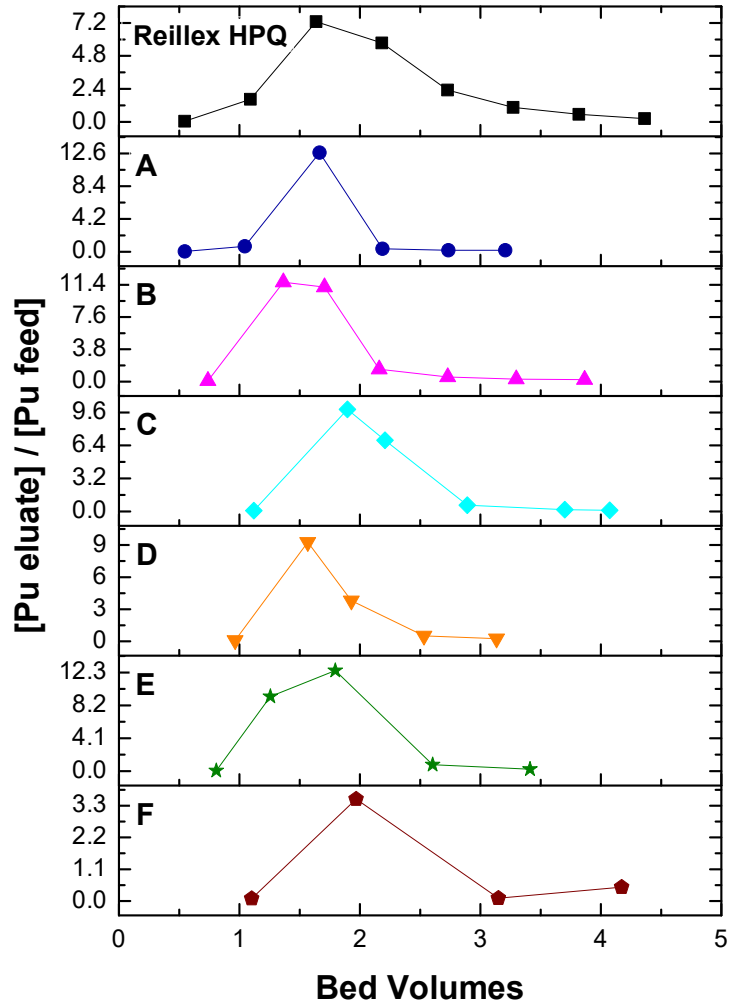


Figure 3.9: Elution curves of Reillex HPQ and tested polyHIPE materials. (Labels A-F refer to the polyHIPE foam samples described in Table 3.2).

of approximately two bed volumes, sometimes fewer. In comparison, quantitative elution of the Pu from the Reillex HPQ column occurs over about four bed volumes, meaning that the collected Pu eluate is much less concentrated than the eluate generated from the foam materials. This broadened elution profile is a direct result of the diffusive mass transfer occurring in the pores of the resin beads. From a process intensification standpoint, the fact that the foams

can release the adsorbed Pu in about half the number of bed volumes required for the Reillex HPQ means a smaller volume of hazardous material to handle after the separation, and that the recovered Pu (which is very valuable) is obtained in a more concentrated form with less loss of material to the dilute heads and tails cuts of the elution. Note that for sample A, the recovered Pu was than 12 times more concentrated than the feed solution.

The bulk capacities of the tested materials are presented as a function of volume and mass in Figure 3.10. It is significant that some of the tested foams exceeded the capacity of the resin when compared volumetrically because the foams are about six times less dense than the resin. Despite having much less mass than a similar volume of resin, the polyHIPE could load 60% more Pu per unit volume than the resin in the case of sample B. When the materials are compared on a gravimetric basis, the capacity difference is much more dramatic. Sample C, which demonstrated the highest Pu capacity per unit mass, had 7.7x the capacity of the resin. Combined with the separation efficiency of the polyHIPE materials, the improvement in capacity compared to the resin suggests that these materials have real potential to significantly improve upon the efficiency of current Pu separation and purification technologies.

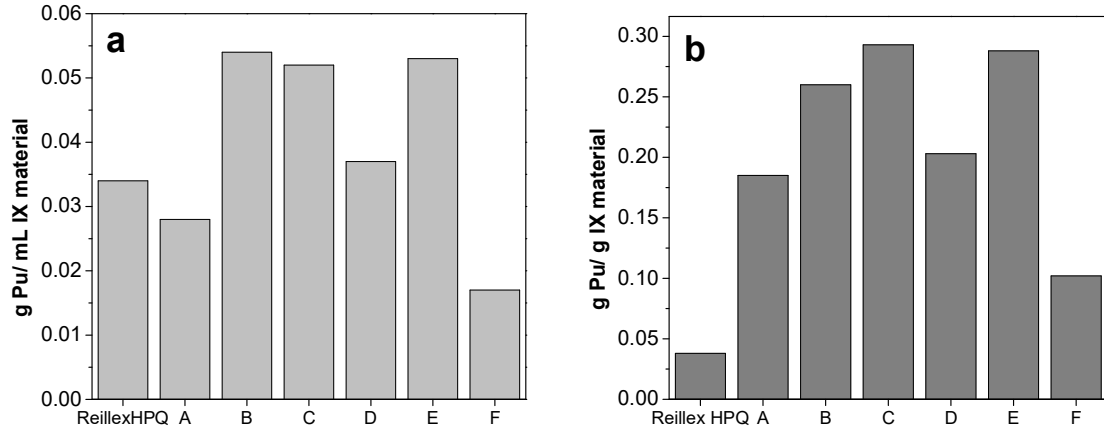


Figure 3.10: Bulk Pu capacity of each ion-exchange (IX) material on a volumetric basis (a) and gravimetric basis (b).

Another important parameter which warranted inquiry is the maintenance of ion-exchange capacity over repeated cycles and the stability of the polyHIPEs in the harsh acid and radiation environments inherent to this separation. A polyHIPE (sample G) was prepared and subjected to four loading and elution cycles to study if there was any effect on the capacity or separation efficiency with repeated use. The loading and elution curves generated from this testing are shown in Figure 3.11.

Over the course of 4 anion-exchange cycles, the number of bed volumes until ~10% breakthrough ranged from about 10 to 12 bed volumes, with the highest capacity exhibited on the first cycle (determined by number of bed volumes until 10% breakthrough) (Figure 3.11, left). The three following cycles had a variability of less than one bed volume at this level of breakthrough. One explanation for this difference in Pu adsorbed until breakthrough between the

first cycle and the following cycles is that some amount of Pu loaded during the first cycle remains bound to the polyHIPE, and after this equilibrium is reached the capacity stabilizes in subsequent cycles. The efficiency of Pu elution is similar for each sample tested, given there is little change in the width of the elution profile between each trial (Figure 3.11, right).

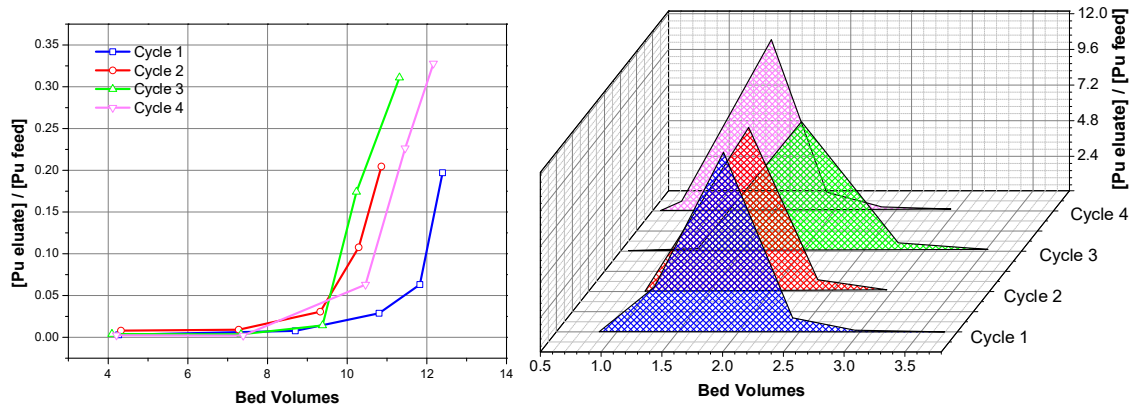


Figure 3.11: Loading and elution curves for polyHIPE sample G over four Pu anion-exchange cycles.

When the bulk capacity of the column is compared across the four loading/elution cycles, a similar trend is observed. After the first cycle there is a slight decrease in the capacity, but the capacity is recovered for the third and fourth cycles (Figure 3.12). Based on this information, the hypothesis is that a small amount of the Pu loaded during the first cycle remains somehow bound to the foam after the first elution, but then some of that may desorb during further cycles until some equilibrium amount is reached, after which the capacity remains relatively steady.

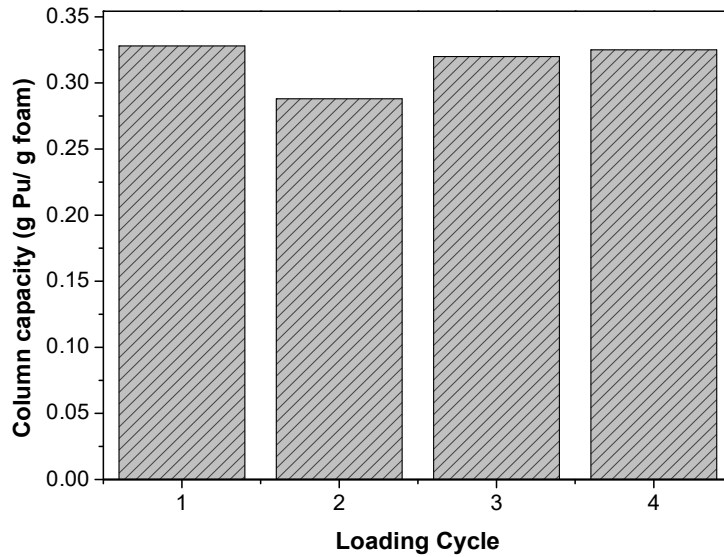


Figure 3.12: Bulk Pu capacity of polyHIPE sample G across four loading/elution cycles.

The polyHIPE materials were also evaluated for their stability to the harsh acid and radiation conditions. Two identical polyHIPE samples were synthesized and one was soaked in 8 M nitric acid for seven weeks and the other was soaked in 8 M nitric acid as well as being irradiated by a Co-60 gamma irradiation source for seven weeks to a total dose of approximately 7.8×10^7 rads. It was found that after about 48 days (approximately 7 weeks) under these conditions, both polyHIPE monoliths had degraded significantly and could not be tested for their Pu capacity (Figure 3.13).

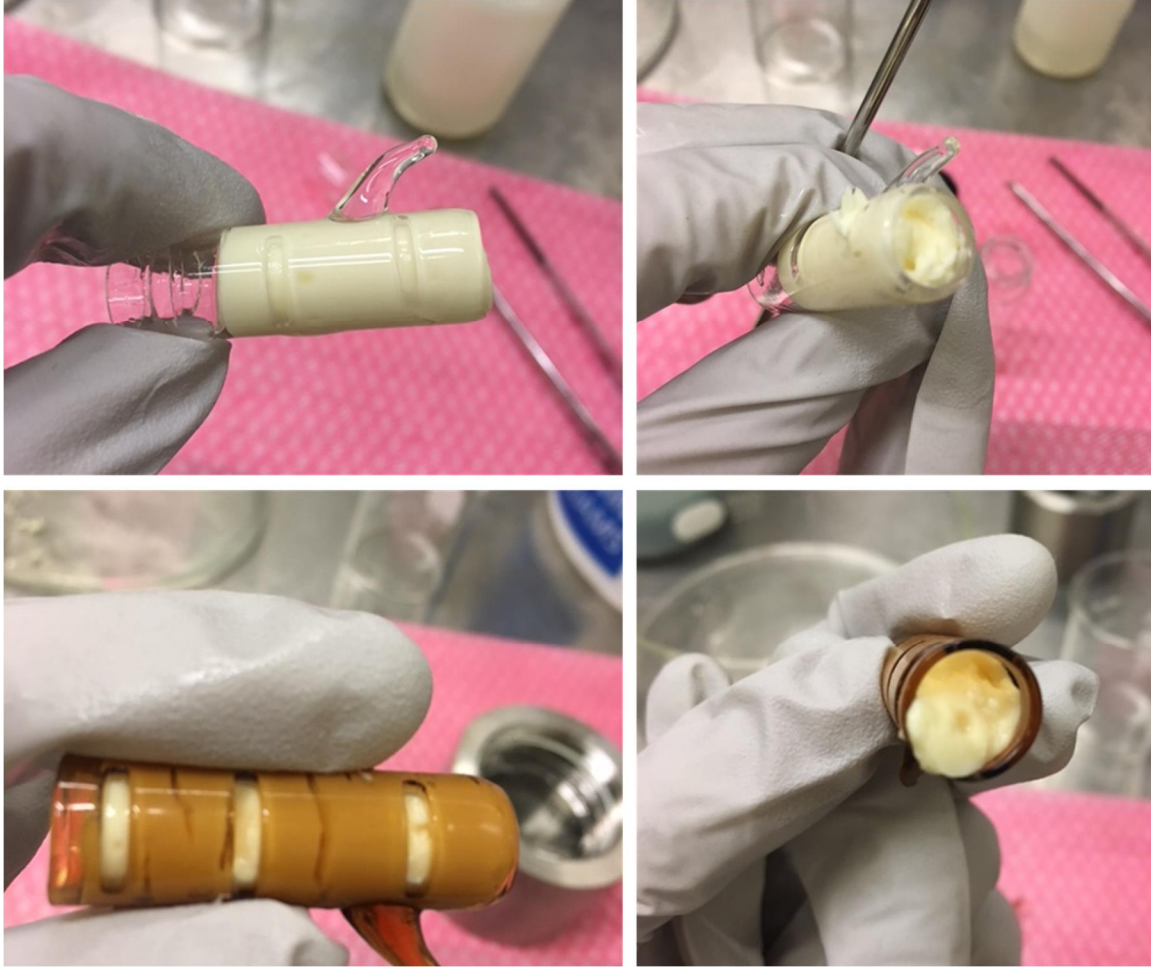


Figure 3.13: Photos of polyHIPeS (top) after soaking in 8 M nitric acid for approx. 7 weeks and (bottom) after soaking in 8 M nitric acid with gamma irradiation for approx. 7 weeks (total dose $\sim 7.8 \times 10^7$ rads). Samples were placed in the glass holders to keep the foam submerged in acid during the soaking.

Due to the proximity of the steel vessel containing the samples to the Co-60 sources, there was a strong spatial dependency on the dose rate and therefore total dose absorbed by the sample. A color contour map of absorbed dose within the steel vessel is provided in Figure 3.14. The value of total absorbed dose within the vessel ranges from 6×10^7 to 1.1×10^8 Rads. A volumetric averaged dose within the vessel was determined to be 7.75×10^7 Rads. All dose rates were

determined using F4 track length estimator tallies modified by ANSI/ANS6.1.11977 Fluence to Dose Conversion Factors.

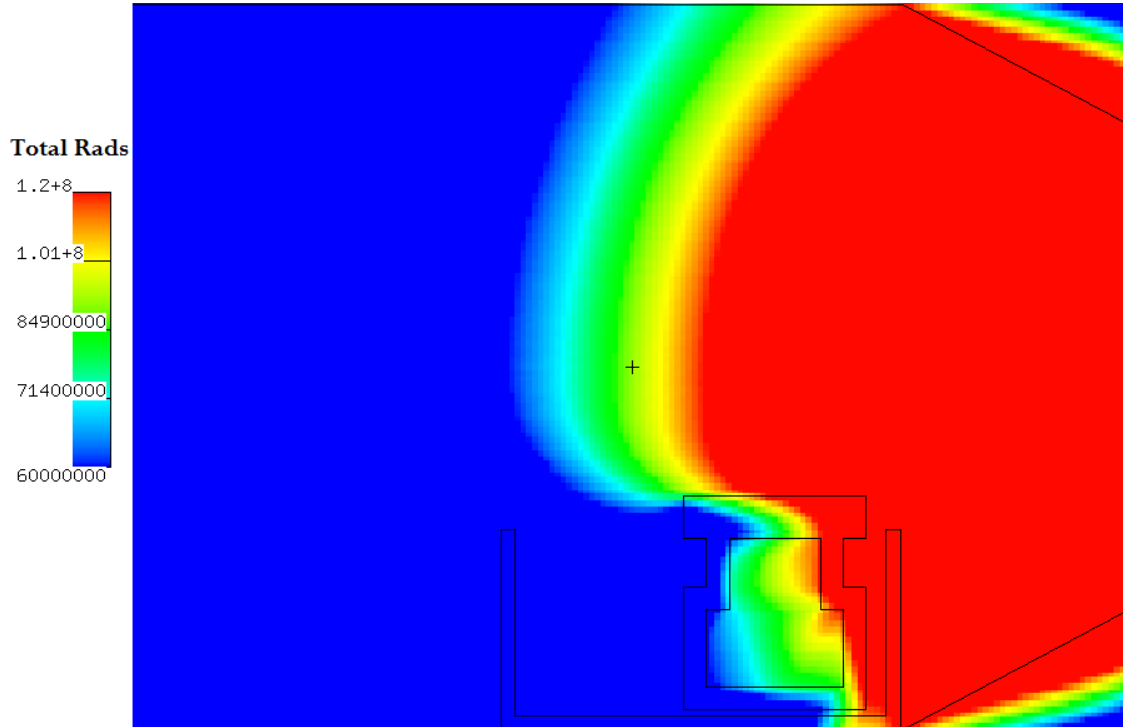


Figure 3.14: Colormap of radiation dose within irradiator vessel (side view)

The Reillex HPQ resin is limited to 1×10^8 rads exposure before change-out when it is used in the HB line process at the Savannah River Site.³⁸ This amount of radiation was thus chosen as the target dose for the foam samples tested (see Figure 3.13). However, it was difficult to understand the effects of this dose of radiation on the foam samples because a sample which was soaked in ~8 M nitric acid for the same amount of time degraded to the extent that it could not be tested. The same was true for the irradiated sample (also soaked in 8 M nitric acid). Under similar conditions (conc. nitric acid, same radiation exposure), the

Reillex loses some anion-exchange capacity, but does not show the same structural degradation seen in the foam samples.³⁹ This is attributed to the 4-vinylpyridine incorporated into the resin backbone, which has been shown to be more radiolytically stable than styrene/divinylbenzene systems.³⁹

It is worth noting that during the cyclic testing of sample G, the time elapsed between cycles two and three was about three months. During that time, the polyHIPE had remained saturated with the 0.35 M nitric acid and based on the testing results detailed above, did not appear to have degraded or lost an appreciable amount of anion-exchange capacity. As a result, these materials appear to be relatively stable to the dilute acid and exposure to radiation over that amount of time. The ability to store the polyHIPE monolith saturated in dilute nitric acid between loading cycles is consistent with the common way that the Reillex HPQ is treated. The resin is generally only saturated with concentrated nitric acid when it is actively being primed or loaded with Pu out of caution to avoid potentially violent reactions between the organic polymer and nitric acid.³⁸

3.5 Conclusion

In this work, a new synthetic approach to P4VP-grafted polyHIPE materials was explored and their capabilities as ion-exchange media for Pu separations was evaluated. The ability to incorporate many NMP initiation sites

into the surface of the foam using a functional co-monomer in the initial high internal-phase emulsion enabled the growth of a brush of P4VP with a sufficient number of ion-exchange sites to exceed the anion-exchange capacity of a commercial resin on both a volumetric and gravimetric basis. The exposed nature of the P4VP brush on the surface of the polyHIPE foam enabled excellent separation efficiency in the form of narrow elution profiles, and the purified Pu was obtained in very concentrated form compared to the resin. The polyHIPE materials were found to retain their separation capabilities over the course of four anion-exchange cycles and were found to be stable for months in dilute nitric acid with exposure to radiation. Based on the results of these experiments, these polyHIPE materials appear to be a suitable replacement for ion-exchange resins used in the separation and purification of Pu where higher efficiency and loading is desired.

Many exciting aspects of these materials such as their high ion-exchange capacity per unit mass and excellent separation efficiency indicate that these materials may have applications in other areas of actinide science and separations in general. For example, growing a brush of polymer containing an organophosphorus ligand which can selectively chelate different actinides may offer an attractive route to separating or purifying other actinide elements. The high gravimetric capacity of these polyHIPEs may also allow for high efficiency

capture and sequestration of radioactive materials or fission products with little practical use (given the mass of material which would then need to be sequestered would be very low compared to other sequestration technologies). Simple tuning of the chemistry of the polymer brush grown using this synthetic approach to polyHIPEs renders these materials very versatile and viable alternatives to many existing separation technologies.

3.6 References

- [1] Marsh, S. F. Reillex™ HPQ: A New, Macroporous Polyvinylpyridine Resin for Separating Plutonium using Nitrate Ion Exchange. *Solvent Extr. Ion Exch.* **1989**, *7*, 889–908.
- [2] Navratil, J. D.; Yuezhou, W. Actinide Ion Exchange Technology in the Back End of the Nuclear Fuel Cycle. *Nukleonika* **2001**, *46*, 75–80.
- [3] Bhattacharyya, A.; Mohapatra, P. K.; Manchada, V. K. Solvent Extraction and Extraction Chromatographic Separation of Am³⁺ and Eu³⁺ from Nitrate Medium using Cyanex® 301. *Solvent Extr. Ion Exch.* **2007**, *25*, 27–39.
- [4] Barr, M. E.; Jarvinen, G. D.; Moody, E. W.; Vaughn, R.; Silks, L. A.; Bartsch, R. A. Plutonium(IV) Sorption by Soluble Anion-Exchange Polymers. *Sep. Sci. Technol.* **2002**, *37*, 1065–1078.
- [5] Griffith, C. S.; De Los Reyes, M.; Scales, N.; Hanna, J. V.; Luca, V. Hybrid Inorganic-Organic Adsorbents Part 1: Synthesis and Characterization of Mesoporous Zirconium Titanate Frameworks Containing Coordinating Organic Functionalities. *ACS Appl. Mater. Interfaces* **2010**, *2*, 3436–3446.
- [6] De Los Reyes, M.; Majewski, P. J.; Scales, N.; Luca, V. Hydrolytic Stability of Mesoporous Zirconium Titanate Frameworks Containing Coordinating Organic Functionalities. *ACS Appl. Mater. Interfaces* **2013**, *5*, 4120–4128.
- [7] Veliscek-Carolan, J.; Jolliffe, K. A., Hanley, T. L. Selective Sorption of Actinides by Titania Nanoparticles Covalently Functionalized with Simple Organic Ligands. *ACS Appl. Mater. Interfaces* **2013**, *5*, 11984–11994.

- [8] De Decker, J.; Rochette, J.; De Clercq, J.; Florek, J.; Van Der Voort, P. Carbamoylmethylphosphine Oxide-Functionalized MIL-101(Cr) as Highly Selective Uranium Adsorbent. *Anal. Chem.* **2017**, *89*, 5678–5682.
- [9] Zakharchenko, E. A.; Malikov, D. A.; Molochnikova, N. P.; Myasoedova, G. V., Kulyako, Y. M. Sorption Recovery of U(VI), Pu(IV), and Am(III) from Nitric Acid Solutions with Solid-Phase Extractants based on Taunit Carbon Nanotubes and Polystyrene Supports. *Radiochemistry (Moscow, Russ. Fed.)* **2014**, *56*, 27–31.
- [10] Zhang, A.; Hu, Q.; Wang, W.; Kuraoka, E. Application of a Macroporous Silica-Based CMPO-Impregnated Polymeric Composite in Group Partitioning of Long-Lived Minor Actinides from Highly Active Liquid by Extraction Chromatography. *Ind. Eng. Chem. Res.* **2008**, *47*, 6158–6165.
- [11] Ansari, S. A.; Pathak, P.; Mohapatra, P. K.; Manchanda, V. K. Chemistry of Diglycolamides: Promising Extractants for Actinide Partitioning. *Chem. Rev.* **2012**, *112*, 1751–1772.
- [12] Yarbrow, S. L.; Schreiber, S. B. Using Process Intensification in the Actinide Processing Industry. *J. Chem. Technol. Biotechnol.* **2003**, *78*, 254–259.
- [13] Silverstein, M. S. PolyHIPEs: Recent Advances in Emulsion-Templated Porous Polymers. *Prog. Polym. Sci.* **2014**, *39*, 199–234.
- [14] Choudhury, S.; Connolly, D.; White, B. Supermacroporous polyHIPE and Cryogel Monolithic Materials as Stationary Phases in Separation Science: A Review. *Anal. Methods* **2015**, *7*, 6967–6982.
- [15] Barlik, N.; Keskinler, B.; Kocakerim, M. M.; Akay, G. Surface Modification of Monolithic PolyHIPE Polymers for Anion Functionality and their Ion Exchange Behavior. *J. Appl. Polym. Sci.* **2015**, *132*, 42286.
- [16] Barlik, N.; Keskinler, B.; Kocakerim, M. M.; Akay, G. Functionalized PolyHIPE Polymer Monoliths as an Anion-Exchange Media for Removal of Nitrate Ions from Aqueous Solutions. *Desalin. Water Treat.* **2016**, *57*, 26440–26447.
- [17] Hus, S.; Kolar, M.; Krajnc, P. Separation of Heavy Metals from Water by Functionalized Glycidyl Methacrylate Poly(High Internal Phase Emulsions). *J. Chromatogr. A* **2016**, *1437*, 168–175.

- [18] Inoue, H.; Yamanaka, K.; Yoshida, A.; Aoki, T.; Teraguchi, M.; Kaneko, T. Synthesis and Cation Exchange Properties of a new Porous Cation Exchange Resin having an Open-Celled Monolith Structure. *Polymer* **2004**, *45*, 3–7.
- [19] Moine, L.; Deleuze, H.; Maillard, B. Preparation of High Loading PolyHIPE Monoliths as Scavengers for Organic Chemistry. *Tetrahedron Lett.* **2003**, *44*, 7813–7816.
- [20] Tripp, J. A.; Needham, T. P.; Ripp, E. M.; Konzman, B. G.; Homnick, P. J. A Continuous-Flow Electrophile Scavenger Prepared by a Simple Grafting Procedure. *React. Func. Polym.* **2010**, *70*, 414–418.
- [21] Mert, E. H.; Kaya, M. A.; Yildirim, H. Preparation and Characterization of Polyester-Glycidyl Methacrylate PolyHIPE Monoliths to use in Heavy Metal Removal. *Des. Monomers Polym.* **2012**, *15*, 113–126.
- [22] Savina, I. N.; Galaev, I. Y.; Mattiasson, B. Ion-Exchange Macroporous Hydrophilic Gel Monolith with Grafted Polymer Brushes. *J. Mol. Recognit.* **2006**, *19*, 313–321.
- [23] Luo, Y.; Wang, A.; Gao, X. One-Pot Interfacial Polymerization to Prepare PolyHIPEs with Functional Surface. *Colloid Polym. Sci.* **2015**, *293*, 1767.
- [24] Krajnc, P.; Leber, N.; Stefanec, D.; Kontrec, S.; Podgornik, A. Preparation and Characterisation of Poly(High Internal Phase Emulsion) Methacrylate Monoliths and their Application as Separation Media. *J. Chromatogr. A* **2005**, *1065*, 69–73.
- [25] Pulko, I.; Kolar, M.; Krajnc, P. Atrazine Removal by Covalent Bonding to Piperazine Functionalized PolyHIPEs. *Sci. Total Environ.* **2007**, *386*, 114–123.
- [26] Koler, A.; Paljevac, M.; Cmager, N.; Iskra, J.; Kolar, M.; Krajnc, P. Poly(4-vinylpyridine) polyHIPEs as Catalysts for Cycloaddition Click Reaction. *Polymer* **2017**, *126*, 402–407.
- [27] Benicewicz, B. C.; Jarvinen, G. D.; Kathios, D. J.; Jorgensen, B. S. Open Celled Polymeric Foam Monoliths for Heavy Metal Separations Study. *J. Radioanal. Nucl. Chem.* **1998**, *235*, 31–35.
- [28] Pribyl, J.; Fletcher, B.; Steckle, W.; Taylor-Pashow, K.; Shehee, T.; Benicewicz, B. Photoinitiated Polymerization of 4-Vinylpyridine on

- PolyHIPE Foam Surface toward Improved Pu Separations. *Anal. Chem.* **2017**, *89*, 5174–5178.
- [29] Leung, P. S.-W.; Teng, Y.; Toy, P. H. Rasta Resin-PPh₃ and its use in Chromatography-Free Wittig Reactions. *Synlett* **2010**, *13*, 1997–2001.
- [30] Williams, J. M.; Gray, J. A.; Wilkerson, M. H. Emulsion Stability and Rigid Foams from Styrene or Divinylbenzene Water-in-Oil Emulsions. *Langmuir* **1990**, *6*, 437–444.
- [31] Hawker, C. J. Molecular Weight Control by a “Living” Free-Radical Polymerization Process. *J. Am. Chem. Soc.* **1994**, *116*, 11185–11186.
- [32] Hawker, C. J.; Frechet, J. M. J.; Grubbs, R. B.; Dao, J. Preparation of Hyperbranched and Star polymers by a “Living”, Self-Condensing Free Radical Polymerization. *J. Am. Chem. Soc.* **1995**, *117*, 10763–10764.
- [33] Hawker, C. J. Architectural Control in “Living” Free Radical Polymerization: Preparation of Star and Graft Polymers. *Angew. Chem., Int. Ed. Engl.* **1995**, *34*, 1456–1459.
- [34] Ohno, K.; Ma, Y.; Huang, Y.; Mori, C.; Yahata, Y.; Tsujii, Y.; Maschmeyer, T.; Moraes, J.; Perrier, S. Surface-Initiated Reversible Addition-Fragmentation Chain Transfer (RAFT) Polymerization from Fine Particles Functionalized with Trithiocarbonates. *Macromolecules* **2011**, *44*, 8944–8953.
- [35] Larsson, E.; Pendergraph, S. A.; Kaldeus, T.; Malmstrom, E.; Carlmark, A. Cellulose Grafting by Photoinduced Controlled Radical Polymerization. *Polym. Chem.* **2015**, *6*, 1865–1874.
- [36] Zheng, Y.; Abbas, Z. M.; Sarkar, A.; Marsh, Z.; Stefik, M.; Benicewicz, B. C. Surface-Initiated Reversible Addition-Fragmentation Chain Transfer Polymerization of Chloroprene and Mechanical Properties of Matrix-Free Polychloroprene Nanocomposites. *Polymer* **2018**, *135*, 193–199.
- [37] Kuliasha, C. A.; Fedderwitz, R. L.; Calvo, P. R.; Sumerlin, B. S.; Brennan, A. B. Engineering the Surface Properties of Poly(dimethylsiloxane) Utilizing Aqueous RAFT Photografting of Acrylate/Methacrylate Monomers. *Macromolecules* **2018**, *51*, 306–317.
- [38] Hallman, D. F. *Technical Requirements For Plutonium Processing Using Strong Base Anion Resin for HB-Line Phase II*; WSRC-TR-2001-00354; Westinghouse Savannah River Company: Aiken, SC, 2001.

- [39] Marsh, S. F. *The Effects of Ionizing Radiation on Reillex™ HPQ, a New Macroporous Polyvinylpyridine Resin, and on Four Conventional Polystyrene Anion Exchange Resins*; LA-11912; Los Alamos National Lab: Los Alamos, NM, 1990.

CHAPTER 4

SYNTHESIS AND CHARACTERIZATION OF POLYETHYLENE GRAFTED NANOPARTICLES TOWARD POLYETHYLENE NANOCOMPOSITES

4.1 Abstract

Polyethylene and nanosilica represent the most ubiquitous commodity plastic and nanocomposite filler, respectively. Despite their importance, there are surprisingly few examples in the literature of successfully combining these two materials to form polyethylene nanocomposites. Synthesizing well-defined polyethylene grafted to a surface with the aim of minimizing the surface energy between a nanofiller and polyethylene matrix represents a significant challenge in the nanocomposites community due to the difficulty of preparing well-defined polyethylene and attaching it to surfaces. Presented here is a new synthetic approach developed with the aim of making polyethylene grafted nanoparticles with predictable graft density and molecular weight of the grafted polymer. Control of these molecular parameters is essential to controlling the nanocomposite dispersion morphology. The synthesis and characterization of well-defined polyethylene grafted nanoparticles as well as some challenges inherent to this approach are discussed in detail.

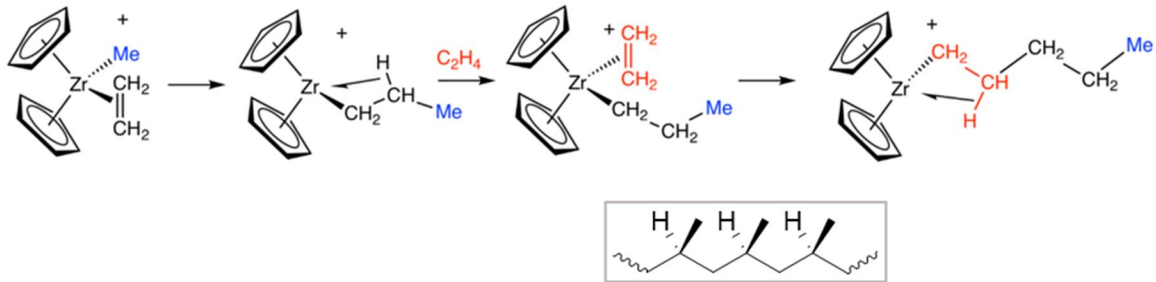
4.2 Introduction

Polyolefin materials represent the largest class of commodity thermoplastics in the world and they find use in every aspect of daily life.¹ The largest subclass of commodity polyolefins, polyethylenes (PE), are abundantly used in applications from packaging to artificial joints.² PE is the material of

choice in a variety of applications which demand chemical inertness, high strength, low density, ductility, etc. and many different classes of PE are synthesized commercially (low density PE, high density PE, linear low density PE). PE is also semicrystalline and processing the polymer to have crystalline regions can further affect the mechanical properties.³

Despite the commercial relevance and excellent properties of PE, there are relatively few examples in the literature of polyethylene nanocomposites. This stems from the synthetic challenge of making polyethylene and then attaching it to a nanofiller or growing the polymer from a surface. Commercially, polyethylene is produced by reacting ethylene gas with a Ziegler-Natta catalyst comprised of a transition metal complex (commonly titanium or zirconium, but nickel is also common) in combination with an organoaluminum co-catalyst (e.g. triethylaluminum).⁴ The polymerization occurs through olefin insertion between the metal center and a coordinated alkyl group (Scheme 4.1), and results in polymers with a broad molecular weight distribution (sometimes $\bar{M}_w/\bar{M}_n > 10$) but can also produce polyolefins with excellent stereochemical fidelity (e.g. isotactic polypropylene).⁵⁻⁶ Use of the Ziegler-Natta catalyst is not a versatile technique to synthesize polyolefin nanocomposites because it is extremely water and air-sensitive, sometimes requires high pressures of ethylene gas, and there is very poor control of molecular weight (MW). Fundamental investigation of

nanocomposites in our group has shown that control over graft density and MW is crucial for obtaining predictable nanofiller dispersion within a polymer matrix, and for realizing the subsequent property enhancements.⁷⁻⁸



Scheme 4.1: Mechanism of Ziegler-Natta polymerization of polyethylene (simplified for clarity), and structure of isotactic polypropylene (inset).

There have been a few attempts to synthesize polyolefin nanocomposites with varying degrees of success which are briefly summarized here. Polyethylene/palygorskite nanocomposites were prepared by *in situ* coordination polymerization, and the resulting micrometer-length palygorskite whiskers could be dispersed in a polyethylene matrix.⁹ The resulting composites showed an improvement in the tensile and impact strengths compared to the unfilled polymer. Polyethylene/nanoclay composites were prepared in a similar fashion and demonstrated improved thermal stability compared to unfilled polyethylene.¹⁰ Nanoclays modified with a three component mixture of oligomers (styrene, lauryl acrylate, and vinyl benzyl chloride) were dispersed in both polyethylene and polypropylene, but based on transmission electron microscopy (TEM) images there were substantial areas of aggregation in the

composite.¹¹ Despite this aggregation, there were some observed improvements in the measured peak heat release rate (a measure of the thermal stability). Better dispersion of montmorillonite clays was achieved by anchoring an early transition metal complex (Ni) on the surface of the Lewis acidic clay surface, which also activates the catalyst for the *in situ* coordination polymerization of ethylene.¹² The resulting matrix-free nanocomposites showed an appreciable increase in the flexural modulus, and interestingly the activation of the catalyst on the clay surface seemed to decrease the rate of chain walking during the polymerization, and the clay-supported polymer had a melting point $\sim 15^\circ\text{C}$ higher than polymer made with the same catalyst activated by $\text{B}(\text{C}_6\text{F}_5)_3$.

Polyolefin composites with carbon-based fillers have also been explored. Dodecylamine functionalized graphene was solution mixed with linear low-density polyethylene.¹³ The modified micron-sized sheets appeared to be fairly well-dispersed within the matrix, and a 118% increase in the storage modulus was observed at 8 wt.% loading of the modified graphene. Carbon nanotubes also functionalized with dodecylamine were dispersed in a polyethylene matrix, and also exhibited improvements in the storage modulus compared to the unfilled polymer.¹⁴ Graphene oxide functionalized with a Ziegler-Natta catalyst was used to grow polypropylene from the graphene oxide surface *in situ* in a similar fashion to the nanoclays discussed above, and the resulting composite

exhibited high electrical conductivity and a low percolation threshold (0.2 vol. % graphene oxide).¹⁵

Silica nanoparticles are of great interest in the nanocomposites community because nanosilica is easy to synthesize or cheaply available in many different sizes and has been extensively studied as a filler in non-olefin materials.¹⁶⁻¹⁸ Achieving good dispersion of small silica nanoparticles (>50 nm) in polyolefin matrices remains a challenge, but there are some examples of dispersing larger nanoparticles in polyolefin matrices. Octenyl-modified silica nanoparticles (diameter 150-200 nm) were dispersed in polyethylene via catalytic emulsion polymerization, and the resulting composites showed relatively good dispersion.¹⁹ Alternatively, a grafting-to approach was used to condense hydroxyl terminated polypropylene to the surface silanol groups on silica nanoparticles (diameter=26 nm) at 200° C.²⁰ The grafting density of the attached polymer was relatively low (a common problem with grafting-to approaches), and the resulting composites had large aggregates. A more recent report of grafting end-functionalized polyethylene to silica particles (diameter=100-300 nm) achieved better dispersion.²¹ Iodine-terminated polyethylene was also attached to iron oxide via a grafting-to ligand exchange process, and the resulting composites exhibited an order of magnitude increase in the storage modulus and increased softening temperature.²² An interesting approach to form

silica particles within a polyethylene matrix consisted of trapping polyethylene among droplets of polymerizing tetraethylorthosilane (TEOS) stabilized by a polyethylene-block-poly(ethylene glycol surfactant).²³ The resulting particles were well-dispersed in the nanocomposite, but were fairly large (diameter=150-300 nm). Finally, in what is arguably the most successful example of dispersing small silica nanoparticles in a polyolefin matrix to date was achieved by grafting chains of poly(stearyl methacrylate) from 15 nm diameter silica particles.²⁴ The 18-carbon-long side chains along the polymer backbone allowed for good dispersion of the nanoparticles in linear low-density polyethylene.

In light of the work which has been done on polyolefin nanocomposites, specifically nanocomposites with polyethylene, no single route exists which allows for independent control of the graft density and molecular weight of the surface-grafted polymer except for the method described by Khani et al.²⁴ However, that approach relied on long alkyl side chains to achieve dispersion in linear low-density polyethylene which has a high degree of short branching along the polymer backbone. High density polyethylene (HDPE) is truly underexplored in the nanocomposites community because of its linearity and high degree of crystallinity which results in its immiscibility even with other classes of polyethylene. To date, there are no reports of well-dispersed nanofillers in high density polyethylene. There is great potential in using HDPE's

crystallinity to template the assembly of nanoparticles on the nanoscale. Recent work leveraged the semi-crystallinity of poly(ethylene oxide) (PEO) to template the assembly of poly(methyl methacrylate) grafted silica nanoparticles (PMMA-g-SiO₂).²⁵ In this study, PMMA-g-SiO₂ particles were homogeneously dispersed in PEO, and then the PEO was heated above the melting point and isothermally crystallized. The slowly growing spherulites pushed the nanoparticles to the interlamellar amorphous regions between crystal spherulites, creating a nanoscale “brick and mortar” structure. Nearly an order of magnitude increase in the Young’s modulus was observed for the ordered composite compared to the randomly dispersed composite at the same filler loading. This work has exciting implications for semicrystalline polyolefin materials, especially HDPE which has excellent mechanical properties even without nanofiller.

In this work, we present a new surface-initiated ring opening metathesis polymerization (SI-ROMP) strategy to prepare linear polyethylene-grafted silica nanoparticles with excellent control of the graft density and molecular weight of the grafted polymer. The synthesis, challenges, and thorough characterization of these new materials will be discussed in detail.

4.3 Experimental

4.3.1 Materials and Instrumentation

Silica nanoparticles (MEK-ST, 30 wt.% in methyl ethyl ketone, diameter = 14 ± 4 nm) were supplied by Nissan Chemical Corporation and Grubbs 2nd Generation Catalyst 1,3-Bis(2,4,6-trimethylphenyl-2-imidazolidinylidene) dichloro(phenylmethylene) (tricyclohexylphosphine)ruthenium, C848) was generously donated by Materia. [(5-Bicyclo[2.2.1]hept-2-enyl)ethyl]trimethoxysilane was supplied by Gelest. Dry tetrahydrofuran (THF) was dispensed from a dry still solvent system and used immediately. All other chemicals were supplied by Oakwood Chemicals, Alfa Aesar, or Acros Organics. All chemicals were used as received unless otherwise noted. Thermogravimetric analysis (TGA) was performed on a TA Instruments Q5000 thermogravimetric analyzer under nitrogen at a heating ramp rate of 10 deg C/min. Differential scanning calorimetry (DSC) measurements were made using a TA Instruments Q2000 under a nitrogen atmosphere at a heating ramp rate of 10 deg C/min. DSC samples were hermetically sealed in aluminum pans for analysis. Molecular weights (M_n) and dispersities (\bar{D}) were determined using a gel permeation chromatograph (GPC) equipped with a Varian 290-LC pump, a Varian 390-LC refractive index detector, and three Styragel columns (HR1, HR3, and HR4, molecular weight ranges of 100–5000, 500–30 000, and 5000–500 000,

respectively). THF was used as eluent at 30 °C and a flow rate of 1.0 mL/min. The GPC was calibrated with poly(1,4-butadiene) standards obtained from Polymer Laboratories. ¹H NMR spectra were obtained from Bruker Avance III-HD 300 MHz NMR in CDCl₃. Dynamic light scattering measurements were made on a Malvern Zetasizer instrument in glass cuvettes at a scattering angle of 90° and THF as the solvent. DLS measurements were made at a sample concentration of 2-3 mg/mL. Transmission electron microscopy (TEM) images were recorded on JEOL 200CX Transmission Electron Microscope at an acceleration voltage of 120 kV.

4.3.2 Synthesis of norbornyl tagged SiO₂ (Nb-g-SiO₂)

To begin, 20 g of MEK-ST silica nanoparticle dispersion was weighed in a glass vial and added to a 100 mL 3-neck round bottom flask equipped with a stir bar, rubber septum, and glass stopper. The particle solution was diluted with 20 mL THF and [(5-Bicyclo[2.2.1]hept-2-enyl)ethyl]trimethoxysilane was added via micropipet. The flask was attached to a water condenser, sparged with dry argon for five minutes, then lowered into a 70° C oil bath and allowed to stir overnight. Trimethylmethoxysilane (1 mL) was then added to the heated solution via syringe, and the particle mix was allowed to stir an additional two hours. The particle mix was then cooled to room temperature, and the particles were precipitated in a large excess of hexanes (200 mL). The precipitated particles

were added to centrifuge tubes, and the particles were recovered by centrifugation at 5000 rpm for five minutes. The particles were then dried *in vacuo* for two hours and stored at -25° C for further use.

4.3.3 Synthesis of Grubbs catalyst-tethered SiO₂ and surface-initiated ROMP (SI-ROMP) of cis-cyclooctene

In a typical experiment, 250 mg of Nb-g-SiO₂ (1 eq. of [(5-Bicyclo[2.2.1]hept-2-enyl)ethyl]trimethoxysilane) were weighed out and added to a flame-dried 20 mL septum-capped vial. 10 mL of dry THF was quickly added to the vial, and the particles were dispersed by sonicating for five minutes. Meanwhile, 5 mL dry THF was added to a 100 mL flame-dried round bottom flask equipped with a 10mm x 30 mm egg-shaped magnetic stir bar. The THF was sparged with dry argon for five minutes, then Grubbs' second generation catalyst (Grubbs II, 1.15 eq. with respect to the norbornyl silane) was added under argon and dissolved by stirring. The dispersed particle solution was then sparged for 10 minutes with dry argon, then added via syringe dropwise to the stirring catalyst solution. The catalyst/particle mix was allowed to stir under argon protection for 45 minutes at 25° C. While the catalyst/particle mix was stirring, a 1 M solution of cis-cyclooctene in THF (varying amounts depending on target MW) was degassed by sparging with dry argon in a 50 or 100 mL flame-dried round bottom flask along with butylated hydroxytoluene (BHT, 10 mol. % with respect

to monomer). After 45 minutes of the particle/catalyst mix stirring, the prepared monomer solution was slowly cannula transferred to the particle mixture under dry Argon. The solution immediately became viscous, but the polymerization mix was allowed to stir an additional 30-60 minutes. The polymerization was quenched by adding 2 mL (excess) of ethyl vinyl ether and stirring for 15 minutes. The resulting polycyclooctene grafted silica nanoparticles (PCO-g-SiO₂) were then precipitated in methanol and recovered by centrifugation at 5000 rpm for five minutes.

A small sample was cleaved with hydrofluoric acid for GPC analysis.

4.3.4 Hydrogenation of grafted polymer

Hydrogenations were performed according to a modified literature procedure.²⁷ In a typical experiment, the grafted polycyclooctene was hydrogenated using the following procedure; 0.7 g of vacuum-dried PCO-g-SiO₂ (1 eq. of polymer) was added to a 500 mL oven-dried 3-neck round bottom flask equipped with a magnetic stir bar. The flask was equipped with a glass stopper and rubber septum then attached to a water condenser. The flask was sparged with dry argon for two minutes, then 150 mL of dry o-xylene was transferred under argon via cannula. The polymer mixture was lowered into an oil bath set to 90° C and allowed to stir for 10 minutes to dissolve the PCO-g-SiO₂.

Meanwhile, *p*-toluenesulfonyl hydrazide (1.18 g, 1 eq. with respect to polymer)

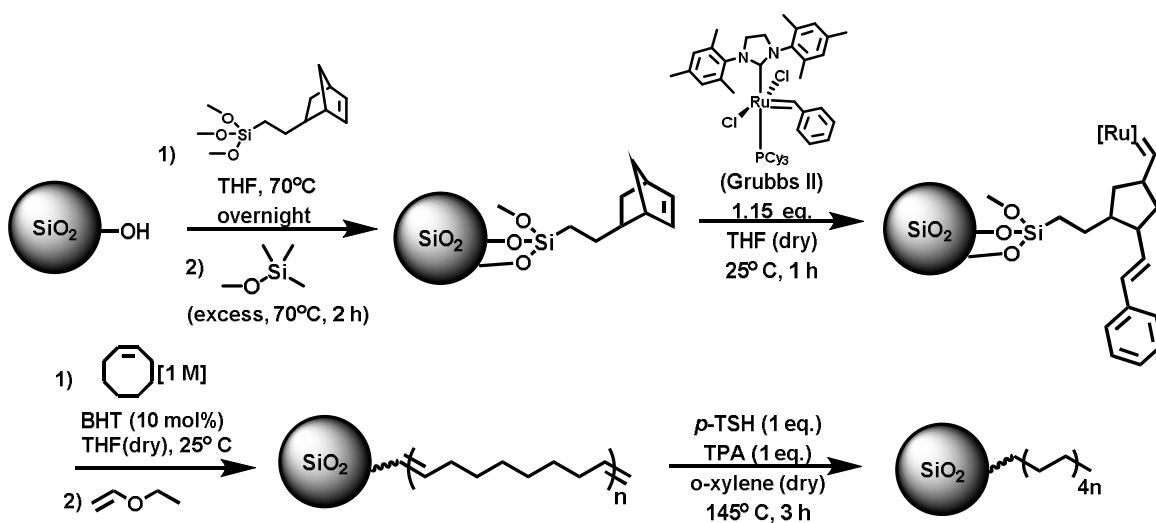
was weighed, then added to the stirring reaction solution under argon. Then, tripropylamine (TPA, 1.2 mL, 1 eq. with respect to polymer) was added to the reaction mix via syringe. The mixture was heated at 145° C for three hours, then cooled to room temperature. When cooled, the particles began to precipitate from the solution due to the poor solubility of the grafted polyethylene in o-xylene at room temperature. The particles were precipitated in an excess of methanol (300 mL), allowed to settle, then recovered by vacuum filtration through a 0.2 µm nylon filter. The particles were washed with a copious amount of water and methanol to remove the by-product of the hydrogenation, then dried *in vacuo*.

4.4 Results and Discussion

A synthetic strategy was developed which allows for the controlled synthesis of linear polyethylene grafted on silica nanoparticles detailed in Scheme 4.2. To begin, silica nanoparticles were modified with a norbornyl silane coupling agent at varying feed ratios as well as an alkylsilane to cap any unreacted silanol groups. This norbornyl group was then used to tether Grubbs' second generation ruthenium catalyst (Materia C848) to the silica nanoparticles. Many methods of catalyst attachment to surfaces have been explored in the literature,²⁸⁻³⁰ but the benefit of using a norbornyl group rather than a simple alkene group, for example, is that the relief of ring strain after the catalyst reacts

with the norbornene moiety generates an essentially irreversible tether compared to an alkene exchange with the catalyst's benzylidene ligand. Also, varying the feed ratio of the norbornyl silane to nanoparticles allows for the attachment for a variety of brush densities. Subsequent addition of the monomer solution to the catalyst-tethered particles results in grafted polycyclooctene (PCO-g-SiO₂). *Cis*-cyclooctene contains sufficient ring strain that the polymerization produces linear polymer (no branching) with up to 95% trans geometry in the final polymer.³¹ After a mild hydrogenation procedure, the grafted polymer is transformed into linear polyethylene. A library of samples was made according to this procedure, and the characterization data for these samples is shown in

Table 4.1.



Scheme 4.2: Synthetic approach toward nanosilica grafted well-defined polyethylene

Table 4.1: Physical and chemical characteristics of selected samples

Sample	M _n (kg/mol) ^a	Đ	Calculated average graft density (σ , chains/nm ²) ^b	Norbornyl silane feed ratio (mmol/g)	Char yield before hydrog. (%)	Char yield after hydrog. (%)	Avg. Diameter (nm) ^c
A	10/10	1.3	0.17	0.10	47.7	46.0	24
B	50/50	?	0.16	0.10	14.4	12.1	62
C	10/10	1.4	0.27	0.21	40.2	39.8	55
D	50/50	1.3	0.22	0.21	8.7	6.1	78
E	101/100	1.7	0.24	0.21	2.4	1.7	118
F	10/10	1.5	0.60	0.42	11.1	9.1	69
G	49/50	1.4	0.61	0.42	2.0	1.4	130

^aMolecular weight expressed as experimental/theoretical ^bAverage graft density calculated based on the MW of grafted polymer and char yield before hydrogenation ^cNumber average diameter of PCO-g-SiO₂ determined by DLS

A main benefit of the described synthetic approach is that the graft density and molecular weight of the grafted polymer are independently tunable as seen in Table 4.1. The graft density of the polymer is dictated by the feed ratio of norbornyl silane to nanoparticles, and the molecular weight of the grafted polymer is controlled by the monomer to catalyst ratio. Each molecular variable is tunable and easily-characterized which is necessary for targeting specific dispersion states when combined with a matrix, for instance. Another advantage of this procedure is that the polymer can be fully characterized by gel-permeation chromatography (GPC) before the hydrogenation, which renders it insoluble except at very high temperatures in harsh organic solvents (e.g. trichlorobenzene). Polyethylene prepared directly by Ziegler-Natta chemistry is challenging to analyze for molecular weight and Đ characteristics using widely

available GPC equipment due to its poor solubility in common organic solvents at common operating temperatures. After the hydrogenation, there is a decrease in the observed char yield due to the saturation of the polymer backbone.

In an attempt to understand the kinetics of the polymerization on particles and in solution, two kinetic studies were conducted at 0° C, respectively. There are many instances in the literature which demonstrate that the rate of a polymerization initiated from a surface can differ greatly from the rate of polymerization of the same monomer in solution.³²⁻³³ However, even at 0° C, full monomer conversion was observed both for the surface-initiated and solution polymerizations in five minutes (Figure 4.1). Based on this result, it was not possible to determine the rate difference, if any.

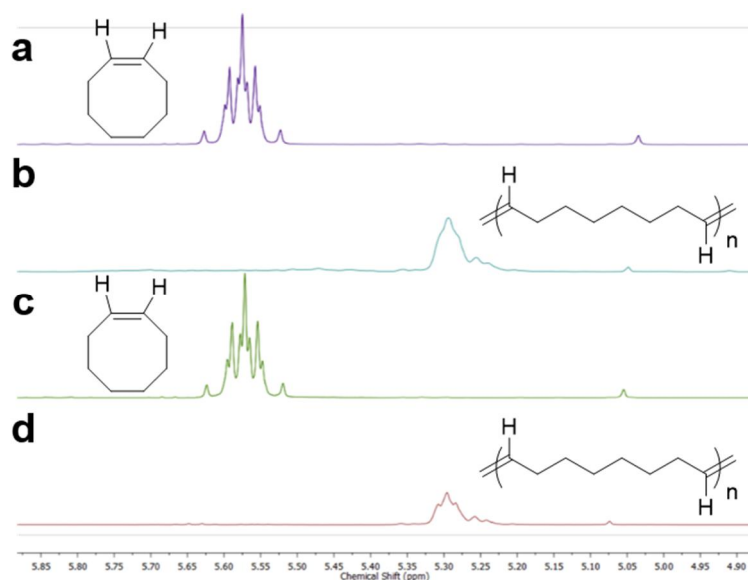


Figure 4.1: NMR spectra of monomer conversion of (a) t=0 min, solution polymerization (b) t=5 min, solution polymerization (c) t=0 min, surface-initiated polymerization and (d) t=5 min, surface-initiated polymerization. [M]:[catalyst] = [200]:[1], [cis-cyclooctene]=1 M in THF.

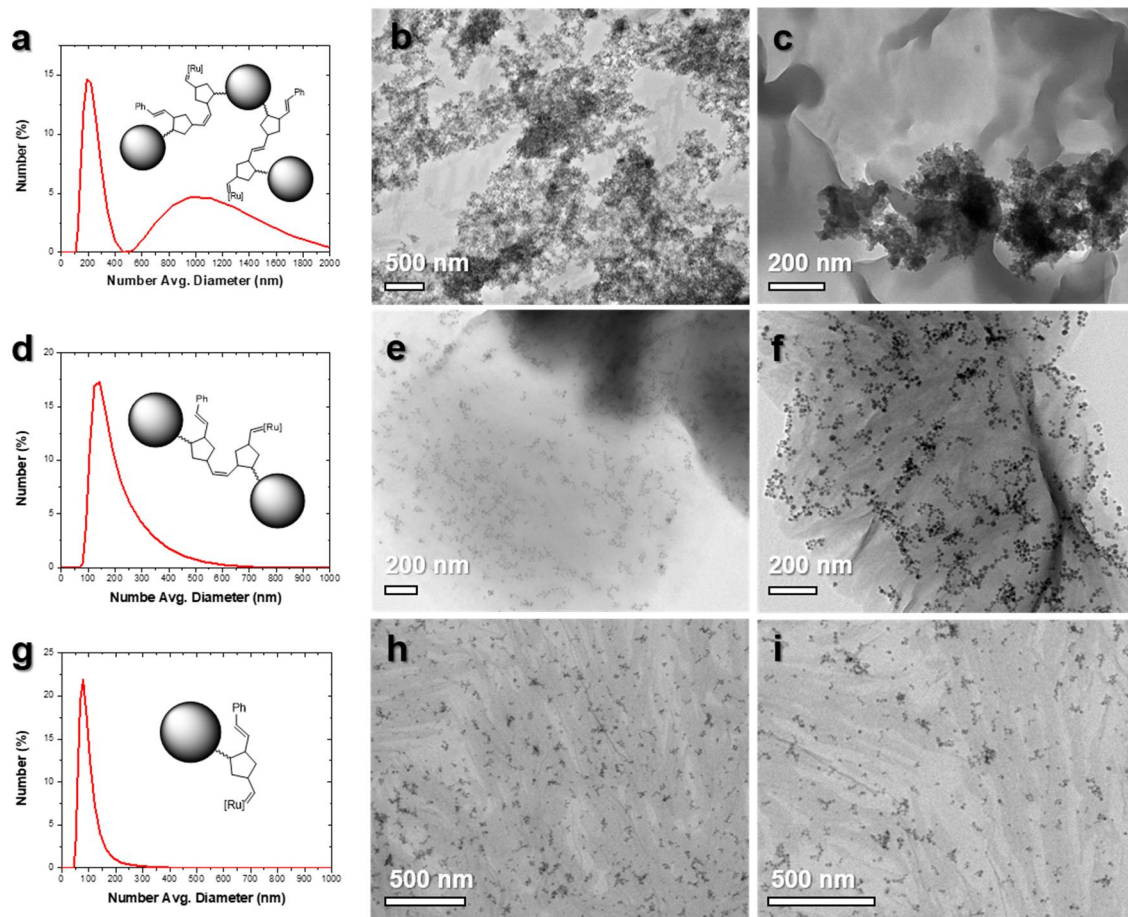


Figure 4.2: DLS curves and TEM images of PCO-g-SiO₂ synthesized with (a-c) 0.8 eq. catalyst with respect to norbornyl silane, (d-f) 1.0 eq. catalyst with respect to norbornyl silane, (g-i) 1.15 eq. catalyst with respect to norbornyl silane.

A challenge to this synthetic approach which needed to be addressed was the issue of significant particle agglomeration when the norbornyl functionalized nanoparticles were combined with the fast-initiating second generation Grubbs catalyst. Figure 4.2 shows the dispersion state of the PCO-g-SiO₂ nanoparticles drop cast onto a TEM grid which were made from different catalyst ratios with respect to the amount of norbornyl silane, as well as corresponding DLS curves.

ROMP is relatively unencumbered by steric hindrance,³⁴ so it is possible for particles to irreversibly couple during this step of the synthesis.

It was found that using a slight excess of catalyst with respect to the norbornyl silane, as well as slowly adding the Nb-g-SiO₂ particles to a concentrated catalyst solution were both essential measures needed to minimize particle coupling and resulted in predominantly singly dispersed polymer-grafted particles (Figure 4.2, g-i). These images, in combination with the DLS result (number average particle diameter = 78 nm) suggest that the majority of nanoparticles are singly dispersed after the polymerization. In general, the measured particle diameters for each sample agree fairly well with the theoretical brush heights based on the graft density and molecular weight of each sample.³⁵ The DLS results for samples A-G are shown in Figure 4.3, as well as the DLS size of the bare silica particles for comparison.

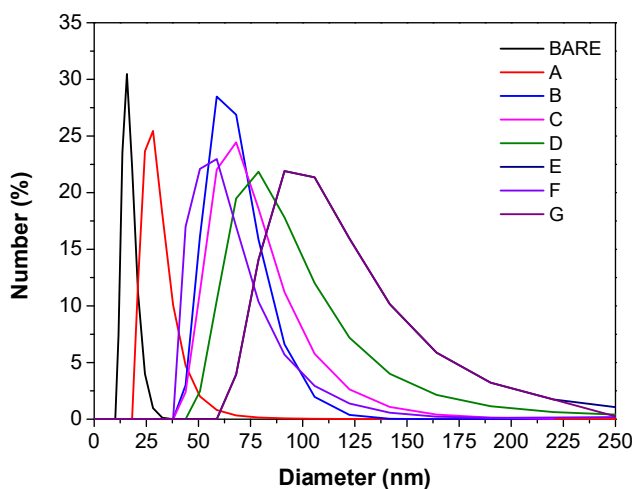


Figure 4.3: DLS curves for samples A-G and bare silica nanoparticles

The final hydrogenation step of the described synthesis is arguably the most important in preparing the PCO-g-SiO₂ nanoparticles for mixing with high density polyethylene (HDPE). HDPE is completely linear (contains no alkyl branches along the polymer backbone) and has a very high melting point because of the high degree of chain packing which occurs in the crystalline regions of the polymer. The theoretical melting point for perfectly linear polyethylene is 134° C, and there have been a few reports of synthesized HDPE reaching that melting point.³⁶ To understand the degree of hydrogenation of the PCO-g-SiO₂, differential scanning calorimetry (DSC) was used to compare the thermal properties of the particles before and after the hydrogenation step (Figure 4.4). Before hydrogenation, there is no discernible melting or crystallization transition in the PCO-g-SiO₂ samples. After the hydrogenation, melting points ranging from 94° C to 127° C were observed. The lowest melting point (94° C, Figure 4.4E) after the initial hydrogenation was likely due to the high molecular weight of the grafted polymer in combination with the density of the brush, which limited the extent of the hydrogenation reaction. A second hydrogenation conducted on the same sample (Figure 4.4E, blue curve) increased the melting point of the sample to 129° C. Nearly exhaustive hydrogenation of the grafted polymer should minimize phase-separation with a HDPE matrix.

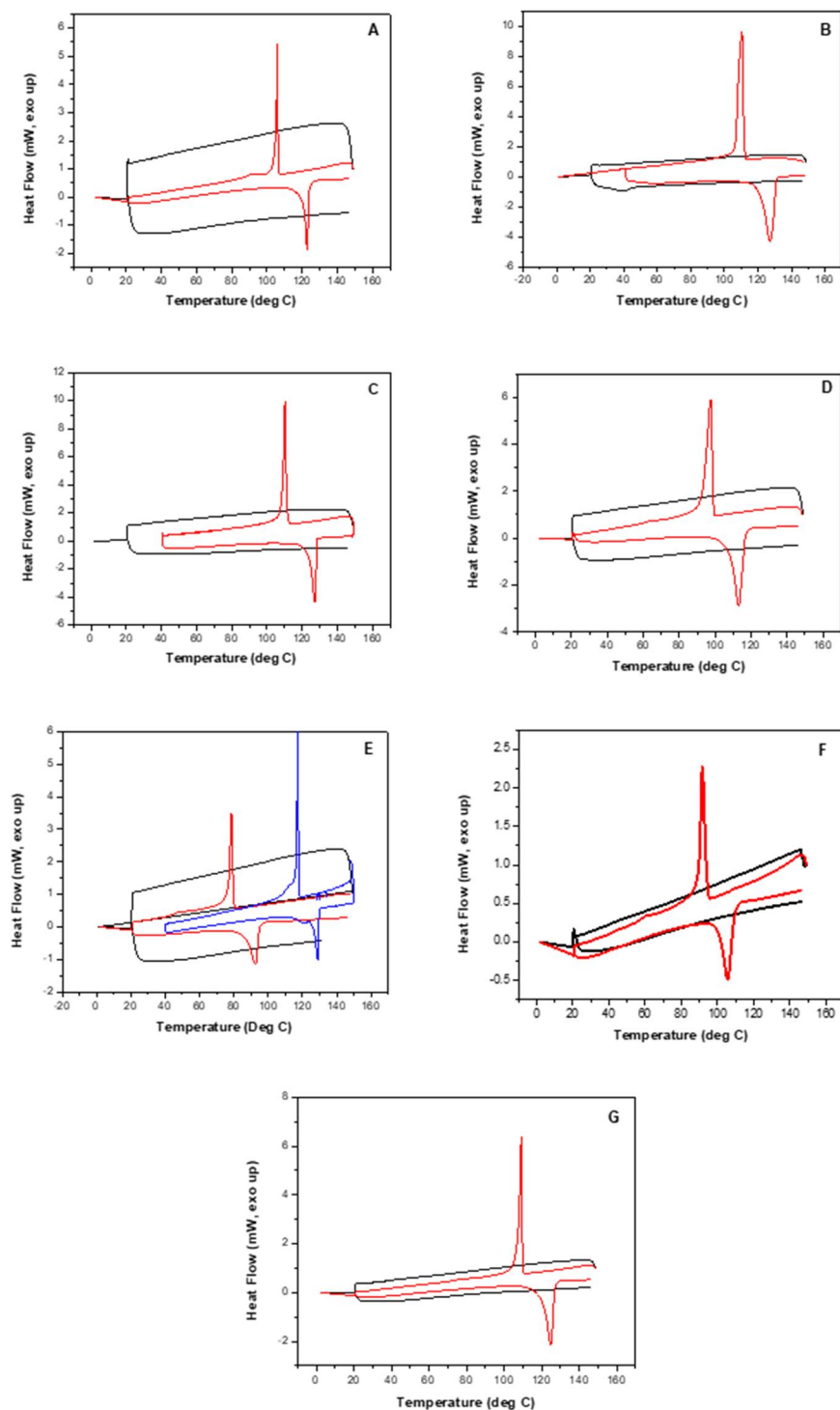


Figure 4.4: DSC curves before hydrogenation (black), after hydrogenation (red), after second hydrogenation (blue). Displayed curves represent the first cooling and second heating cycle. Labels A-G refer to the samples detailed in Table 4.1.

4.5 Conclusion

In this work, a novel approach to polyethylene grafted nanosilica was detailed along with thorough characterization of the resulting nanomaterial. In a departure from previous work in the literature, this synthetic approach allows for fine control of molecular parameters including graft density and molecular weight of the grafted polymer, no branching by virtue of the ROMP mechanism, and could in principle be applied to many different types of nanoparticles. Many of the previous examples of polyethylene grafted on nanoparticles lacked control of one or more of these parameters, and often demonstrated the dispersion of very large (>100 nm) nanoparticles which lowers the surface area where load transfer can occur in the nanocomposite. These controls, combined with a nearly exhaustive hydrogenation procedure which resulted in grafted polymer with a melting point near the theoretical melting point of perfect HDPE suggest that this synthetic approach may allow for nanofiller miscibility with HDPE.

This synthetic approach also represents a new addition to the synthetic toolbox constantly in development in our group. A reliable route to SI-ROMP means that new classes of monomers (i.e. norbornenes, cyclooctenes, cyclooctadienes, etc.) which are not possible to polymerize via the controlled radical polymerization techniques which dominate the nanocomposites literature.

4.6 References

- [1] PlasticsEurope Annual Review 2017-2018. <https://www.plasticseurope.org/en/resources/publications/498-plasticseurope-annual-review-2017-2018> European polymer report. (Accessed September 10, 2018).
- [2] Dorigato, A.; Pegoretti, A. (Re)processing effects on linear low-density polyethylene/silica nanocomposites. *J. Polym. Res.* **2013**, *20*, 92.
- [3] Nowlin, T. E.; Mink, R. I.; Kissin, Y. V. Supported Magnesium/Titanium-Based Ziegler Catalysts for Production of Polyethylene. In *Handbook of Transition Metal Polymerization Catalysts (Online ed.)* Hoff, R. and Mather, R. T., Ed.; John Wiley & Sons. Hoboken, NJ, 2010; p. 131.
- [4] Eisch, J. J. Fifty years of Ziegler-Natta polymerization: from serendipity to science. A personal account. *Organometallics* **2012**, *31*, 4917–4932.
- [5] Yadav, Y. S.; Jain, P. C. Melting behavior of isotactic polypropylene isothermally crystallized from the melt. *Polymer* **1986**, *27*, 721–727.
- [6] Bassett, D. C.; Olley, R. H. On the lamellar morphology of isotactic polypropylene spherulites. *Polymer* **1984**, *25*, 935–946.
- [7] Akcora, P.; Liu, H.; Kumar, S. K.; Moll, J.; Li, Y.; Benicewicz, B. C.; Schadler, L. S.; Acehan, D.; Panagiotopoulos, A. Z.; Pryamitsyn, V.; Ganesan, V.; Ilavsky, J.; Thiyagarajan, P.; Colby, R. H.; Douglas, J. F. Anisotropic self-assembly of spherical polymer-grafted nanoparticles. *Nature Mater.* **2009**, *8*, 354–359.
- [8] Natarajan, B.; Neely, T.; Rungta, A.; Benicewicz, B.; Schadler, L. S. Thermomechanical properties of bimodal brush modified nanoparticle composites. *Macromolecules* **2013**, *46*, 4909–4918.
- [9] Du, Z.; Zhang, W.; Zhang, C.; Jing, Z.; Li, H. A novel polyethylene/palygorskite nanocomposite prepared via in-situ coordinated polymerization. *Polym. Bull* **2002**, *49*, 151–158.
- [10] He, F.-A.; Zhang, L.-M.; Jiang, H.-L.; Chen, L.-S.; Wu, Q.; Wang, H.-H. A new strategy to prepare polyethylene nanocomposites by using a late-transition metal catalyst supported on AlEt₃-activated organoclay. *Compos. Sci. Technol.* **2007**, *67*, 1727–1733.

- [11] Zhang, J.; Jiang, D. D.; Wilkie, C. A. Polyethylene and polypropylene nanocomposites based on a three component oligomerically-modified clay. *Polym. Degrad. Stab.* **2006**, *91*, 641–648.
- [12] Scott, S. L.; Peoples, B. C.; Yung, C.; Rojas, R. S.; Khanna, V.; Sano, H.; Suzuki, T.; Shimizu, F. Highly dispersed clay-polyolefin nanocomposites free of compatibilizers via the in situ polymerization of α -olefins by clay-supported catalysts. *Chem. Commun.* **2008**, *0*, 4186–4188.
- [13] Kuila, T.; Bose, S.; Mishra, A. K.; Khanra, P.; Kim, N. H.; Lee, J. H. Effect of functionalized graphene on the physical properties of linear low density polyethylene nanocomposites. *Polym. Test.* **2012**, *31*, 31–38.
- [14] Ferreira, F. V.; Franceschi, W.; Menezes, B. R. C.; Brito, F. S.; Lozano, K.; Coutinho, A. R.; Cividanes, L. S.; Thim, G. P. Dodecylamine functionalization of carbon nanotubes to improve dispersion, thermal and mechanical properties of polyethylene-based nanocomposites. *Appl. Surf. Sci.* **2017**, *410*, 267–277.
- [15] Dong, J.-Y.; Liu, Y. Synthesis of polypropylene nanocomposites using graphite oxide-intercalated Ziegler-Natta catalyst. *J. Organomet. Chem.* **2015**, *798*, 311–316.
- [16] Virtanen, S.; Krentz, T. M.; Nelson, J. K.; Schadler, L. S.; Bell, M.; Benicewicz, B. C.; Hillborg, H.; Ahaio, S. Dielectric breakdown strength of epoxy bimodal polymer brush grafted core functionalized silica nanocomposites. *IEEE Trans. Dielectr. Electr. Insul.* **2014**, *21*, 563–570.
- [17] Khani, M. M.; Abbas, Z. M.; Benicewicz, B. C. Well-defined polyisoprene-grafted silica nanoparticles via the RAFT process. *J. Polym. Sci., Part A: Polym. Chem.* **2017**, *55*, 1493–1501.
- [18] Huang, Y.; Zheng, Y.; Sarkar, A.; Xu, Y.; Stefik, M.; Benicewicz, B. Matrix-free polymer nanocomposite thermoplastic elastomers. *Macromolecules* **2017**, *50*, 4742–4753.
- [19] Dong, J.-Y.; Liu, Y. Synthesis of polypropylene nanocomposites using graphite oxide-intercalated Ziegler-Natta catalyst. *J. Organomet. Chem.* **2015**, *798*, 311–316.
- [20] Monteil, V.; Stumbaum, J.; Thomann, R.; Mecking, S. Silica/polyethylene nanocomposite particles from catalytic emulsion polymerization. *Macromolecules* **2006**, *39*, 2056–2062.

- [21] Toyonaga, M.; Chamminkwan, P.; Terano, M.; Taniike, T. Well-defined polypropylene/polypropylene-grafted silica nanocomposites: roles of number and molecular weight of grafted chains on mechanistic reinforcement. *Polymers* **2016**, *8*, 300.
- [22] Peng, Z.; Li, Q.; Li, H.; Youliang, H. Polyethylene-modified nanosilica and its fine dispersion in polyethylene. *Ind. Eng. Chem. Res.* **2017**, *56*, 5892–5898.
- [23] Bieligmeyer, M.; Taheri, S. M.; German, I.; Boisson, C.; Probst, C.; Milius, W.; Altstadt, V.; Breu, J.; Schmidt, H.-W.; D'Agosto, F.; Forster, S. Completely miscible polyethylene nanocomposites. *J. Am. Chem. Soc.* **2012**, *134*, 18157–18160.
- [24] Sertchook, H.; Elimelech, H.; Makarov, C.; Khalfin, R.; Cohen, Y.; Shuster, M.; Babonneau, F.; Avnir, D. Composite particles of polyethylene@silica. *J. Am. Chem. Soc.* **2007**, *129*, 98–108.
- [25] Khani, M. M.; Woo, D.; Mumpower, E. L.; Benicewicz, B. C. Poly(alkyl methacrylate)-grafted silica nanoparticles in polyethylene nanocomposites. *Polymer* **2017**, *109*, 339–348.
- [26] Zhao, D.; Gimenez-Pinto, V.; Jimenez, A. M.; Zhao, L.; Jestin, J.; Kumar, S. K.; Kuei, B.; Gomez, E. D.; Prasad, A. S.; Schadler, L. S.; Khani, M. M.; Benicewicz, B. C. Tunable multiscale nanoparticle ordering by polymer crystallization. *ACS Cent. Sci.* **2017**, *3*, 751–758.
- [27] Petzetakis, N.; Stone, G. M.; Balsara, N. P. Synthesis of well-defined polyethylene-polydimethylsiloxane-polyethylene triblock copolymers by diimide-based hydrogenation of polybutadiene blocks. *Macromolecules* **2014**, *47*, 4151–4159.
- [28] Cao, E.; Pichavant, L.; Prouzet, E.; Heroguez, V. The formation and study of poly(ethylene oxide)-poly(norbornene) block-copolymers on the surface of titanium dioxide particles: a novel approach towards application of si-ROMP to larger surface modification. *Polym. Chem.* **2016**, *7*, 2751–2758.
- [29] Kalluru, S. H.; Cochran, E. W. Synthesis of polyolefin/layered silicate nanocomposites via surface-initiated ring-opening metathesis polymerization. *Macromolecules* **2013**, *46*, 9324–9332.

- [30] Haque, H. A.; Kakehi, S.; Hara, M.; Nagano, S.; Seki, T. High-density liquid crystalline azobenzene polymer brush attained by surface-initiated ring-opening metathesis polymerization. *Langmuir* **2013**, *29*, 7571–7575.
- [31] Martinez, H.; Ren, N.; Matta, M. E.; Hillmyer, M. A. Ring-opening metathesis polymerization of 8-membered cyclic olefins. *Polym. Chem.* **2014**, *5*, 3507–3532.
- [32] Zheng, Y.; Abbas, Z. M.; Sarkar, A.; Marsh, Z.; Stefik, M.; Benicewicz, B. C. Surface-Initiated Reversible Addition-Fragmentation Chain Transfer Polymerization of Chloroprene and Mechanical Properties of Matrix-Free Polychloroprene Nanocomposites. *Polymer* **2018**, *135*, 193–199.
- [33] Kuliasha, C. A.; Fedderwitz, R. L.; Calvo, P. R.; Sumerlin, B. S.; Brennan, A. B. Engineering the Surface Properties of Poly(dimethylsiloxane) Utilizing Aqueous RAFT Photografting of Acrylate/Methacrylate Monomers. *Macromolecules* **2018**, *51*, 306–317.
- [34] Ganewatta, M. S.; Ding, W.; Rahman, M. A.; Yuan, L.; Wang, Z.; Hamidi, N.; Robertson, M. L.; Tang, C. Bioboased plastics and elastomers from renewable rosin via “living” ring-opening metathesis polymerization. *Macromolecules* **2016**, *49*, 7155–7164.
- [35] Dukes, D.; Li, Y.; Lewis, S.; Benicewicz, B.; Schadler, L.; Kumar, S. Conformational transitions of spherical polymer brushes: synthesis, characterization, and theory. *Macromolecules* **2010**, *43*, 1546–1570.
- [36] Sworen, J. C.; Smith, J. A.; Wagener, K. B.; Baugh, L. S.; Rucker, S. P. Modeling random methyl branching in ethylene/propylene copolymers using metathesis chemistry: synthesis and thermal behavior. *J. Am. Chem. Soc.* **2003**, *125*, 2228–2240.

CHAPTER 5
SUMMARY AND OUTLOOK

In this dissertation, new synthetic strategies to generate polymer brushes for advanced applications were discussed, and the resulting materials represent advancements in materials for anion exchange separations and nanocomposites. Each of the chapters contained herein builds on the knowledge of polymer brushes and surface modification which has been developed in this group throughout nearly the past two decades, but the work here also represents a departure from previous work in terms of substrate, surface-attachment chemistry, and the polymerization chemistry used to synthesize the brushes.

Chapter 2 discussed the development of polyHIPE foam monoliths grafted with chains of poly(4-vinylpyridine) (P4VP) which is an excellent ion-exchange moiety for Pu(IV) in concentrated acidic conditions. In this work, which relied on a photoinitiated free radical polymerization to graft the P4VP on the foam surface, the idea that macroporous foams could exhibit better separation kinetics compared to a resin-based material was demonstrated. This was evident in the narrow plutonium elution profiles achieved by the foam monoliths in comparison to the relatively broad profiles characteristic of a resin. However, the foam materials had a relatively low capacity due to the low grafting efficiency of the photoinitiated polymerization. The opacity of the foams limited the penetration depth of the light used to initiate the polymerization, resulting in uneven grafting and overall poor plutonium capacity.

In Chapter 3, a new synthetic approach was developed to overcome the poor grafting efficiency of the system described in Chapter 2, while also seeking to incorporate and controlled radical polymerization technique which would allow for the controlled synthesis of surface-grafted P4VP. A co-monomer containing a dormant nitroxide was incorporated into the foam structure, and after curing, the nitroxide groups could be activated a high temperature to mediate the surface polymerization of P4VP. The functional co-monomer could be incorporated into the pre-foam emulsion at very high weight fractions without affecting the quality of the cured foam, which was also a convenient way to vary the surface density of the grafted chains. The resulting P4VP-grafted polyHIPE foams exceeded the capacity of a commercial resin commonly used for the Pu anion exchange separation conducted at the Savannah River Site while still maintaining efficient separation kinetics and recyclability of these materials was demonstrated. The anion-exchange separation of plutonium is conducted in a very harsh acid and radiological environment, but the synthesized foam monoliths showed no loss in capacity or efficiency over 4 anion exchange cycles conducted over approximately three months. To our knowledge, this is the first example of the use of nitroxide-mediated polymerization to graft a polymer brush from the surface of polyHIPE foams.

Given, the potential for this type of material to conduct very efficient separations on a large scale, future work could focus on a slightly less tedious preparation of polymer grafted polyHIPEs. For example, some recent work on polyHIPEs has focused on macromolecules as stabilizers for the pre-foam emulsion instead of small molecule surfactants or particles. The main focus of this work has been to improve the mechanical properties of the polyHIPEs, but there is also the potential that a functional amphiphilic polymer could both stabilize the emulsion as well as provide a functional polymer brush post-curing, all in one synthetic step. This would of course be important for commercialization of such a material, but also present an opportunity to incorporate multiple chemical functionalities while also synthesizing polyHIPEs with robust mechanical properties.

In Chapter 4, focus was shifted back toward a more conventional surface (silica nanoparticles), but the polymerization chemistry was again unique from previous work in our group. A synthetic approach toward linear polyethylene-grafted silica nanoparticles was developed with SI-ROMP and the resulting materials were thoroughly characterized. This work represents an attempt to synthesize nanoparticles grafted with well-defined linear polyethylene which can be synthesized at any graft density or molecular weight which is desired. Control over each of these molecular parameters has not yet been demonstrated

in the polyolefin nanocomposite literature, but control of those features is essential to controlling the dispersion state of nanofiller blended with a polymer matrix. Use of a norbornyl silane coupling agent to tether a Grubbs catalyst to the surface of the silica nanoparticles was an effective strategy to control the graft density of the polymer, but also presented the challenge that the particles could irreversibly couple when the catalyst was added, resulting in large aggregates in the final material. To overcome this challenge, the ratio of catalyst to norbornyl silane was tuned to ensure the particles did not couple before the polymer could be grown from the surface of the particles. A mild hydrogenation procedure was effective at saturating the backbone of the polymer, and the grafted polymer exhibited a melting point very close to the theoretical melting point of perfectly linear polyethylene in some cases. The use of surface-initiated ROMP is a valuable tool to add to the nanocomposite synthetic toolbox because it enables the grafting of new classes of monomers on nanoparticle substrates. Controlled radical polymerization has dominated the polymer brush literature for the past decade because of the ease of synthesizing well-defined polymer brushes, often with very mild conditions. A continuation of this work should include the investigation of brushes of the numerous norbornene derivatives, or the use of functional cyclooctenes or cyclooctadienes, and their properties as fillers or

matrix-free composites on their own. In principle, this technique could be applied to substrates other than silica.

APPENDIX A
NMR SPECTRA

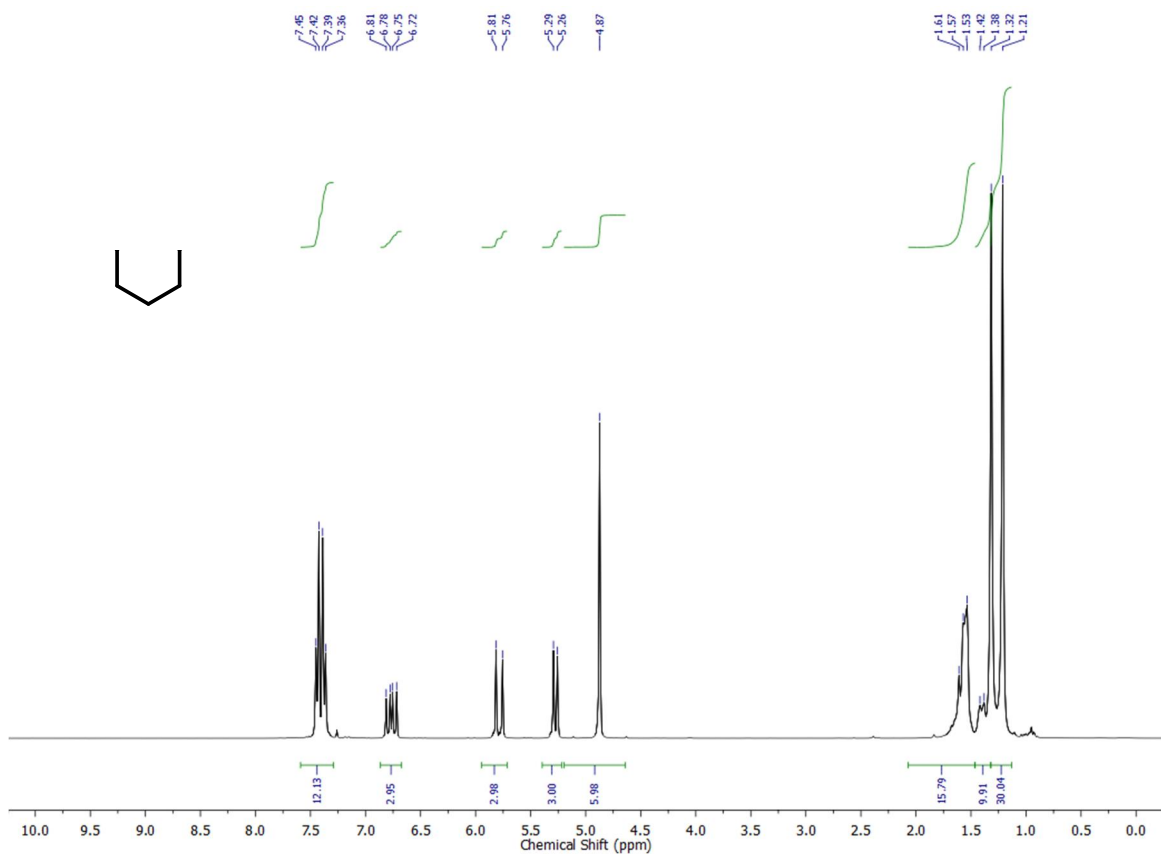


Figure A.1: ^1H NMR (300 MHz, CDCl_3) spectrum of compound 3.1

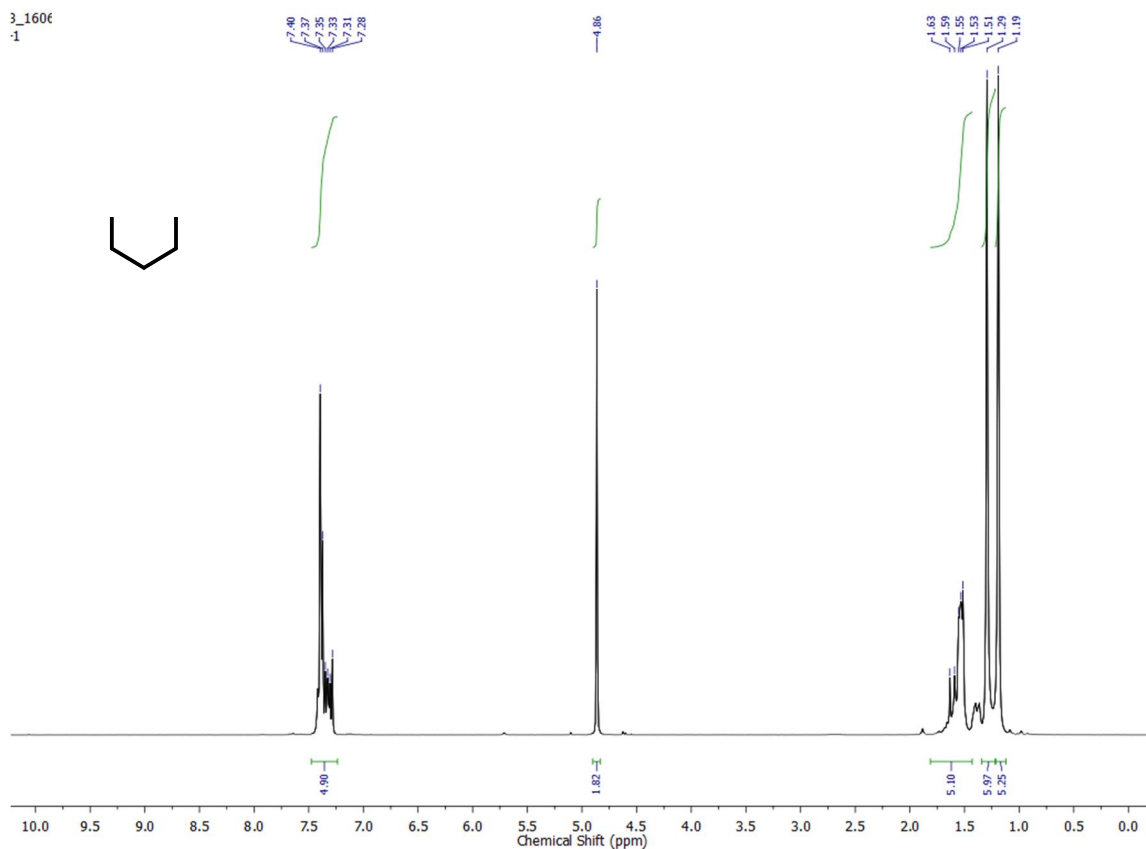



Figure A.2: ^1H NMR (300 MHz, CDCl_3) spectrum of compound 3.2

APPENDIX B
PERMISSION TO REPRINT



Note: Copyright.com supplies permissions but not the copyrighted content itself.

1 ————— 2 ————— 3
 PAYMENT — REVIEW — CONFIRMATION

Step 3: Order Confirmation

Thank you for your order! A confirmation for your order will be sent to your account email address. If you have questions about your order, you can call us 24 hrs/day, M-F at +1.855.239.3415 Toll Free, or write to us at info@copyright.com. This is not an invoice.

Confirmation Number: 11751701
Order Date: 09/26/2018

Payment Information

Julie Pribyl
 University of South Carolina
 pribyl@email.sc.edu
 +1 (303) 332-1593
 Payment Method: n/a

If you paid by credit card, your order will be finalized and your card will be charged within 24 hours. If you choose to be invoiced, you can change or cancel your order until the invoice is generated.

Order Details

Polymer chemistry

<p>Order detail ID: 71573522 Order License ID: 4436620267819 ISSN: 1759-9962 Publication Type: e-Journal Volume: Issue: Start page: Publisher: Royal Society of Chemistry Author/Editor: Royal Society of Chemistry (Great Britain)</p>	<p>Permission Status: ✔ Granted Permission type: Republish or display content Type of use: Thesis/Dissertation <input type="checkbox"/> View details</p>
--	--


Note: This item will be invoiced or charged separately through CCC's [RightsLink](#) service. [More info](#) \$ 0.00

Total order items: 1

This is not an invoice.

Order Total: 0.00 USD

Figure B.1: Permission to reprint Scheme 2.1B



Note: Copyright.com supplies permissions but not the copyrighted content itself.

1
PAYMENT
2
REVIEW
3
CONFIRMATION

Step 3: Order Confirmation

Thank you for your order! A confirmation for your order will be sent to your account email address. If you have questions about your order, you can call us 24 hrs/day, M-F at +1.855.239.3415 Toll Free, or write to us at info@copyright.com. This is not an invoice.

Confirmation Number: 11751702
Order Date: 09/26/2018

Payment Information

Julia Pribyl
University of South Carolina
pribyl@email.sc.edu
+1 (303) 332-1593
Payment Method: n/a

If you paid by credit card, your order will be finalized and your card will be charged within 24 hours. If you choose to be invoiced, you can change or cancel your order until the invoice is generated.

Order Details

Chemical communications

<p>Order detail ID: 71573536 Order License Id: 4436620729523 ISSN: 1364-548X Publication Type: e-Journal Volume: Issue: Start page: Publisher: ROYAL SOCIETY OF CHEMISTRY Author/Editor: Royal Society of Chemistry (Great Britain)</p>	<p>Permission Status: ✔ Granted Permission type: Republish or display content Type of use: Thesis/Dissertation View details</p>
--	---

Note: This item will be invoiced or charged separately through CCC's **RightsLink** service. [More info](#) \$ 0.00

Total order items: 1
This is not an invoice.
Order Total: 0.00 USD

Figure B.2: Permission to reprint Scheme 1.2C



RightsLink®

Home Account Info Help



Title: Hierarchical Porous Polystyrene Monoliths from PolyHIPE
Author: Xinjia Yang, Liangxiao Tan, Lingling Xia, et al
Publication: Macromolecular Rapid Communications
Publisher: John Wiley and Sons
Date: Jul 15, 2015
Copyright © 2015, John Wiley and Sons

Logged in as:
Julia Pribyl
University of South Carolina
Account #: 3001318491
[Logout](#)

Order Completed

Thank you for your order.


This Agreement between University of South Carolina -- Julia Pribyl ("You") and John Wiley and Sons ("John Wiley and Sons") consists of your license details and the terms and conditions provided by John Wiley and Sons and Copyright Clearance Center.

Your confirmation email will contain your order number for future reference.

[printable details](#)

License Number	4436620878788
License date	Sep 26, 2018
Licensed Content Publisher	John Wiley and Sons
Licensed Content Publication	Macromolecular Rapid Communications
Licensed Content Title	Hierarchical Porous Polystyrene Monoliths from PolyHIPE
Licensed Content Author	Xinjia Yang, Liangxiao Tan, Lingling Xia, et al
Licensed Content Date	Jul 15, 2015
Licensed Content Volume	36
Licensed Content Issue	17
Licensed Content Pages	6
Type of use	Dissertation/Thesis
Requestor type	University/Academic
Format	Print and electronic
Portion	Figure/table
Number of figures/tables	1
Original Wiley figure/table number(s)	Figure 2c
Will you be translating?	No
Title of your thesis / dissertation	DESIGNED POLYMER BRUSH INTERFACES FOR PLUTONIUM SEPARATIONS AND POLYETHYLENE NANOCOMPOSITES
Expected completion date	Oct 2018
Expected size (number of pages)	1
Requestor Location	University of South Carolina 541 Main Street, Room 233

Figure B.3: Permission to reprint Figure 1.5



Note: Copyright.com supplies permissions but not the copyrighted content itself.

1 PAYMENT 2 REVIEW 3 CONFIRMATION

Step 3: Order Confirmation

Thank you for your order! A confirmation for your order will be sent to your account email address. If you have questions about your order, you can call us 24 hrs/day, M-F at +1.855.239.3415 Toll Free, or write to us at info@copyright.com. This is not an invoice.

Confirmation Number: 11751709
Order Date: 09/26/2018

If you paid by credit card, your order will be finalized and your card will be charged within 24 hours. If you choose to be invoiced, you can change or cancel your order until the invoice is generated.

Payment Information

Julia Pribyl
University of South Carolina
pribyl@email.sc.edu
+1 (303) 332-1593
Payment Method: n/a

Order Details

Soft matter

Order detail ID: 71573556	Permission Status: ✔ Granted
Order License Id: 4436621175845	Permission type: Republish or display content
ISSN: 1744-6848	Type of use: Thesis/Dissertation
Publication Type: e-Journal	View details
Volume:	
Issue:	
Start page:	
Publisher: ROYAL SOCIETY OF CHEMISTRY	
Author/Editor: Royal Society of Chemistry (Great Britain)	

Note: This item will be invoiced or charged separately through CCC's RightsLink service. [More info](#) \$ 0.00

Total order items: 1 **This is not an invoice.** **Order Total: 0.00 USD**

Figure B.4: Permission to reprint Figure 1.6

Title: Designed Interfaces in Polymer Nanocomposites: A Fundamental Viewpoint
Author: Linda S. Schadler, Sanat K. Kumar, Brian C. Benicewicz, Sarah L. Lewis, Shane E. Harton
Publication: MRS Bulletin
Publisher: Cambridge University Press
Date: Oct 30, 2010
 Copyright © COPYRIGHT: © Materials Research Society 2007

Logged in as:
 Julia Pribyl
 University of South Carolina
 Account #: 3001318491

[LOGOUT](#)

Order Completed

Thank you for your order.

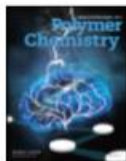
This Agreement between University of South Carolina -- Julia Pribyl ("You") and Cambridge University Press ("Cambridge University Press") consists of your license details and the terms and conditions provided by Cambridge University Press and Copyright Clearance Center.

Your confirmation email will contain your order number for future reference.

[printable details](#)

License Number	4436621289260
License date	Sep 26, 2018
Licensed Content Publisher	Cambridge University Press
Licensed Content Publication	MRS Bulletin
Licensed Content Title	Designed Interfaces in Polymer Nanocomposites: A Fundamental Viewpoint
Licensed Content Author	Linda S. Schadler, Sanat K. Kumar, Brian C. Benicewicz, Sarah L. Lewis, Shane E. Harton
Licensed Content Date	Oct 30, 2010
Licensed Content Volume	32
Licensed Content Issue	4
Start page	335
End page	340
Type of Use	Dissertation/Thesis
Requestor type	Not-for-profit
Portion	Text extract
Number of pages requested	1
Order reference number	
Territory for reuse	World
Title of your thesis / dissertation	DESIGNED POLYMER BRUSH INTERFACES FOR PLUTONIUM SEPARATIONS AND POLYETHYLENE NANOCOMPOSITES
Expected completion date	Oct 2018
Estimated size(pages)	1
Requestor Location	University of South Carolina 541 Main Street, Room 233

Figure B.5: Permission to reprint Figure 1.8



Title: Controlling the thermomechanical properties of polymer nanocomposites by tailoring the polymer-particle interface
Author: Amitabh Bansal, Hoichang Yang, Chunzhao Li, et al
Publication: Journal of Polymer Science Part B: Polymer Physics
Publisher: John Wiley and Sons
Date: Sep 5, 2006
Copyright © 2006, John Wiley and Sons

Logged in as:
Julia Pribyl
University of South Carolina
Account #:
3001318491
[LOGOUT](#)

Order Completed

Thank you for your order.

This Agreement between University of South Carolina -- Julia Pribyl ("You") and John Wiley and Sons ("John Wiley and Sons") consists of your license details and the terms and conditions provided by John Wiley and Sons and Copyright Clearance Center.

Your confirmation email will contain your order number for future reference.

[printable details](#)

License Number	4436621413711
License date	Sep 26, 2018
Licensed Content Publisher	John Wiley and Sons
Licensed Content Publication	Journal of Polymer Science Part B: Polymer Physics
Licensed Content Title	Controlling the thermomechanical properties of polymer nanocomposites by tailoring the polymer-particle interface
Licensed Content Author	Amitabh Bansal, Hoichang Yang, Chunzhao Li, et al
Licensed Content Date	Sep 5, 2006
Licensed Content Volume	44
Licensed Content Issue	20
Licensed Content Pages	7
Type of use	Dissertation/Thesis
Requestor type	University/Academic
Format	Print and electronic
Portion	Figure/table
Number of figures/tables	1
Original Wiley figure/table number(s)	Figure 3
Will you be translating?	No
Title of your thesis / dissertation	DESIGNED POLYMER BRUSH INTERFACES FOR PLUTONIUM SEPARATIONS AND POLYETHYLENE NANOCOMPOSITES
Expected completion date	Oct 2018
Expected size (number of pages)	1

Figure B.6: Permission to reprint Figure 1.9

SPRINGER NATURE

Title: Anisotropic self-assembly of spherical polymer-grafted nanoparticles
Author: Pinar Akcora, Hongjun Liu, Sanat K. Kumar, Joseph Moll, Yu Li et al.
Publication: Nature Materials
Publisher: Springer Nature
Date: Mar 22, 2009
 Copyright © 2009, Springer Nature

Logged in as:
 Julia Pribyl
 University of South Carolina
 Account #:
 3001318491
[LOGOUT](#)

Order Completed

Thank you for your order.

This Agreement between University of South Carolina -- Julia Pribyl ("You") and Springer Nature ("Springer Nature") consists of your license details and the terms and conditions provided by Springer Nature and Copyright Clearance Center.

Your confirmation email will contain your order number for future reference.

[printable details](#)

License Number	4436630170451
License date	Sep 26, 2018
Licensed Content Publisher	Springer Nature
Licensed Content Publication	Nature Materials
Licensed Content Title	Anisotropic self-assembly of spherical polymer-grafted nanoparticles
Licensed Content Author	Pinar Akcora, Hongjun Liu, Sanat K. Kumar, Joseph Moll, Yu Li et al.
Licensed Content Date	Mar 22, 2009
Licensed Content Volume	8
Licensed Content Issue	4
Type of Use	Thesis/Dissertation
Requestor type	academic/university or research institute
Format	print and electronic
Portion	figures/tables/illustrations
Number of figures/tables/illustrations	1
High-res required	no
Will you be translating?	no
Circulation/distribution	<501
Author of this Springer Nature content	no
Title	DESIGNED POLYMER BRUSH INTERFACES FOR PLUTONIUM SEPARATIONS AND POLYETHYLENE NANOCOMPOSITES
Instructor name	Brian C. Benicewicz
Institution name	University of South Carolina
Expected presentation date	Oct 2018
Portions	Figure 2
Requestor Location	University of South Carolina

Figure B.7: Permission to reprint Figure 1.10



Title: Grafting Bimodal Polymer
Brushes on Nanoparticles Using
Controlled Radical
Polymerization

Author: Atri Rungta, Bharath Natarajan,
Tony Neely, et al

Publication: Macromolecules

Publisher: American Chemical Society

Date: Dec 1, 2012

Copyright © 2012, American Chemical Society

Logged in as:

Julia Pribyl
University of South Carolina

Account #:
3001318491

LOGOUT

PERMISSION/LICENSE IS GRANTED FOR YOUR ORDER AT NO CHARGE

This type of permission/license, instead of the standard Terms & Conditions, is sent to you because no fee is being charged for your order. Please note the following:

- Permission is granted for your request in both print and electronic formats, and translations.
- If figures and/or tables were requested, they may be adapted or used in part.
- Please print this page for your records and send a copy of it to your publisher/graduate school.
- Appropriate credit for the requested material should be given as follows: "Reprinted (adapted) with permission from (COMPLETE REFERENCE CITATION). Copyright (YEAR) American Chemical Society." Insert appropriate information in place of the capitalized words.
- One-time permission is granted only for the use specified in your request. No additional uses are granted (such as derivative works or other editions). For any other uses, please submit a new request.

If credit is given to another source for the material you requested, permission must be obtained from that source.

Figure B.8: Permission to reprint Scheme 1.5



RightsLink®

Home

Account Info

Help



Title: Ligand Engineering of Polymer Nanocomposites: From the Simple to the Complex

Author: Ying Li, Timothy M. Krentz, Lei Wang, et al

Publication: Applied Materials

Publisher: American Chemical Society

Date: May 1, 2014

Copyright © 2014, American Chemical Society

Logged in as:

Julia Pribyl
University of South Carolina

Account #:
3001318491

LOGOUT

PERMISSION/LICENSE IS GRANTED FOR YOUR ORDER AT NO CHARGE

This type of permission/license, instead of the standard Terms & Conditions, is sent to you because no fee is being charged for your order. Please note the following:

- Permission is granted for your request in both print and electronic formats, and translations.
- If figures and/or tables were requested, they may be adapted or used in part.
- Please print this page for your records and send a copy of it to your publisher/graduate school.
- Appropriate credit for the requested material should be given as follows: "Reprinted (adapted) with permission from (COMPLETE REFERENCE CITATION). Copyright (YEAR) American Chemical Society." Insert appropriate information in place of the capitalized words.
- One-time permission is granted only for the use specified in your request. No additional uses are granted (such as derivative works or other editions). For any other uses, please submit a new request.

If credit is given to another source for the material you requested, permission must be obtained from that source.

Figure B.9: Permission to reprint Figure 1.11



RightsLink®

Home

Account Info

Help



ACS Publications
Most Trusted. Most Cited. Most Read.

Title: Photoinitiated Polymerization of 4-Vinylpyridine on polyHIPE Foam Surface toward Improved Pu Separations

Author: Julia Pribyl, Brock Fletcher, Warren Steckle, et al

Publication: Analytical Chemistry

Publisher: American Chemical Society

Date: May 1, 2017

Copyright © 2017, American Chemical Society

Logged in as:

Julia Pribyl
University of South Carolina
Account #:
3001318491

LOGOUT

PERMISSION/LICENSE IS GRANTED FOR YOUR ORDER AT NO CHARGE

This type of permission/license, instead of the standard Terms & Conditions, is sent to you because no fee is being charged for your order. Please note the following:

- Permission is granted for your request in both print and electronic formats, and translations.
- If figures and/or tables were requested, they may be adapted or used in part.
- Please print this page for your records and send a copy of it to your publisher/graduate school.
- Appropriate credit for the requested material should be given as follows: "Reprinted (adapted) with permission from (COMPLETE REFERENCE CITATION). Copyright (YEAR) American Chemical Society." Insert appropriate information in place of the capitalized words.
- One-time permission is granted only for the use specified in your request. No additional uses are granted (such as derivative works or other editions). For any other uses, please submit a new request.

Figure B.10: Permission to reprint Chapter 2